NSIDE TRACK with Hatem Zeine, Ossia, Inc. | 28

DRO-Based Synthesizer Cuts Phase Noise | 74

microwaves&rf

ANUARY 2014 TRUSTED ENGINEERING RESOURCE FOR 50 YEARS www.mwrf.com

2014 TECH FORECAST: TECHNOLOGIES TO WATCH p | 36

A Penton® Publication

Periodicals Postage Paid • USPS 100 Approved Poly

Planar Monolithics Industries, Inc.

Offering State-Of-The-Art RF and Microwave Components
& Integrated Assemblies From DC to 40GHz

- Amplifiers
- Attenuators - Variable
- DLVA & ERDLVA & SDLVA's
- DTO's & Frequency Synthesizers
- Filters
- Form, Fit & Function Products
- IFM's & Frequency Discriminators
- Integrated MIC/MMIC Modules
- I/Q Vector Modulators
- Limiters & Detectors
- Log Amplifiers
- Pulse & Bi-Phase Modulators
- Phase Shifters
- Rack & Chassis Mount Products
- Receiver Front Ends & Transceivers
- Single Sideband Modulators
- SMT & QFN Products
- Solid-State Switches
- Switch Matrices
- Switch Filter Banks
- Threshold Detectors
- USB Products

FREQUENCY SYNTHESIZERS

Model No. PFS-618-CD-1

- 6.0 to 18.0GHz
- 100kHz Frequency Step Size
- +/-1MHz Frequency Accuracy
- 1uS Settling Time to 1MHz
- 1uS Tuning Speed
- +10dBm Output Power
- Phase Noise:
  - -78dBc/Hz @ 1kHz Offset
  - -96dBc/Hz @ 100kHz Offset
  - -100dBc/Hz @ 10MHz Offset
- DC to 10MHz Modulation BW

Frequency Range	6.0 to 18.0GHz
Frequency Step Size, Nominal (LSB)	100kHz
Power Output Level	+10dBm Min.
Power Variation	5dB P-P (±2.5dB) Max.
Frequency Accuracy	±1MHz Max.
Frequency Aging	±2 PPM / Year
Settling Time to 1MHz	1usec
Tuning Control	Binary, TTL 17 Bits (Parallel)
Tuning Speed	1usec
SSB Noise	6.0 to 18.0GHz Max.
@ 1kHz Offset	-78dBc / Hz
@ 100kHz Offset	-96dBc / Hz
@ 10MHz Offset	-100dBc / Hz
Spurious Output	-55dBc Max.
Harmonics	-30dBc Max.
Sub-Harmonics	-55dBc Max.
Reference	Internal Reference
Frequency Modulation	
Modulation Bandwidth	DC to 10MHz
Frequency Deviation	±400MHz Min., 100MHz / Volt
Control	Analog
Sensitivity	1.1 : 1
Power Supply	+12V @ 2.5A Max. (1.4A measured) -12V @ 0.6A Max. (0.1A measured) +5V @ 4A Max (1.6A measured) -5V @ 2A Max. (0.1A measured)
Connectors	
Control	37 Pin Sub-D Male
Power	9 Pin Sub-D Male
RF Output	SMA Female
Modulation Input	SMA Female
Size	6.48" x 6.23" x 1.6"

West Coast Operation:
4921 Robert J. Mathews Pkwy, Suite 1
El Dorado Hills, CA 95762 USA
Tel: 916-542-1401 Fax: 916-265-2597

East Coast Operation:
7311-F Grove Road
Frederick, MD 21704 USA
Tel: 301-662-5019 Fax: 301-662-1731

Email: sales@pmi-rf.com
Website: www.pmi-rf.com

Hermetic Sealing, High Reliability to Mil-Std-883, Small Quantity Requirements accepted.
We offer Custom Designs

ISO9001/2008 REGISTERED

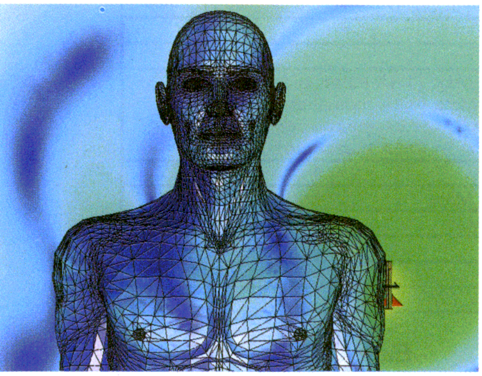

theNEW NARDA

The Engineer's First Choice for RF & Microwave Products

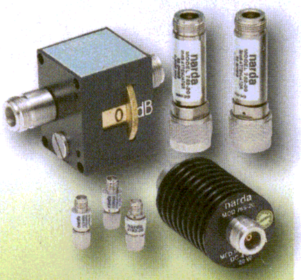

Attenuators
- Fixed, Step, or Variable
- Power Levels Up to 500W
- DC to 40 GHz

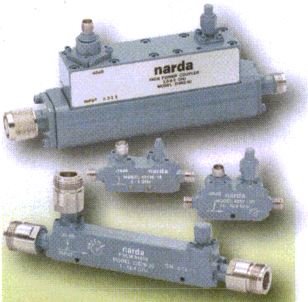

Directional Couplers
- Broadband Coverage
- High Power (up to 1 kW CW)
- Flat Frequency Response
- .05-40 GHz

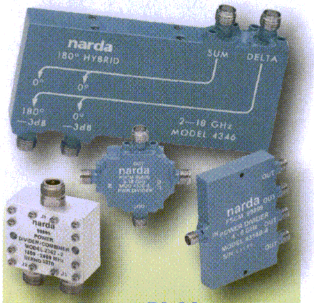

Power Dividers
- Low VSWR
- 2-, 3-, 4-, 6-, and 8-way
- High Isolation
- .25-45 GHz

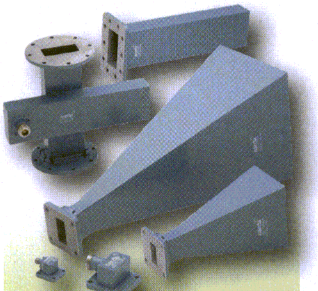

Waveguide Products
- Newly Expanded Line, Including 130 New Products
- 1.7-40 GHz
- Gain Horns, Adapters, Terminations, and Couplers

Terminations
- Low VSWR
- High Power (up to 500W CW)
- DC-40 GHz

SEM Switches
- Electro-Mechanical
- SPDT through SP12T
- DC-26.5 GHz

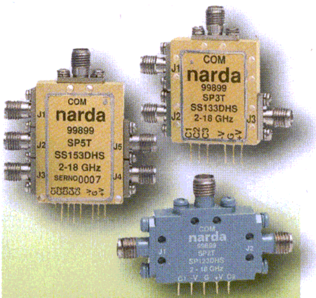

PIN Switches
- Solid-State
- Small Package Size
- Fast Switching Speeds
- .1-40 GHz

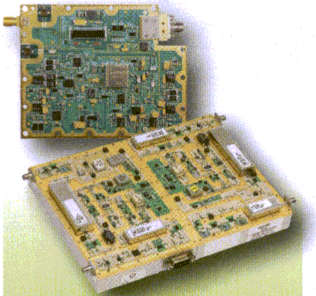

Custom IMA Solutions
- Simple & Complex Modules and Subsystems
- EW, Satcom, Radar Applications
- DC-60 GHz

Narda has over 700 catalog products, as well as custom products, to meet your specific program requirements.

Please contact us for details.

narda

an L3 company

www.nardamicrowave.com • 631.231.1700

Six decades of technological innovation.


AWR
© 2014 AWR Corporation. All rights reserved.
Add a macroscope to your Microwave Office.
See the big picture quickly in one design environment with VSS. Zoom in to make circuit tweaks. Then zoom out to see the system impact. VSS does system budget analysis and identifies sources of IM products, harmonics, and noise directly on your Microwave Office circuits. VSS's powerful simulator defines complex systems — radio and circuit designs, baseband signal processing, algorithmic development, and digital fixed-point implementations too. Grab a test copy at awrcorp.com/VSS.
Stop waiting and start designing™
VSS SYSTEM SIMULATOR

VOLUME 53, ISSUE 1

In This Issue

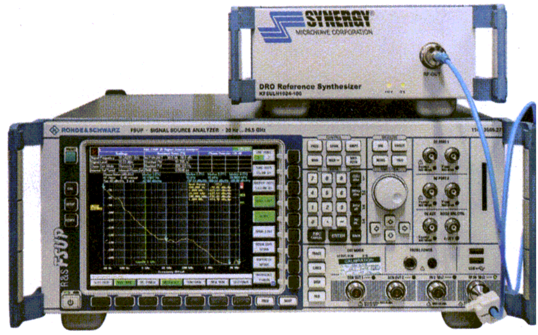

74

FEATURES

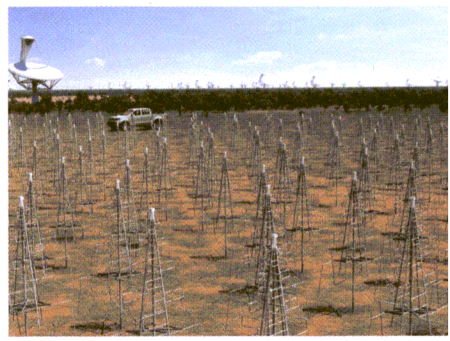

20

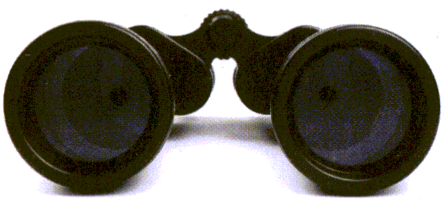

36

INDUSTRY TRENDS & ANALYSIS

PRODUCT TECHNOLOGY

NEWS & COLUMNS

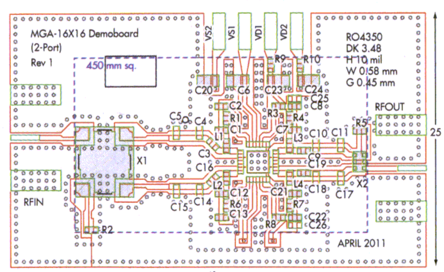

50

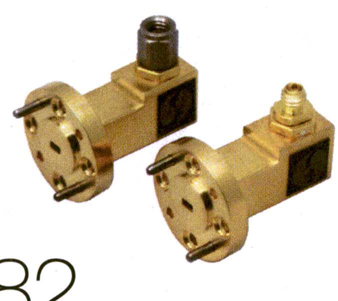

82

JOIN US ONLINE

follow us @MicrowavesRF

become a fan at facebook.com/microwavesRF

Penton Design Engineering & Sourcing Group

BPA WORLDWIDE BUSINESS

abm The Association of Business Information & Media Companies

Micro Lambda's Bench Test Boxes... Simple and Easy to Use!

MLBS-Synthesizer Test Box – 600 MHz to 20 GHz
Standard models cover the 0.6 to 2.5 GHz, 2 to 8 GHz, 8 to 20 GHz and 2 to 20 GHz frequency bands. All versions of the MLSP synthesizer product family can be easily inserted into the test box. Tuning consists of a control knob, key pad, USB and Ethernet connections. Units provide +10 dBm to +13 dBm output power levels and are specified over the lab environment of +15°C to +55°C and are CE certified.

Units are provided with a power cord, USB cable, Ethernet cable, CD incorporating a users manual, quick start guide and PC interface software.

MLBF-Filter Test Box – 500 MHz to 50 GHz
Standard models utilize any Bandpass or Bandreject filter manufactured by Micro Lambda today. Bandpass filter models cover 500 MHz to 50 GHz and are available in 4, 6 and 7 stage configurations. Bandreject (notch) filter models cover 500 MHz to 20 GHz and are available in 10, 12, 14 and 16 stage configurations. Units are specified to operate over the lab environment of +15°C to +55°C and are CE certified.

Units are provided with a power cord, USB cable, Ethernet cable, CD incorporating a users manual, quick start guide and PC interface software.

See our complete line of wideband, low noise components

MLSP-series Synthesizers
600 MHz to 20 GHZ

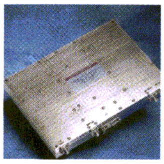

MLSW-series Synthesizers
600 MHz to 16 GHz

MLTO-series TO-8 Oscillators
2 to 16 GHz

MLSMO-series Surface Mount Oscillators
2 to 16 GHz

www.microlambdawireless.com

MICRO LAMBDA WIRELESS, INC.

"Look to the leader in YIG-Technology"

46515 Landing Parkway, Fremont CA 94538 • (510) 770-9221 • sales@microlambdawireless.com

Industry pros are talking about us behind our backs ***...and we love it!***

IW designs and manufactures high performance microwave cable and cable assemblies for both military and commercial markets. Applications include telecommunications, data links, satellite systems, airborne electronic warfare and counter measures, missile systems, UAV applications, avionics and instrumentation, fire control systems, medical electronics, and geophysical exploration.

We offer a wide variety of products providing extremely low attenuation at frequencies up to 67 GHz and ranging from .050 inch to 0.50 inch in diameter. Our unique PTFE lamination process, combined with our high performance shield design, has made us one of the leaders in low-loss microwave transmission lines. IW's broad range of microwave cables and connectors assures every customer the proper cable assembly for each of their specific application needs.

Our major products include:

- Low-loss microwave cables optimized for use to 11, 18, 26.5, 40, 50, and 67 GHz
- Microwave cable assemblies with connectors for SMA, TNC, N, SC, 7/16, 1.85mm, 2.4mm, 2.92mm, 3.5mm, 7mm, ZMA, SMP, SMPM & more
- RE-FLEX™ semi flexible assemblies
- TUF-FLEX™ assemblies – improved crush resistance without using armor
- Water-blocked cables for submarines
- Composite cables – combination microwave/signal/power/data
- PTFE insulated hook-up wires
- Multi-conductor cables
- Dielectric cores
- Twisted pair and triaxial cables
- Low smoke, zero halogen cable jackets
- Cable protection options such as armor, PEEK, NOMEX, Neoprene weatherproofing, PET monomer braid

AS9100:2009 and ISO 9001:2008 certified.

INSULATED WIRE, INC.
203.791.1999
www.iw-microwave.com
sales@iw-microwave.com

Scan code to find out how you can ***get connected***

We're how the microwave industry ***gets connected!***

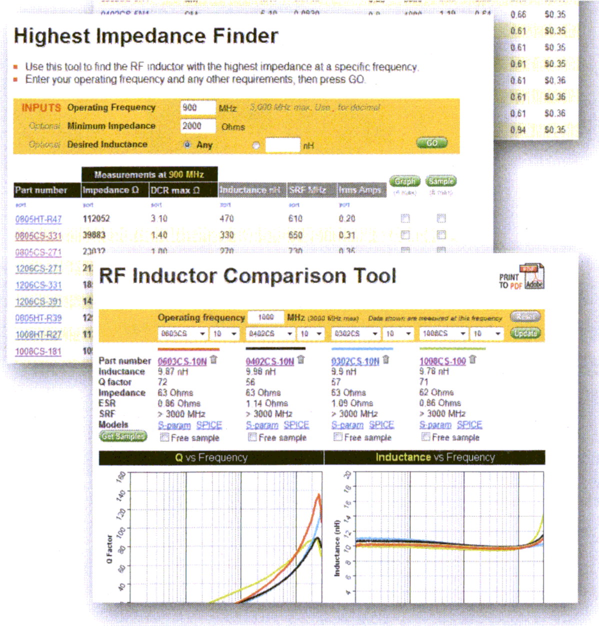

The best inductor selection tools.

coilcraft.com/tools

Now in a handy pocket size.

coilcraft.com/mobile

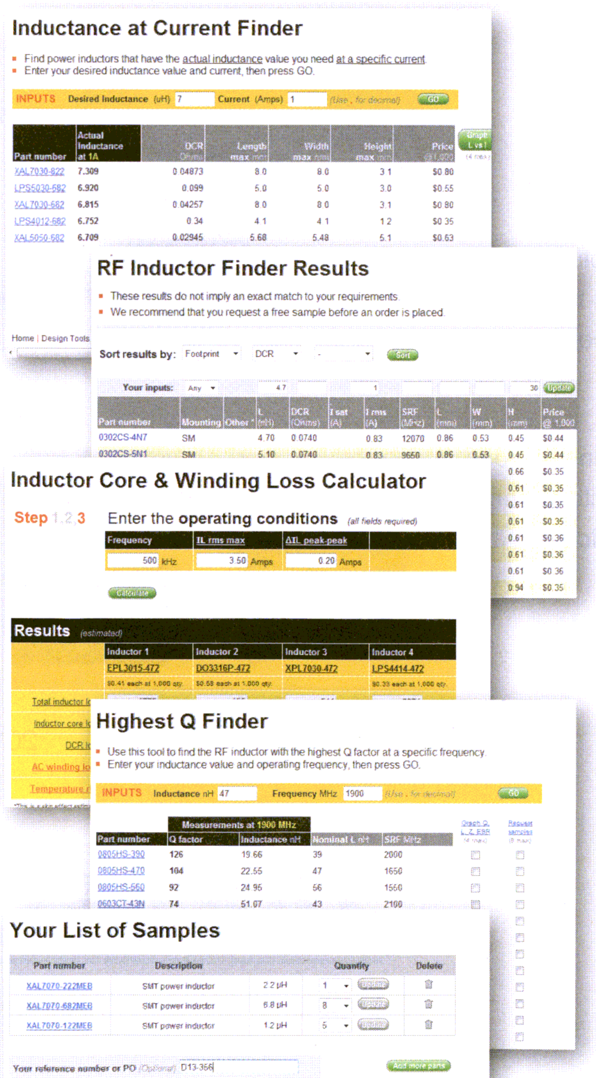

Coilcraft®

WWW.COILCRAFT.COM

on microwaves&rf.com

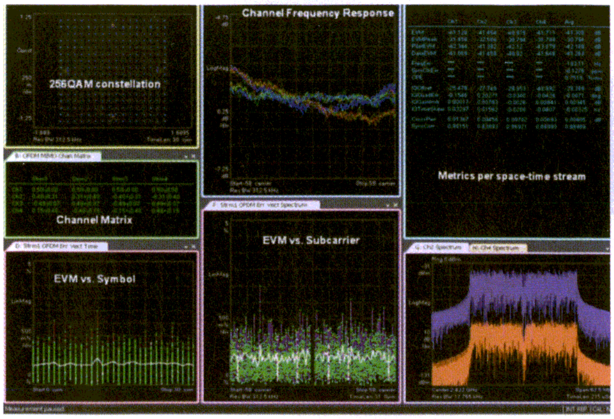

WHAT'S THE DIFFERENCE BETWEEN IEEE 802.11AC AND 802.11AD?

The IEEE 802.11ac and 802.11ad specifications both promise to deliver increased capacity, speed, and performance in different ways, allowing users on-the-go to enjoy even their highest-data-rate applications. In this Web-exclusive report, Agilent Technologies' *Liz Ruetsch* breaks down the differences between the two.

To read the article in its entirety, go to *www.mwrf.com/test-amp-measurement/what-s-difference-between-ieee-80211ac-and-80211ad*

NEWS UPDATES SENT TO YOUR DESKTOP

Don't believe everything you read, unless it's in the latest issue of *Microwaves & RF UPDATE*. The industry's longest-running weekly e-mail newsletter, it combines insightful commentary with the latest product and industry business news. It is sent directly to your computer desktop each week, and often contains the little things that engineers love, such as links to free white papers and even design software. If you're not already reading it, subscriptions are free, and available from the *Microwaves & RF* website at *www.mwrf.com.*

- Microwave Meetings

News

Putting Software Through Its Paces
Jack Browne, Technical Contributor
In addition to offering demonstrations of its powerful computer-aided-engineering (CAE) software tools at booth No. 330, AWR will be sponsoring several social gatherings at the 2013 IMS.
READ THE FULL ARTICLE

Corralling Materials For Microwave Circuits
Jack Browne, Technical Contributor
Engineers in need of a starting point for their high-frequency printed-circuit boards (PCBs) will find them by comparing notes with members of Rogers Corp.'s Advanced Circuit Materials division at IMS booth No. 1459. Visitors to the booth will learn about Rogers' next generation RO4000® circuit materials.
READ THE FULL ARTICLE

Top Articles Right Now

1. 5 RF Transmitter Measurements Every Engineer Should Know
2. What's The Difference Between IEEE 802.11ac And 802.11ad?
3. Filtering EMI And RFI Noise
4. RF MEMS Switches Are Primed For Mass-Market Applications
5. Software Speeds PA Design

join us online

DAVID A. HALL BOB NELSON

ALSO, BE SURE CHECK OUT THESE OTHER RECENT ARTICLES IN OUR CONTRIBUTED TECHNICAL EXPERT SERIES.

Visit *www.mwrf.com/community/contributors.*

THE EFFECT OF MOORE'S LAW ON RF INSTRUMENTS

DAVID A. HALL—*Senior Product Marketing Manager for RF and Communications, National Instruments*

UNDERSTANDING MEASUREMENT UNCERTAINTIES IN SPECTRUM ANALYSIS

BOB NELSON—*Product Support Engineer, Agilent Technologies*

REVISIT IMS2013

IMS 2013

The 2013 installment of the RF/microwave industry's flagship event, the *International Microwave Symposium*, has come and gone. Luckily for you, it needn't live on just in memory. Visit *www.mwrf.com/ims-2013-microwaves-rf-reports-event* to check out our show coverage, as well as *www.engineering tv.com* to view videos from the event.

MWRF.COM HAS ARCHIVES OF PRINT AND ONLINE ARTICLES DATING BACK TO OCTOBER 2002.

Visit mwrf.com today and click the "Back Issues" link. And while you're taking a look around the site, click on "Product Directory" to gain access to our complete directory of products and suppliers.

Editorial

JEAN-JACQUES DELISLE
Technical Engineering Editor
jean-jacques.delisle@penton.com

The Designer's Conundrum

The past two months have been thrilling for me. Not only did I make a big move from Rochester, N.Y., to New York City, but I began working with the *Microwaves & RF* team as technical editor. Nancy Friedrich, Jack Browne, and the rest of the team have done a tremendous job in giving me an introduction to a different side of the RF industry from what I am used to, and I am excited to really dig in. Already I have interviewed several CEOs, chatted with experts in a range of fields, researched products/design trends, and had the opportunity to immerse myself in a field that I am passionate about. So when Nancy asked me to write a guest editorial this month, I jumped at the chance to share my excitement and mission.

Throughout college and once I began working, the complex problems just waiting for solutions are what drew me so strongly to the RF design field. My studies and work focused on everything from the design and testing of ICs, control systems, sensors, and test fixtures to sustainable energy solutions and more. But none of these fields alone really matched the complexity and detail necessary to design RF technologies, as this field requires a level of consideration and thought that is staggering.

I relished the challenge, quickly learning that a little bit of knowledge in this field is dangerous, a good amount of knowledge is helpful, and expertise in an RF field makes you feel like you have magical powers. I also learned that with great power come great difficulties, roadblocks, and headaches. With RF technology, if you make a little mistake it's big, big mistakes cost a lot of money, and often you are reinventing the wheel anyway.

There have been many RF experts since Tesla befuddled everyone almost a century ago, but most people don't know any more about RF then they did back then. Many of these experts are just as secretive as Tesla, or just too overworked to share the bounty of their knowledge. The roadblock could also be the math involved. Either way, I found that there were great solutions to a lot of design problems I ran into, but I either didn't know the right terminology to describe it, or the solution was in a scope so different from what I was working in, I didn't know what I was looking at. Oh—and of course, some RF fields change every year.

These frustrations and design challenges are what make me really excited about working with *Microwaves & RF*, as the magazine and website are geared toward providing knowledge and direction to designers for all matters RF while staying updated. There is a lot more out there than just what is shared in scientific journals, and my goal is to help get that information into the hands of RF designers in a timely fashion, and in a way that adds value. mw

JOIN US ONLINE
become a fan: facebook.com/microwaves & RF

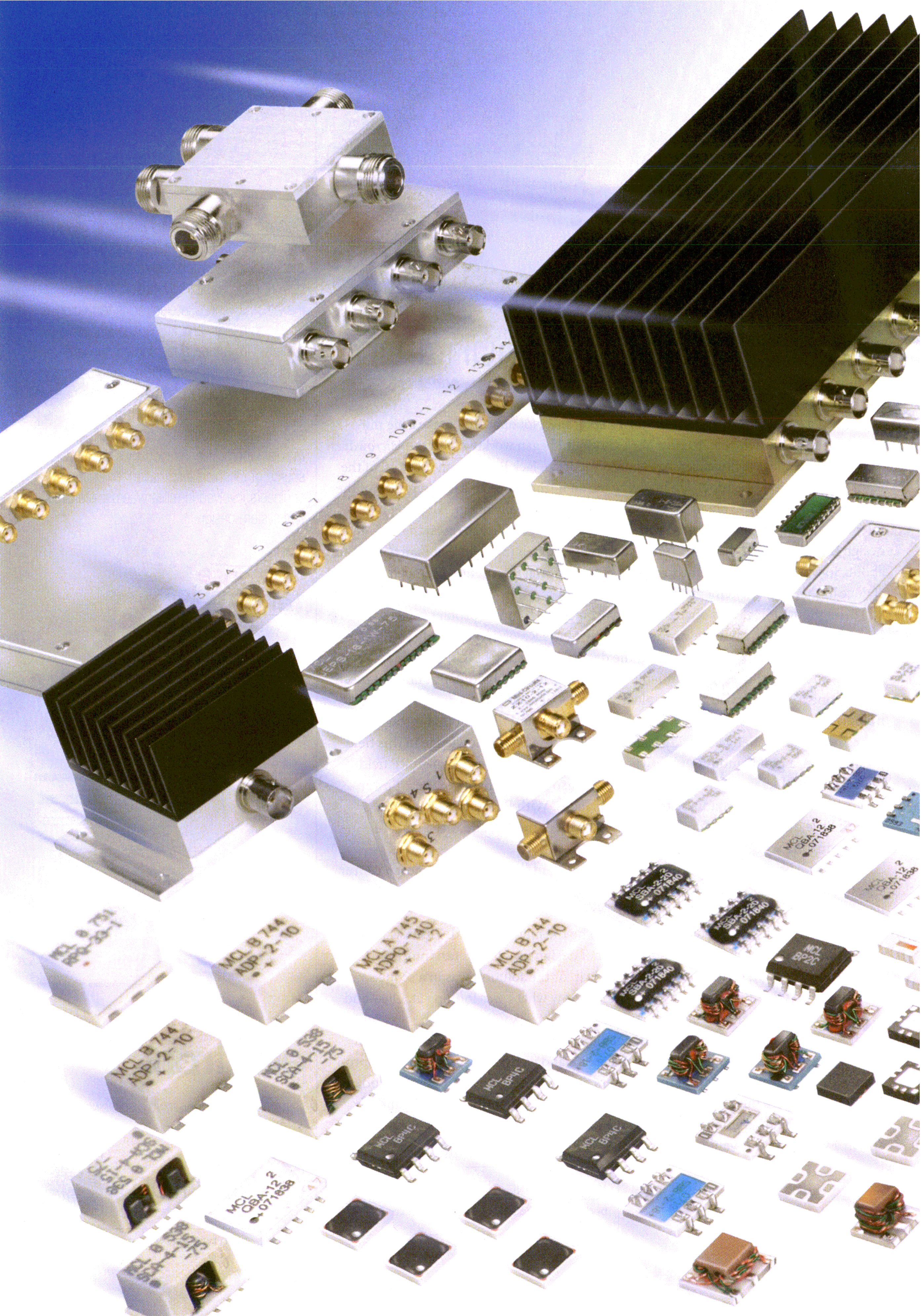

MCL B 744
ADP-2-10
MCL B 744
ADP-2-10
MCL B 744
ADP-2-10
MCL
BP4C
MCL
BP4C
MCL
BP4C
MCL
BP2C

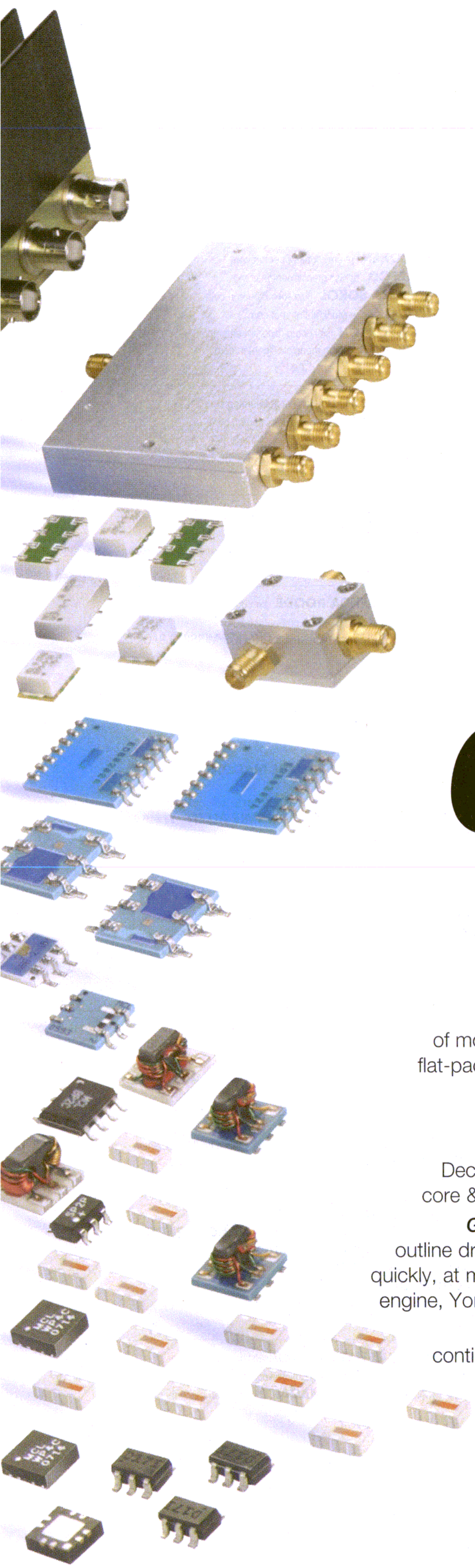

448 re

JANUARY | 2014 microwaves&rf

A Penton® Publication

EDITORIAL

CONTENT DIRECTOR: **NANCY K. FRIEDRICH** nancy.friedrich@penton.com
TECHNICAL CONTRIBUTOR: **JACK BROWNE** jack.browne@penton.com
TECHNICAL ENGINEERING EDITOR: **JEAN-JACQUES DELISLE** jean-jacques.delisle@penton.com
CONTENT PRODUCTION DIRECTOR: **MICHAEL BROWNE** michael.browne@penton.com
PRODUCTION EDITOR: **RICHARD GAWEL** richard.gawel@penton.com
PRODUCTION EDITOR: **JEREMY COHEN** jeremy.cohen@penton.com
PRODUCTION EDITOR: **DENISE GRECO** denise.greco@penton.com
ASSOCIATE CONTENT PRODUCER: **ILIZA SOKOL** iliza.sokol@penton.com
EUROPEAN EDITOR: **PAUL WHYTOCK** p.whytock@btinternet.com
ASSOCIATE EDITOR: **SALLY WARD-FOXTON** sally.ward-foxton@penton.com
EDITORIAL INTERN: **SARAH MANGIOLA** sarah.mangiola@penton.com

ART DEPARTMENT

GROUP DESIGN DIRECTOR: **ANTHONY VITOLO** tony.vitolo@penton.com
CREATIVE DIRECTOR: **DIMITRIOS BASTAS** dimitrios.bastas@penton.com
SENIOR ARTIST: **JAMES MILLER** james.miller@penton.com
CONTRIBUTING ART DIRECTOR **RANDALL RUBENKING** randall.rubenking@penton.com

PRODUCTION

GROUP PRODUCTION MANAGER: **JUSTIN MARCINIAK** justin.marciniak@penton.com
PRODUCTION MANAGER: **VICKI MCCARTY** vicki.mccarty@penton.com
CLASSIFIED PRODUCTION COORDINATOR: **LINDA SARGENT** linda.sargent@penton.com

AUDIENCE MARKETING

AUDIENCE DEVELOPMENT DIRECTOR: **BRENDA ROODE** brenda.roode@penton.com
ONLINE MARKETING SPECIALIST: **DAN KRAFT** dan.kraft@penton.com
FREE SUBSCRIPTION/STATUS OF SUBSCRIPTION/ADDRESS CHANGE/MISSING BACK ISSUES
T | 866.505.7173 microwaves&RF@halldata.com

SALES & MARKETING

BRAND DIRECTOR, e|DESIGN: **TRACY SMITH** **T** | 913.967.1324 **F** | 913.514.6881
tracy.smith@penton.com

REGIONAL SALES REPRESENTATIVES
BRAND CHAMPION: NORTHEAST/EASTERN CANADA: **DAVE MADONIA** **T** | 212.204.4331
F | 913.514.3966 dave.madonia@penton.com
SOUTH: **BILL YARBOROUGH** **T** | 713.636.3809 **F** | 713.380.5318 bill.yarborough@penton.com
NORTHWEST/NORTHERN CALIFORNIA/WESTERN CANADA: **JAMIE ALLEN** **T** | 415.608.1959
F | 913.514.3667 jamie.allen@penton.com
MIDWEST/MID-ATLANTIC: **STEPHANIE CAMPANA** **T** | 312.840.8437 **F** | 913.514.3645
stephanie.campana@penton.com

PLEASE SEND INSERTION ORDERS TO: orders@penton.com
PENTON REPRINTS: **WRIGHT'S MEDIA** **T** | 877.652.5295 penton@wrightsmedia.com
CIRCULATION: **CUSTOMER SERVICE** **T** | 866.505.7173 **F** | 847.763.9673 electronicdesign@halldata.com

EUROPEAN SALES
EUROPE: **MARK DURHAM** **T** | +44 (0)7958 564137 mark.durham@penton.com
ASIA: **HELEN LAI** **T** | 886 2-2727 7799 helen@twoway-com.com
JAPAN: **HIROKAZU MORITA** **T** | +81 3 3261 4591 **F** | +81 3 3261 6126
TAIWAN: **CHARLES LIU** **T** | 886 2-2727 7799 **F** | 886 2 2728-3686
KOREA: **JO YOUNG SANG** **T** | (011)82-2-739-7840
LIST RENTALS, CUSTOMER SERVICE--SUBSCRIPTIONS:
ONLINE MARKETING MANAGER: **SARAH NOWOWIEJSKI** **T** | (212) 204 4295
sarah.nowowiejski@penton.com
PENTON REPRINTS: **WRIGHT'S MEDIA** **T** | (877) 652-5295 penton@wrightsmedia.com

ONLINE

ONLINE DEVELOPMENT DIRECTOR: **VIRGINIA GOULDING** virginia.goulding@penton.com
COMMUNITY LEADER: **RYAN MALEC** ryan.malec@penton.com

DESIGN ENGINEERING & SOURCING GROUP

VICE PRESIDENT & MARKET LEADER: **BILL BAUMANN**
EXECUTIVE DIRECTOR OF CONTENT AND USER ENGAGEMENT: **NANCY FRIEDRICH**
GROUP DIRECTOR OF OPERATIONS: **CHRISTINA CAVANO**
GROUP DIRECTOR OF MARKETING: **JANE COOPER**
RESEARCH MANAGER: **JULIE RITCHIE**
MARKETING & EVENTS SPECIALIST: **ADRIAN PIAZZA**

PENTON MEDIA INC.

CHIEF EXECUTIVE OFFICER: **DAVID KIESELSTEIN** david.kieselstein@penton.com
CHIEF FINANCIAL OFFICER: **NICOLA ALLAIS** nicola.allais@penton.com
SENIOR VP, DESIGN ENGINEERING GROUP: **BOB MACARTHUR** bob.macarthur@penton.com

1166 AVENUE OF THE AMERICAS, 10TH FLOOR
NEW YORK, NY 10036 **T** | 212.204.4200

Penton
Design Engineering & Sourcing Group

Electronic Design | Machine Design | Microwaves & RF | Medical Design | Source ESB | Hydraulics & Pneumatics | Global Purchasing | Distribution Resource | Power Electronics | Mobile Dev & Design | Defense Electronics | Auto Electronics | Electronic Design Europe | Engineering TV

RF Amplifiers and Sub-Assemblies for Every Application

Delivery from Stock to 2 Weeks ARO from the catalog or built to your specifications!

- Competitive Pricing & Fast Delivery
- Military Reliability & Qualification
- Various Options: Temperature Compensation, Input Limiter Protection, Detectors/TTL & More
- Unconditionally Stable (100% tested)

ISO 9001:2000 and AS9100B CERTIFIED

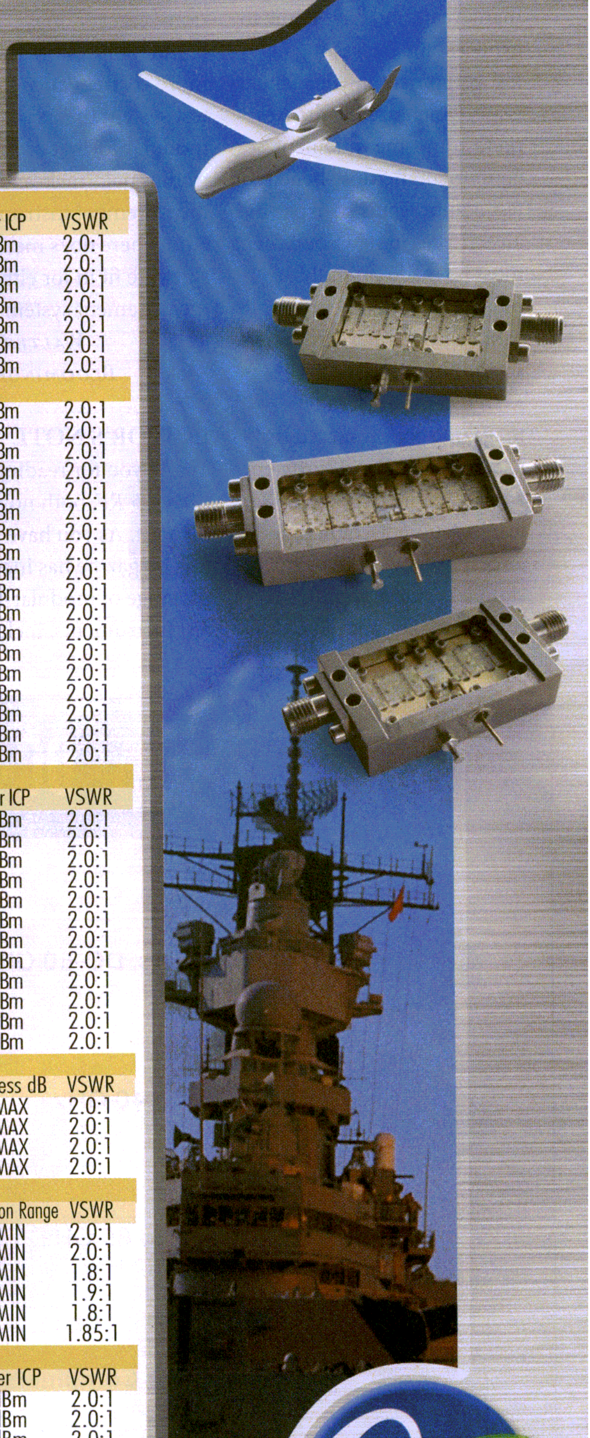

OCTAVE BAND LOW NOISE AMPLIFIERS

Model No.	Freq (GHz)	Gain (dB) MIN	Noise Figure (dB)	Power-out @ P1-dB	3rd Order ICP	VSWR
CA01-2110	0.5-1.0	28	1.0 MAX, 0.7 TYP	+10 MIN	+20 dBm	2.0:1
CA12-2110	1.0-2.0	30	1.0 MAX, 0.7 TYP	+10 MIN	+20 dBm	2.0:1
CA24-2111	2.0-4.0	29	1.1 MAX, 0.95 TYP	+10 MIN	+20 dBm	2.0:1
CA48-2111	4.0-8.0	29	1.3 MAX, 1.0 TYP	+10 MIN	+20 dBm	2.0:1
CA812-3111	8.0-12.0	27	1.6 MAX, 1.4 TYP	+10 MIN	+20 dBm	2.0:1
CA1218-4111	12.0-18.0	25	1.9 MAX, 1.7 TYP	+10 MIN	+20 dBm	2.0:1
CA1826-2110	18.0-26.5	32	3.0 MAX, 2.5 TYP	+10 MIN	+20 dBm	2.0:1

NARROW BAND LOW NOISE AND MEDIUM POWER AMPLIFIERS

Model No.	Freq (GHz)	Gain (dB) MIN	Noise Figure (dB)	Power-out @ P1-dB	3rd Order ICP	VSWR
CA01-2111	0.4 - 0.5	28	0.6 MAX, 0.4 TYP	+10 MIN	+20 dBm	2.0:1
CA01-2113	0.8 - 1.0	28	0.6 MAX, 0.4 TYP	+10 MIN	+20 dBm	2.0:1
CA12-3117	1.2 - 1.6	25	0.6 MAX, 0.4 TYP	+10 MIN	+20 dBm	2.0:1
CA23-3111	2.2 - 2.4	30	0.6 MAX, 0.45 TYP	+10 MIN	+20 dBm	2.0:1
CA23-3116	2.7 - 2.9	29	0.7 MAX, 0.5 TYP	+10 MIN	+20 dBm	2.0:1
CA34-2110	3.7 - 4.2	28	1.0 MAX, 0.5 TYP	+10 MIN	+20 dBm	2.0:1
CA56-3110	5.4 - 5.9	40	1.0 MAX, 0.5 TYP	+10 MIN	+20 dBm	2.0:1
CA78-4110	7.25 - 7.75	32	1.2 MAX, 1.0 TYP	+10 MIN	+20 dBm	2.0:1
CA910-3110	9.0 - 10.6	25	1.4 MAX, 1.2 TYP	+10 MIN	+20 dBm	2.0:1
CA1315-3110	13.75 - 15.4	25	1.6 MAX, 1.4 TYP	+10 MIN	+20 dBm	2.0:1
CA12-3114	1.35 - 1.85	30	4.0 MAX, 3.0 TYP	+33 MIN	+41 dBm	2.0:1
CA34-6116	3.1 - 3.5	40	4.5 MAX, 3.5 TYP	+35 MIN	+43 dBm	2.0:1
CA56-5114	5.9 - 6.4	30	5.0 MAX, 4.0 TYP	+30 MIN	+40 dBm	2.0:1
CA812-6115	8.0 - 12.0	30	4.5 MAX, 3.5 TYP	+30 MIN	+40 dBm	2.0:1
CA812-6116	8.0 - 12.0	30	5.0 MAX, 4.0 TYP	+33 MIN	+41 dBm	2.0:1
CA1213-7110	12.2 - 13.25	28	6.0 MAX, 5.5 TYP	+33 MIN	+42 dBm	2.0:1
CA1415-7110	14.0 - 15.0	30	5.0 MAX, 4.0 TYP	+30 MIN	+40 dBm	2.0:1
CA1722-4110	17.0 - 22.0	25	3.5 MAX, 2.8 TYP	+21 MIN	+31 dBm	2.0:1

ULTRA-BROADBAND & MULTI-OCTAVE BAND AMPLIFIERS

Model No.	Freq (GHz)	Gain (dB) MIN	Noise Figure (dB)	Power-out @ P1-dB	3rd Order ICP	VSWR
CA0102-3111	0.1-2.0	28	1.6 Max, 1.2 TYP	+10 MIN	+20 dBm	2.0:1
CA0106-3111	0.1-6.0	28	1.9 Max, 1.5 TYP	+10 MIN	+20 dBm	2.0:1
CA0108-3110	0.1-8.0	26	2.2 Max, 1.8 TYP	+10 MIN	+20 dBm	2.0:1
CA0108-4112	0.1-8.0	32	3.0 MAX, 1.8 TYP	+22 MIN	+32 dBm	2.0:1
CA02-3112	0.5-2.0	36	4.5 MAX, 2.5 TYP	+30 MIN	+40 dBm	2.0:1
CA26-3110	2.0-6.0	26	2.0 MAX, 1.5 TYP	+10 MIN	+20 dBm	2.0:1
CA26-4114	2.0-6.0	22	5.0 MAX, 3.5 TYP	+30 MIN	+40 dBm	2.0:1
CA618-4112	6.0-18.0	25	5.0 MAX, 3.5 TYP	+23 MIN	+33 dBm	2.0:1
CA618-6114	6.0-18.0	35	5.0 MAX, 3.5 TYP	+30 MIN	+40 dBm	2.0:1
CA218-4116	2.0-18.0	30	3.5 MAX, 2.8 TYP	+10 MIN	+20 dBm	2.0:1
CA218-4110	2.0-18.0	30	5.0 MAX, 3.5 TYP	+20 MIN	+30 dBm	2.0:1
CA218-4112	2.0-18.0	29	5.0 MAX, 3.5 TYP	+24 MIN	+34 dBm	2.0:1

LIMITING AMPLIFIERS

Model No.	Freq (GHz)	Input Dynamic Range	Output Power Range Psat	Power Flatness dB	VSWR
CLA24-4001	2.0 - 4.0	-28 to +10 dBm	+7 to +11 dBm	+/- 1.5 MAX	2.0:1
CLA26-8001	2.0 - 6.0	-50 to +20 dBm	+14 to +18 dBm	+/- 1.5 MAX	2.0:1
CLA712-5001	7.0 - 12.4	-21 to +10 dBm	+14 to +19 dBm	+/- 1.5 MAX	2.0:1
CLA618-1201	6.0 - 18.0	-50 to +20 dBm	+14 to +19 dBm	+/- 1.5 MAX	2.0:1

AMPLIFIERS WITH INTEGRATED GAIN ATTENUATION

Model No.	Freq (GHz)	Gain (dB) MIN	Noise Figure (dB)	Power-out @ P1-dB	Gain Attenuation Range	VSWR
CA001-2511A	0.025-0.150	21	5.0 MAX, 3.5 TYP	+12 MIN	30 dB MIN	2.0:1
CA05-3110A	0.5-5.5	23	2.5 MAX, 1.5 TYP	+18 MIN	20 dB MIN	2.0:1
CA56-3110A	5.85-6.425	28	2.5 MAX, 1.5 TYP	+16 MIN	22 dB MIN	1.8:1
CA612-4110A	6.0-12.0	24	2.5 MAX, 1.5 TYP	+12 MIN	15 dB MIN	1.9:1
CA1315-4110A	13.75-15.4	25	2.2 MAX, 1.6 TYP	+16 MIN	20 dB MIN	1.8:1
CA1518-4110A	15.0-18.0	30	3.0 MAX, 2.0 TYP	+18 MIN	20 dB MIN	1.85:1

LOW FREQUENCY AMPLIFIERS

Model No.	Freq (GHz)	Gain (dB) MIN	Noise Figure dB	Power-out @ P1-dB	3rd Order ICP	VSWR
CA001-2110	0.01-0.10	18	4.0 MAX, 2.2 TYP	+10 MIN	+20 dBm	2.0:1
CA001-2211	0.04-0.15	24	3.5 MAX, 2.2 TYP	+13 MIN	+23 dBm	2.0:1
CA001-2215	0.04-0.15	23	4.0 MAX, 2.2 TYP	+23 MIN	+33 dBm	2.0:1
CA001-3113	0.01-1.0	28	4.0 MAX, 2.8 TYP	+17 MIN	+27 dBm	2.0:1
CA002-3114	0.01-2.0	27	4.0 MAX, 2.8 TYP	+20 MIN	+30 dBm	2.0:1
CA003-3116	0.01-3.0	18	4.0 MAX, 2.8 TYP	+25 MIN	+35 dBm	2.0:1
CA004-3112	0.01-4.0	32	4.0 MAX, 2.8 TYP	+15 MIN	+25 dBm	2.0:1

CIAO Wireless can easily modify any of its standard models to meet your "exact" requirements at the Catalog Pricing.

Visit our web site at www.ciaowireless.com for our complete product offering.

Ciao wireless

Ciao Wireless, Inc. 4000 Via Pescador, Camarillo, CA 93012

Tel (805) 389-3224 Fax (805) 389-3629 sales@ciaowireless.com

MEASURING ADVANCES IN TEST GEAR

I have read your magazine for many years and have come to expect some interesting new test equipment in your January issue, which usually focuses on test-and-measurement equipment. Because bench top test equipment is so expensive, any choices in new equipment must be made carefully. It must serve a number of applications for many years to help spread the cost over time.

In recent years, your magazine has promoted the use of modular measurement equipment like VXI and PXI test instruments, although the largest number of instrument suppliers still support traditional rack-mount test instruments. For companies faced with making commitments to different measurement functions, can you make a recommendation on whether it is more cost-effective to build a test system that is based on a modular format or to stay with traditional, "rack-and-stack" measurement instruments? And where does measurement software fit in for either type of measurement system solution?

Walter Murphy
Bloomingburg, NY

EDITOR'S NOTE

Thank you for reading *Microwaves & RF*, both now and in the past. As you have noted, this magazine has increased its coverage of modular-format test instruments, including PXI and VXI instruments, as the functionality of such instruments has increased. Still, big differences between traditional bench top instruments—such as rack-mount signal generators, spectrum analyzers, and vector network analyzers (VNAs)—and newer modular solutions lie in functionality, bandwidth, and measurement range.

For applications well into the millimeter-wave frequency range (about 30 GHz), for example, the number of choices in the form of modular instruments is extremely limited. The greatest number of instrument choices is still in the form of traditional rack-mount bench top instruments. Although modular instruments provide a certain amount of flexibility and portability, they also suffer challenges in terms of establishing required electromagnetic-interference (EMI) and radio-frequency-interference (RFI) shielding levels.

Many companies and businesses also prefer knowing that a measurement system can be bolted into a 19-in. rack and established as a semi-permanent solution, rather than having test gear that is readily portable (such as a PXI or VXI-based instrument). Still, the functionality of modular instruments is improving, and it is probably just a matter of time before more test instruments will be available in modular formats.

50Ω Matched Input 30MHz to 6GHz Mixer

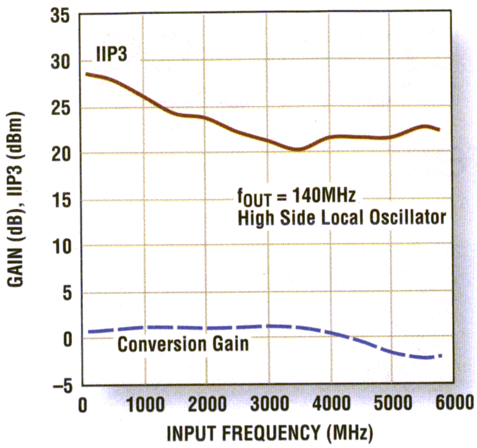

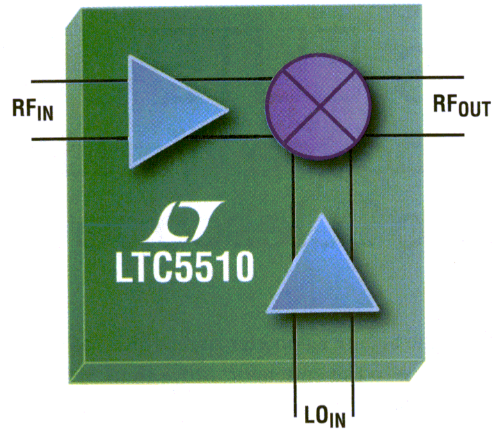

Excellent Dynamic Range, High Port-to-Port Isolation

The LTC®5510's continuous 50Ω matched inputs and high IIP3 from 30MHz to 6GHz set a new level of performance for ultra-wideband scanning receivers, broadcast radios, VHF and white-space receivers, wireless microphone receivers, public safety radios, cable infrastructure receivers and RF test instrumentation. The device's up or downconversion capability provides flexibility while its excellent isolation performance simplifies your design.

Signal Chain Components

Mixer	LTC5567	+26.9dBm IIP3, 1.9dB Gain Mixer	Detector	LTC5582	10GHz, 57dB Dynamic Range RMS Detector
	LTC5569	Dual +26.8dBm IIP3, Low Power Mixer		LTC5587	6GHz 40dB Dynamic Range RMS Detector + ADC
Amplifier	LTC6430-15	+50dBm OIP3 @240MHz, 15dB Gain Differential Amplifier	VGA	LTC6412	31dB Gain Control, Analog VGA with +35dBm OIP3
	LTC6431-15	+47dBm OIP3 @240MHz, 15dB Gain Single-Ended Amplifier		LT®5554	16dB Gain Control, 0.125dB/Step Digital VGA
ADC	LTC2158-14	Dual 14-Bit, 310Msps ADC	Oscillator	LTC6946	Low Phase Noise Integer-N PLL + VCO
	LTC2209	16-Bit, 160Msps ADC		LTC6945	Low Phase Noise Integer-N PLL

Info & Free Samples

www.linear.com/product/LTC5510

1-800-4-LINEAR

Free Wireless Solutions Brochure

www.linear.com/wireless

LINEAR TECHNOLOGY

News

RF's ELITE JOIN FORCES

Behind the World's Largest Radio Telescope

Calling the Square Kilometer Array (SKA) a "project" doesn't do justice to the endeavor. More than 350 scientists and engineers—representing 18 nations and nearly 100 institutions—are currently on track to construct what will be the world's largest radio telescope. Founded in 2011, the SKA Organization (www.skatelescope.org) has now designated several teams to work on separate parts of the telescope, which will eventually come together like pieces of a giant jigsaw puzzle. In the process, they will have to overcome many challenges.

With a total collecting area of approximately one square kilometer, the array will operate over a wide range of frequencies with 50 times more sensitivity than other radio instruments. Such operation will be accomplished through the completion of designated modules or "Work Packages." These RF-centric packages include a dish with phased-array feeds (DSH), a low-frequency aperture array (LFAA), a mid-frequency aperture array (MFAA), and wideband single-pixel feeds (WBSPFs).

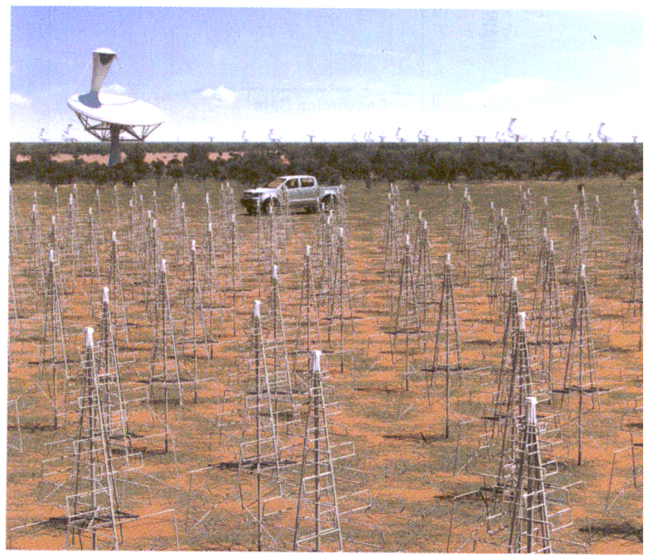

1. An artistic rendition of the low-frequency-aperture-array in Australia shows the hundreds of thousands of dipole antennas that will survey the radio sky in frequencies as low as 50 MHz. 9All images courtesy of the SKA Organization.)

The DSH performs all of the necessary activities to prepare for the procurement of the SKA dishes. Examples include local monitoring and control of the individual dish in pointing and other functionality as well as the SKA dishes' feeds, necessary electronics, and local infrastructure. The team also is tasked with the design and verification of the antenna structure, optics, feed suites, and receivers. The SKA organization describes the greatest challenge for the DSH group as the mass production of several thousand 15-m-wide telescopes with identical performance characteristics. The building of these telescopes required fresh design ideas, keeping in mind the ability to tolerate the harsh desert conditions in which they will operate.

The dishes will be deployed during the second phase of the SKA's construction. They will cover the highest-frequency radio signals being observed—up to 20 GHz. Because the dish is the only one of the SKA's radio receiver types that will have large moving parts, the levels of accuracy needed during steering are extremely high.

In the process of developing the SKA dishes, three prototype antennas are currently being built: DVA-1 in Canada, DVA-C in China, and MeerKAT-1 in South Africa. A single-pixel-feed (SPF) work group will combine feed elements, orthomode transducers (OMTs), and low-noise amplifiers (LNAs) to receive the astronomical radio signals. A phased-array-feed (PAF) work element will incorporate the design of the PAFs, or radio cameras, for the three SKA PAF bands. Those working on the PAF will conduct on-antenna tests of the various arrays in order to determine which type of feed element provides the best performance. They also will investigate the integration of LNAs, analog-to-digital converters (ADCs),

2. SKA dishes in operation, as seen in an artist's rendition.

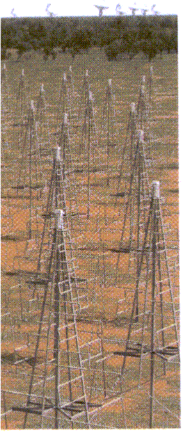

and high-speed data links for an on-antenna digitization scheme. This could potentially reduce the cost, weight, and power consumption of the array.

The LFAA package will cover the SKA's lowest frequency band of 50 to 350 MHz. It will incorporate the antennas, onboard amplifiers, and local processing required of the SKA's aperture-array telescope. It also includes the design of the local-station signal processing and hardware, which is required to combine the antennas and transport antenna data to the station for processing.

3. The mid-frequency aperture array module in Africa is shown here in an artist's rendering.

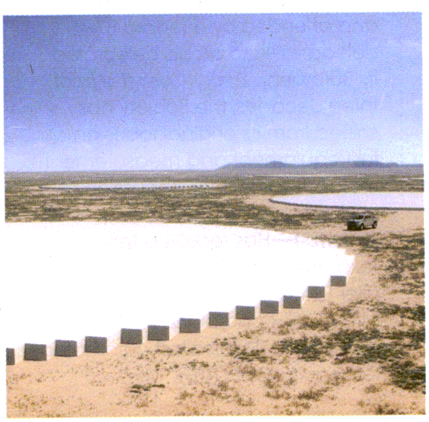

The LFAA package will comprise over a quarter million wide-bandwidth antennas of identical design. This large number of antennas will pose a major obstacle for designers, as testing will need to ensure the longevity of the design and its ability to be replicated exactly. The configuration is very tightly packed with 75% of the antennas within a 2-km diameter core. The remaining collecting area is situated on three spiral arms. They extend out to a radius of 50 km, thereby enabling higher-spatial-resolution observations.

The MFAA module involves the activities necessary for the development of antennas, amplifiers, and processing for frequencies of 400 MHz and upward. This fully sampled field of view situates the array effectively as a 10-gigapixel, ultra-wide-field spectroscopic camera. It will measure the effects of dark energy on the universe in addition to completing high-speed surveys for pulsars and other radio-transient events. To detect very small variations in the observed signals, the antennas will have to be highly sensitive.

WIDEBAND SINGLE-PIXEL FEEDS

Complementing the DSH group's SPF work, the WBSPF group will develop a single-pixel feed for the SKA that covers the broadest possible spectrum. While traditional radio-astronomy receivers only cover approximately a factor of two in frequency, WBSPF technology can potentially cover a range of four to eight. This will be accomplished by the development of new wideband forms of feed (i.e., the metal structures placed at the focal point of the radio telescope dish, which guide the radio waves to the electronics that detect them). As that feed is developed, new wide-frequency-band electronic components also will be designed, such as wideband LNAs.

The wideband receivers could be used to reduce the number of receiver systems on each telescope. Those systems are needed to cover the SKA's frequency range. Alternatively, the receivers could be utilized to expand the SKA's frequency range beyond the current baseline specification. Reducing the number of receivers has the potential to greatly reduce the cost per antenna for receiver (in terms of both capital and operational costs). By combining the WBSPF feeds with higher-capacity data links to the central processor, however, the design team would allow simultaneous processing of data over multiple spectral lines. Higher sensitivities could then be reached on astronomical objects radiating broadband emissions, greatly reducing observation time.

It will be a while before the SKA is fully functional; its first power-on isn't expected until 2020. But with such exciting performance estimates as "the data collected by the SKA in a single day would take nearly two million years to play back on an iPod," the world's largest radio telescope has the potential to be a major game changer—with each of its many parts an engineering feat on its own. ■

SMALL-CELL DEPLOYMENT Boosts Semiconductor Market

SMALL CELLS ARE proving to be a viable solution for boosting network capacity at a lower cost than the equivalent macro capacity. As a result, the semiconductor market for these applications is experiencing rapid growth. While the small-cell market is expected to expand quickly through 2018, however, Mobile Experts has revealed that the supporting system-on-a-chip (SoC), transceiver, and power-amplifier (PA) market will grow even faster.

Small-cell technology, which leverages both cellular and WiFi as well as a flat Internet-protocol (IP) architecture, helps offload data from macro networks as the demand for better rates increases. As mobile network operators (MNOs) attempt a variety of solutions, small cells have proven practical for target areas where people congregate outdoors (when placed on physical infrastructures) and in indoor areas to improve the offloading of traffic (such as homes, offices, and shopping malls).

The firm's market study provides an analysis of large-scale deployments of small cells in Korea and Japan, noting in particular the capacity and cost implications of small cells in a dense urban network. With more than 100,000 indoor hotspot units deployed in Korea using femtocell technology, operators have significantly boosted capacity affordably.

The report offers profiles of key suppliers and details of market shares for semiconductor vendors within the industry as well. Among the companies highlighted is Broadcom, which recently debuted the BCM61630 SoC. This integrated digital baseband processor and RF transceiver is designed for 3G small-cell base stations and femtocell residential access points. As a second-generation wideband-code-division-multiple-access (W-CDMA) SoC, it integrates a complementary-metal-oxide-semiconductor (CMOS) device and has high-speed packet-access data rates with throughput to 21.6 Mb/s. An enterprise version of the device is available for a larger number of users. ■

MACOM ACQUIRES MINDSPEED TECHNOLOGIES

THE SEMICONDUCTOR MAKER Mindspeed Technologies has been a prominent name in wireless communications since the earliest days of heterogeneous networks (HetNets). Now, the small-cell-focused company has become part of MACOM. MACOM has completed a tender offer to purchase all outstanding shares of Mindspeed Technologies. Common stock shares went for $5.05 per share in cash.

MACOM hopes that this acquisition will bolster its standing in the market for high-performance-analog (HPA) solutions for high-speed networking and enterprise applications. Mindspeed's portfolio includes: baseband processors, carrier Ethernet devices, optical laser drivers, customer-premise-equipment (CPE) processors, serial-digital-interface (SDI) cable drivers, and legacy devices, among others. Together with Avago Technologies, Mindspeed also demonstrated a 12-channel, ultra-high-definition serial-digital-interface (UHD-SDI) solution targeting 8K UHDTV broadcast-video applications. The real-time uncompressed 8K video ran at 120 fps over a 100-m optical-fiber cable.

MACOM plans to leverage Mindspeed's high-margin HPA portfolio in order to grow its market share. An agreement was also announced that Mindspeed's wireless-infrastructure business will be divested to Intel Corp. As a result of the merger, Mindspeed's common stock will no longer be listed and traded on the NASDAQ global market. ■

KUDOS

ARMMS RF & MICROWAVE SOCIETY—At its April meeting—sponsored by Teledyne Microwave Solutions and attended by a record 87 delegates—the group celebrated its 30th anniversary. Over the past three decades, the Society has shifted from its original focus on test equipment and measurement methods to a wider discussion of engineering topics.

ADVANTEST—Has received the Texas Instruments (TI) 2012 Supplier Excellence Award. Advantest's M4841 pick-and-place test handler is utilized in TI's installed automated test equipment (ATE).

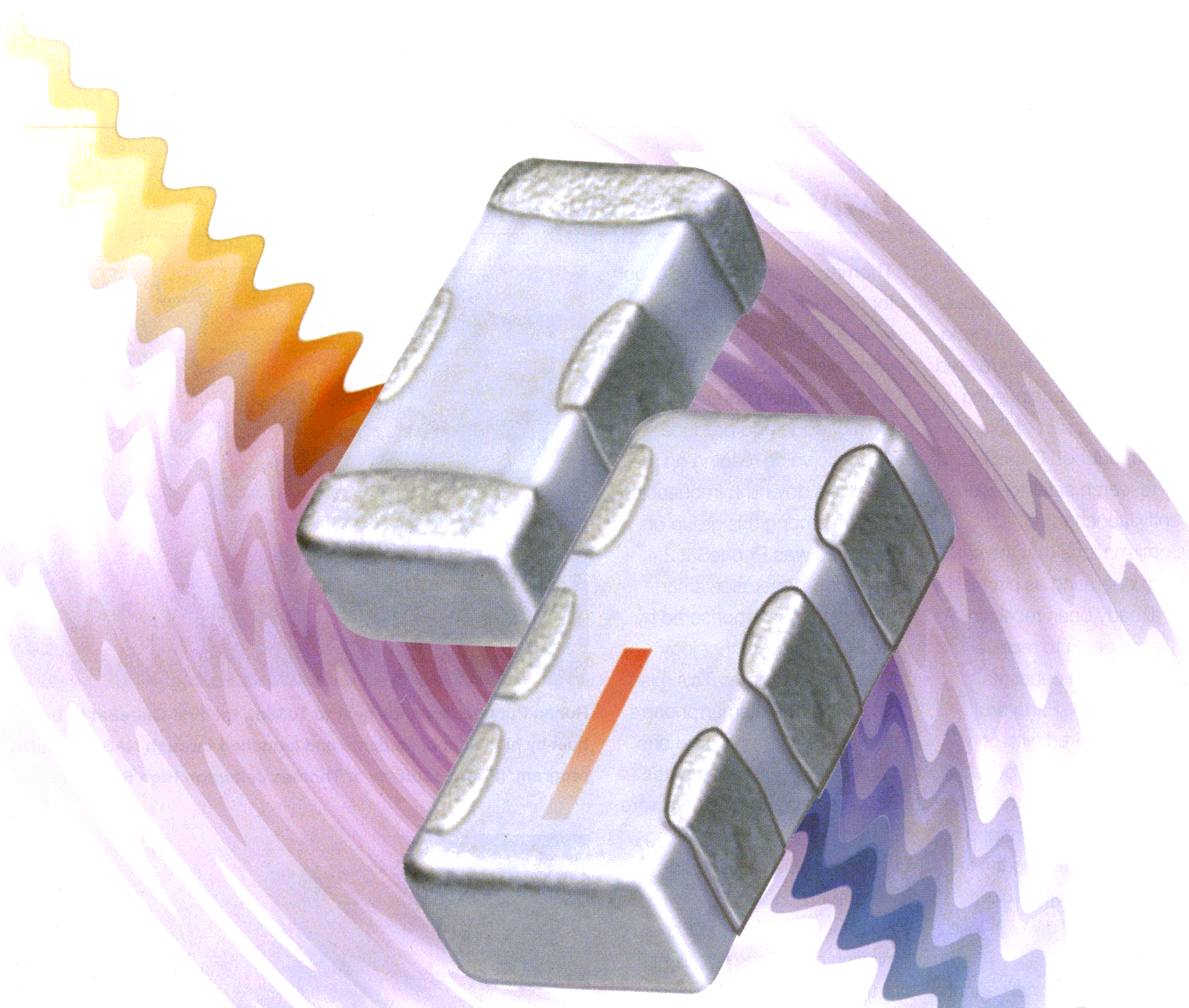

NASA CUBESAT INITIATIVE Launches Student-Built Satellites

AN ONGOING NASA initiative aims to help students discover the excitement of space exploration while confronting related technology and engineering challenges. As part of this program, dubbed CubeSat, 11 small research satellites were recently launched.

Confirmations that the satellites are operating as planned have already been received. As the teams begin to receive signals from the cubesats, which are in low-Earth orbit, they will be tasked with confirming activation and other normal operations of the nanosatellites. The cube-shaped satellites measure about 4 in. on each side, have a volume of about 1 qt., and weigh less than 3 lbs.

NASA's Educational Launch of Nanosatellite (ELaNa) missions, which are conducted under the CubeSat initiative, give students, teachers, and faculty hands-on experience developing flight hardware. In the process, they gain access to a low-cost avenue for research. Cubesats from nine universities, a NASA center, and a high school were launched. The TJ3 Sat from Thomas Jefferson High School for Science and Technology in Alexandra, Va., contains a voice synthesizer module that will take written phrases in the form of code and produce a phonetic voice reading on the satellite's downlink frequencies.

Also among this group of launches was PhoneSat 2.4, a second-generation smartphone cubesat sponsored by NASA's Space Technology Mission Directorate. This mission will test the smartphone's viability as a communications technology for nanosatellites while verifying that its hardware can manage pointing, taking images, and executing software appropriately.

Notably, the fourth ELaNa mission marks the first flight of the Nanosatellite Launch Adapter System (NLAS), a satellite deployment system built by Ames. NLAS is capable of carrying approximately 100 lbs. of secondary payloads into orbit. It also can accommodate various configurations of cubesats. Groups can participate in the program by submitting a proposal to NASA for what they want to accomplish with their cubesat. ■

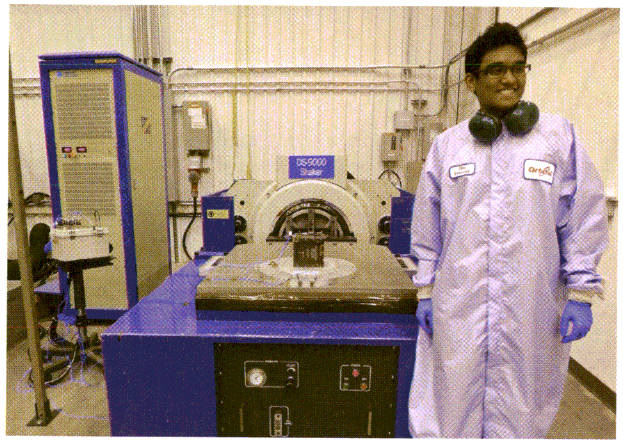

Rohan Punnoose stands next to TJ3Sat, the first CubeSat to be built by high school students and launched through NASA's ELaNA program. (Photo courtesy of Thomas Jefferson High School.)

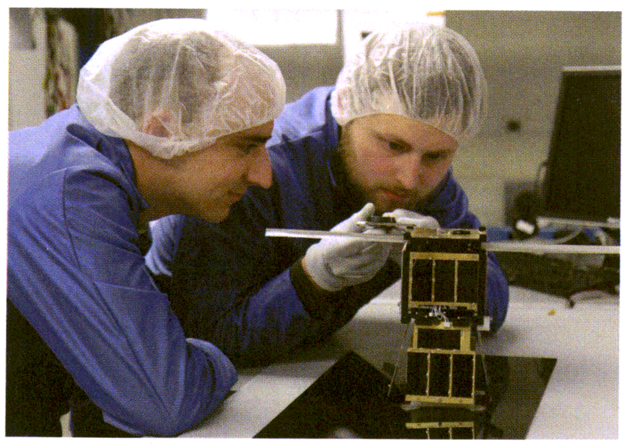

University of Kentucky students Alex Clements and Jason Rexroat conduct final CubeSat acceptance measurements on KYSat-2, a collaborative project between the University of Kentucky and Morehead State University. (Photo courtesy of University of Kentucky.)

PEOPLE

QUALCOMM—Steve Mollenkopf has been named chief executive officer and a member of the firm's board of directors. He will continue to serve in his present role as company president. In addition, Dr. Paul E. Jacobs is assuming the role of executive chairman. Finally, Vice Chairman Steve Altman is retiring from Qualcomm. He will serve as a strategic consultant to the company.

ALTMAN

RAYTHEON CO.— Rebecca R. Rhoads was named president of the company's Global Business Services group. Rhoads will continue on as the company's chief information officer.

RHOADS

AT&T GOVERNMENT SOLUTIONS (AGS)— Paul Girardi was named vice president, business development. In addition, Stacy Schwartz has been named vice president, public safety.

VERIZON—Shellye Archambeau, CEO of MetricStream, was elected to the board of directors.

CONTRACTS

Lockheed Martin— Has been selected by the Mars One Foundation to develop a mission concept study for its Mars lander spacecraft. The lander will be based on the successful 2007 NASA Phoenix spacecraft and will be a technology demonstrator. Slated for a 2018 launch, the mission will provide proof of concept for some of the technologies necessary to establish a permanent human settlement on Mars—the ultimate goal of the foundation. In addition, Lockheed Martin has been awarded more than $200 million in contract options by the U.S. Air Force to complete production of its fifth and sixth next-generation Global Positioning System satellites, known as GPS III.

LOCKHEED MARTIN Scores Mars One, Air Force Deals

RAYTHEON Awarded $12.9-million modification

Comtech Telecommunications Corp.—The firm's Santa Clara, Calif.-based subsidiary, Comtech Xicom Technology Inc., has received an order for approximately $7 million from a unidentified traveling-wave-tube-amplifier (TWTA) system integrator. The order relates to a U.S. Army Satellite Communications program.

Raytheon Co.—Has been awarded a $12.9 million modification to a previously awarded contract to exercise options for Cooperative Engagement Capability (CEC) for the AN/USG-2B Shipboard System and three planar array antenna assembly systems. The firm has also started building the 12th AN/TPY-2 ballistic missile defense radar for the Missile Defense Agency after being awarded a $172.7 million contract, which was previously announced by the Department of Defense in December 2013.

FRESH STARTS

Alliance for Wireless Power (A4WP)—Has debuted Rezence, a new consumer-facing brand that will act as the official name for the organization's wireless power technology. The official launch of the A4WP product certification program is targeted for the end of this year.

Boeing—Will restructure its Boeing Research & Technology organization, the company's central research-and-development unit, through the establishment of research centers in Huntsville, Ala.; Southern California; St. Louis, Mo.; North Charleston, S.C.; and Seattle. The international centers conduct research to benefit the environment, aviation safety, air traffic management, and other areas.

AR—Has broken ground on a major expansion project at its headquarters in Souderton, Pa. The expansion will add a two-story, 10,000-sq. ft. addition and give AR the capabilities to manufacture and test high-power amplifiers in excess of 100 kW.

San-tron—Has achieved AS9100 certification, ensuring safety and reliability of the firm's products used throughout the aerospace product market.

Elbit Systems—Has been selected by the U.S. Department of Homeland Security's Science & Technology Group to provide a technology demonstrator for a secure broadband services solution for first responders. The solution will be based on capabilities developed in Elbit Systems' Land and C4I division, and will incorporate the BlackBerry10 secure workspace within an Android smartphone.

Precision Connector, Inc.—Has updated its website, adding new product sections for adapters, 1.0-mm, SMP, and SSMP connectors. A new PDF brochure was added specifically for cable connectors, making it easier to find and group connectors by cable manufacturer and type.

TRM Microwave—Has acquired Putnam RF Components' high-power product line.

Richardson RFPD—Has launched its SiC Tech Hub. The micro-website will feature news and product releases pertaining to silicon-carbide (SiC) technology. Industrial applications and a wide range of design sources will be featured.

Continua Health Alliance—China Mobile and Verizon Enterprise Solutions have joined the standards group. They join a roster of mobile members that including ATT, KDDI, Korea Telecom (KT), NTT DOCOMO - Mobile, NTT, Orange, Telefonica, Telus, and Vodafone.

Savant Systems—Has chosen GainSpan Wi-Fi technology for its new SmartLighting Wi-Fi control system. The system gives users lighting control and energy monitoring capability from a smartphone, and can be integrated without rewiring the home or commercial facility.

Tsinghua Unigroup Ltd. and Spreadtrum Communications, Inc.—Have completed a previously announced, approximately $1.7-billion merger between Spreadtrum and an affiliate of Tsinghua Unigroup.

Verizon Communications—Has received federal Communications Commision (FCC) approvals to acquire Vodafone's U.S. group. The principal asset is 45% of Verizon Wireless. In addition, Verizon has completed its purchase of wireless assets in rural Missouri from United States Cellular Corp. The purchase will expand Verizon Wireless' brand and network footprint south of St. Louis to the counties of Ste. Genevieve, St. Francois, and Washington.

Iridium Communications, Inc. and Wyless Inc.—Have joined the International M2M Council (IMC), a global organization that promotes the benefits of machine-to-machine communications (M2M). The IMC announced that both companies have become sustaining members of the London-based association, which was formed earlier this year by a group of influential solutions providers in the M2M industry.

Inside TRACK with Hatem Zeine

FOUNDER AND CEO OF OSSIA, INC.

Interview by JEAN-JACQUES DeLISLE

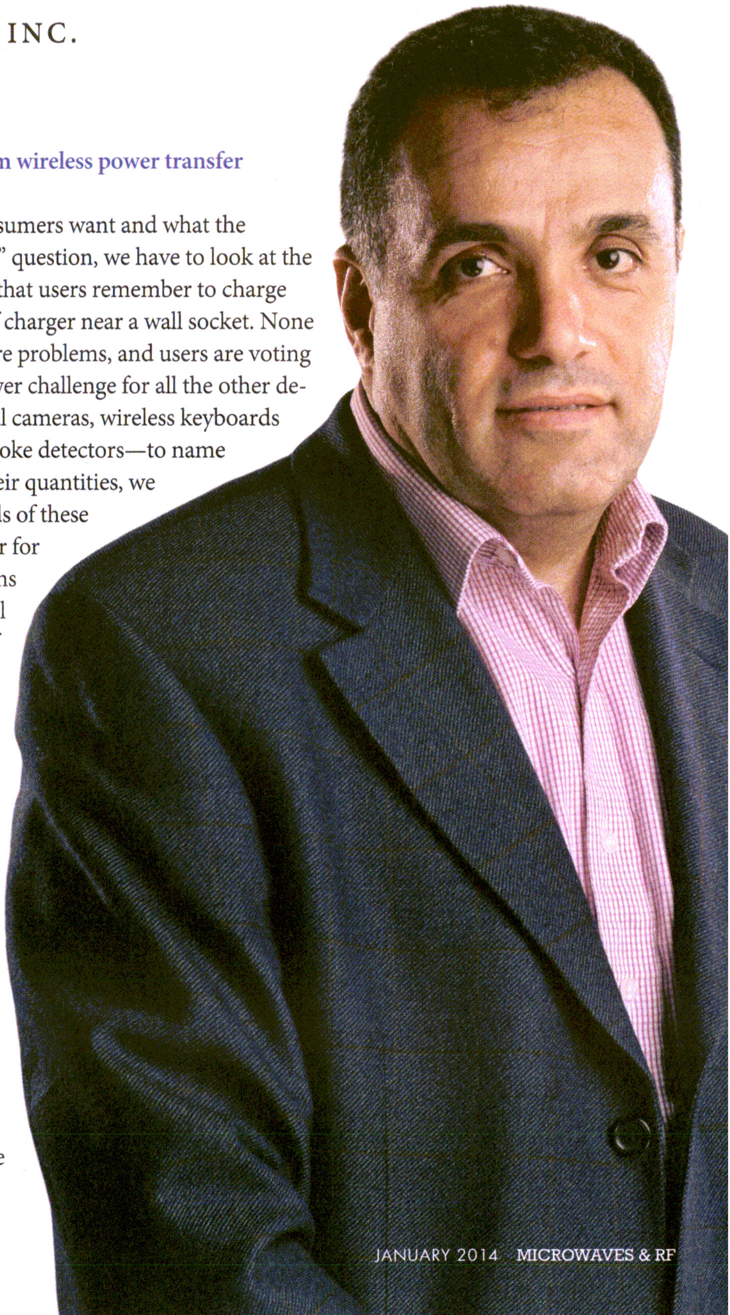

JD: What do you feel consumers are really looking for from wireless power transfer (WPT) technologies?

HZ: This question really has a couple of parts: what the consumers want and what the consumers will end up using/needing. To answer the "want" question, we have to look at the actual problems with our devices. First, cell phones require that users remember to charge their devices. In that process, users have to use some type of charger near a wall socket. None of today's available WPT technologies address these two core problems, and users are voting with their wallets. The "need" presents a larger wireless-power challenge for all the other devices and sensors we have in our life: remote controls, digital cameras, wireless keyboards and mice, tablets, game controllers, motion sensors, and smoke detectors—to name a few. Due to their distribution in our environments and their quantities, we need a radical new solution that can address the power needs of these devices. When we solve this challenge, we will open the door for a truly wireless world that enables all of the intriguing designs of what we call the "Internet of Things." In short, people will stop thinking of their devices' batteries and start thinking of unrestricted use of their devices instead.

JD: Why haven't WPT chargers for mobile devices been more successful?

HZ: Currently, people do not view a WPT charger as a utility. Most people find that the WPT chargers available today do not change their habits or device usage. The added value is not obvious when having a phone with a WPT charging pad, as we still end up needing to remember to charge the device. And when it is charging, it is away from us. The device is not any better in terms of size/weight/design, so the user barely perceives the gain. Remember that all of the market-available WPT chargers power devices at a distance of no more than an inch from a pad that is connected to a wall power socket.

We believe that remote wireless charging will change our habits when users never have to charge their devices because they are receiving power all the time. The devices will then need smaller batteries, hence better designs and use.

JD: Which frequency ranges do you think are the most viable for WPT implementations now and in the future?

HZ: The different use cases of WPT will demand different spectrum sections for us—especially when we consider loss of energy in transmission. Medium- (>20-W) to high-power (>1-kW) applications will inevitably need frequencies that are not absorbed by human flesh, as a mere 5% of power loss could amount to 700 W of power when charging an electric vehicle. This restricts WPT to frequencies below 50 MHz. The caveat of using such frequencies is that the energy cannot be focused at a distance, due to the long wavelength used in lieu of basketball-field-sized chargers. Low-power (<5-W) applications, such as cell phones, can leverage the same frequencies (<50 MHz). But they would restrict the charging distance to a charging pad. Remote power delivery will require a wavelength that can be focused with small transmitters. In addition, the power will have to be focused to a small (device-sized) region. Such wavelengths need to be a minimum of 1 in. to a maximum of 12 in., resulting in frequencies ranging from ~1 to ~12 GHz (give or take a few). Our remote wireless power uses the 2.4-GHz ISM band to deliver safe power at a distance of 30 ft.

JD: Do you feel that the main focus for WPT charging systems has been designed for a charging-pad approach?

HZ: The prevailing technology of wireless charging (which should be called "contactless charging") has been inductive coupling, as seen by electric toothbrushes from the late 1960s and early 1970s. The more recent innovations in magnetic resonance have extended the range of coil-based WPT. But it has not liberated the device from the charger. What we are seeing today is the resurgence of coil-based technology in the marketplace, offering short-range power to devices without attaching contacts. It was simply the only option available.

JD: What major hurdles are faced by companies looking to implement a WPT system?

HZ: I think the biggest obstacle is having enough engineering "manpower" to help make their concept a reality and get to market. Because WPT is an emerging technology, new and innovative engineering techniques are required. Additionally, a real wireless-power solution, such as the one that Ossia has developed with Cota, requires many complex design elements to achieve all of the functionality desired by users. Examples include a 30-ft. charging distance, non-line-of-sight, efficiency, and being able to scale the technology to the next level. Finding engineers with the right RF experience is often challenging, so we are always looking for engineers with this type of background.

JD: Is the major focus of WPT technologies on the commercial, industrial, or military sectors?

HZ: WPT serves all electronic devices, no matter what their application is. The most famous are smartphone chargers because there are so many smartphones and so much hassle with charging them. However, there are applications of wireless/contactless power transmission for industrial robotics, such as warehouse handheld scanners, that have just started being addressed. The tech companies supplying WPT will go where the money is. Where the smartphone market is concerned, it is really the 800-lb. gorilla in the room due to its fast churn and the vast financial resources that are available. We believe that our technologies will have a major impact on consumer devices as well as industrial sensors/controls, as both of these markets are reaching bottlenecks in technology advancement due to power availability.

JD: Does the congestion of electromagnetic interference (EMI) hamper WPT technologies?

HZ: As discussed earlier, different WPT technologies utilize different spectrum segments. All have to follow the guidance set by the FCC in the United States and international legislative bodies elsewhere. Thankfully, wireless power is almost by definition un-encoded.

JD: What are the safety concerns for WPT technologies, and how are they being addressed?

HZ: Safety concerns are paramount in the design of power systems—and even more so for wireless power systems, as the energy is not confined to the wires or components. The ability for the human body to absorb the energy presented by the WPT is a feature that impacts the maximum power levels. For instance, lower frequencies are absorbed less by human flesh. But the energy levels used are much higher, and a small percentage loss would be large and potentially harmful.

JD: Do you believe the WPT market will have room for both short-range and long-range solutions?

HZ: The short-range technologies underneath the wireless-charging consortiums have great value in some vertical markets, where proximity power delivery is of benefit. Examples include electric-vehicle charging and robotics. All of these consortiums continue to demonstrate the importance and need to rapidly adopt a wireless power solution. Yet I believe that this need goes far beyond simply charging a smartphone. It includes charging all types of devices throughout a home, which requires a longer-distance charging solution. In the end, we believe Cota-based systems will power the small devices while Rezence or similar technologies will power the larger, more power-hungry devices like blenders, toasters, and cars.

JD: What technological leap forward would be the most advantageous for WPT technologies?

HZ: We believe that delivering safe, focused, and remote power is a huge leap of utility for users in consumer or industrial markets. Once WPT enters the market, it will ignite the imagination of product designers everywhere. We will see devices that serve us throughout our environment ranging from intelligent door handles to self-heating cups, displays on "inanimate" objects, and feedback from every device. mw

MEGAHERTZ-RANGE WIRELESS-POWER-TRANSFER RECTIFIERS RESONANT TO REGULATE

AS MORE PRODUCTS are designed with wireless charging capability, resonant wireless-power-transfer (WPT) technology is increasingly present in the wireless market. Having faster and more reliable charge rates—while using less expensive or space-consuming electronics—is a major goal for this industry. At the Korea Advanced Institute of Science and Technology, Jun-Han Choi, Sung-Ku Yeo, Seho Park, Jeong-Seok Lee, and Gyu-Hyeong Cho designed and tested several resonant regulating rectifiers for enhanced WPT capability at 6.78 MHz.

On 0.35-micrometer bipolar-CMOS-DMOS (BCD) technology, the team is able to design RWPT circuits that can harvest power to 6 W at 86% efficiency using both the continuous conduction mode and discontinuous conduction mode. The proposed resonant-regulating-rectifier designs do not require an additional inductor for switch-mode regulation, as the resonant tanks are operated using phaser-transformed inductance. Only three switches are used in a rectifier design that achieves 6 W of transferable power.

Such a feat is impressive when compared to other resonant-regulating rectifier systems that have been reported, which have less than 1 W of available power at 13.56 MHz. See "Resonant Regulating Rectifiers (3R) Operating for 6.78 MHz Resonant Wireless Power Transfer (RWPT)," *IEEE Journal of Solid-State Circuits*, Dec. 2013, p. 2989.

UPGRADE FREQUENCY-SELECTIVE SURFACE FILTERS FROM 2D TO 3D

BY INCREASING THE selectivity and out-of-band rejection of bandpass filters for frequency-selective surfaces (FSSs), it is possible to enhance the operation of antenna subreflectors, radomes, and polarizers. Such an approach limits the signal-to-noise ratio (SNR) of the incoming RF signals. Most FSS bandpass filters exhibit low selectivity and unstable angular response. Although cascading enhances the filtering characteristics of these spatial filters, it is still difficult to design bandpass FSS filters to obtain wide out-of-band rejection and stable response under a large incidence angle variation.

Adding stubs, coupled lines, or electromagnetic (EM) bandgap structures can add transmission zeroes at finite frequencies. It is therefore possible to enhance the filtering characteristics of two-dimensional (2D) microstrip filters. Bo Li and Zhongxiang Shen of Nanyang Technological University, Singapore, have adopted this technique to design and test three-dimensional (3D) FSS structures with multiple transmission zeroes introduced at desired frequencies.

Using a modern RF substrate (Rogers 4230) and aluminum to fabricate a surface matrix of 30 × 27 unit cells, the team constructed a 3D FSS with T-type, T-shaped, resonant inserts. The 2D unit cells are fabricated on large printed-circuit boards (PCBs) and then cut into the unit cells. The FSS was tested under transverse-electric polarization with two incident angles.

The FSS was observed to be stable under the different incident angles with transmission poles at 7.9 and 8.4 GHz in the passband and transmission zeroes at 6.1, 10, and 17.9 GHz in the stopband. See "Three-Dimensional Bandpass Frequency-Selective Structures With Multiple Transmission Zeros," *IEEE Transactions on Microwave Theory and Techniques*, Oct. 2013, p. 3578.

SIMPLIFY RF IC TESTING WITH ON-CHIP THERMAL FAULT DETECTORS

TRADITIONALLY, IT HAS been difficult and costly to test RF integrated circuits (ICs) under large-scale manufacture. Attractive alternatives include built-in tests, where the testing operations are on-loaded to take place on the IC itself, or built-in self-tests. If non-invasive fault-detection systems could be integrated within the circuitry of the RF IC, for example, wafer-level, die-level, and chip-level testing could be simplified.

In Grenoble, France, a built-in, temperature-based, non-intrusive sensor for fault detection of a linear amplifier has been designed and tested by Louay Abdallah, Haralampos Stratigopoulos, Salvador Mir, and Josep Altet. The concept behind their temperature sensor is that minor changes from the target circuit's ideal operation will cause a different thermal profile than what is expected. This profile can then be monitored and reported on, as long as the thermal sensor is sufficiently robust.

For the temperature sensor, the designers used an open-loop, operational-transconductance amplifier that uses bipolar transistors in a differential configuration. Because the collector current of bipolar transistors has an exponential dependence on temperature, it is suited to applications in which temperature varying operation can occur. Using the two primary bipolar transistors in the differential topology causes a response in the output voltage. Such a response will be dependent upon the temperature, as long as one pair of the differential amplifier's bipolar transistors are placed near the circuit to be monitored while the other remains relatively isolated. The changes in the transistor's power dissipation in proximity to the monitored circuit vary with temperature. These changes allow for highly sensitive temperature readings. See "Defect-Oriented Non-Intrusive RF Test Using On-Chip Temperature Sensors," *2013 IEEE 31st VLSI Test Symposium*, April 2013.

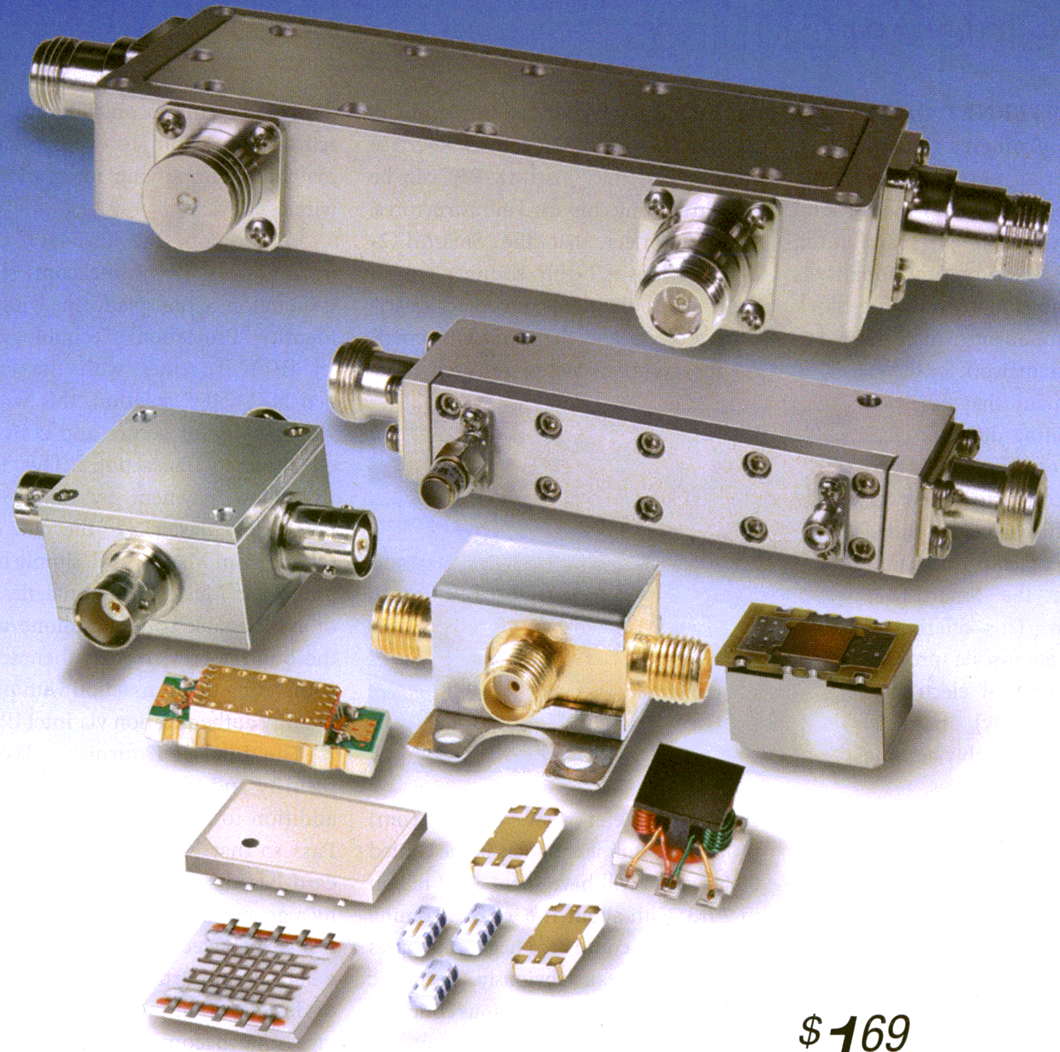

PAUL WHYTOCK | European Editor

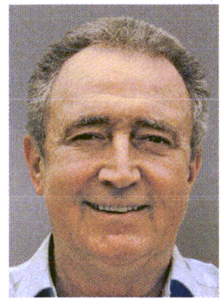

PAUL WHYTOCK

Maintaining Security For The Internet Of Things

THE INTERNET OF THINGS (IoT) promises that one day, almost all personal electronic devices will be connected wirelessly and able to communicate with each other. Of course, before such functionality is readily available, many building-block electronic components will be needed to establish the framework for the IoT.

One company that has been active in creating different electronic function blocks for it is NXP Semiconductors (www.nxp.com), which recently added to its lineup of chip microcontrollers with the SmartMX2-P40 platform. This offering is suitable for large-scale projects in the banking and electronic-government (eGov) markets, which will also inevitably become large parts of IoT activities.

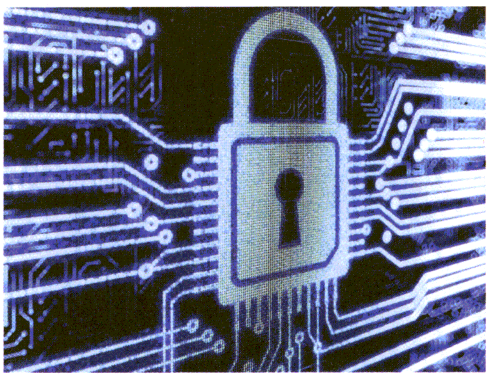

The device is part of NXP's big-picture approach to serving wireless business transactions and IoT services by ensuring electronic security and protection against wireless identity theft. The platform features a reduced-instruction-set-computing (RISC) MRK3-SC core and meets common criteria EAL5+ level certification via the company's Integral Security architecture. The chip microcontroller, which has been optimized for mass-market chip-card projects, is part of NXP's efforts to battle electronic crime (notably, efforts that are anticipated to come with the growth of the IoT).

The SmartMX2-P40 incorporates dedicated coprocessors for asymmetric RSA/ECC and symmetric DES/AES cryptography. It is equipped with a certified hardware abstraction layer (HAL) and crypto library for fast time-to-market. An ISO/IEC 7816 contact interface ensures that the SmartMX-P40 can be used in existing chip-card infrastructures.

NXP offers that the SmartMX2-P40 provides a highly secure platform dedicated to the needs of contact smart-card projects and their end customers. As the company notes, research firms such as eMarketer (www.emarketer.com) project that online shoppers in the United States alone will have spent $262 billion in 2013, with about 16% of that coming from mobile commerce (e.g., purchases on smartphones). Obviously, electronic and wireless security are serious concerns and important parts of design efforts for these wireless electronic devices.

NXP also recently announced that its PN544PC, a derivative of its popular near-field-communication (NFC) radio controller (model PN544), is being integrated into some new computing devices. The PN544, which features a communications distance to 10 cm, is based on an 8-b microprocessor architecture with 5 kb of random-access memory (RAM) and is a versatile component for many financial-functioned NFC card devices. The microcontroller includes a self-test function to verify antenna matching, simplifying integration into wireless devices.

In addition, the PN544PC builds upon Intel's (www.intel.com) Fourth Generation Core platform with Intel Identity Protection Technology (Intel IPT). Together with the embedded NXP NFC solution, this will provide a basis for secure and convenient e-commerce transactions. This feature will allow payment by online shoppers using MasterPass, the new digital service from MasterCard, simply by tapping their MasterCard contactless card or NFC-enabled mobile phone against the built-in NFC reader, then securely completing the transaction with positive identity authentication via Intel IPT.

The Intel IPT furnishes layers of security and identity authentication in addition to those provided by MasterPass so that NFC-enabled, contactless card-based transactions are protected by a generous amount of security functions. Such electronic security planning will be an important and necessary part of design for all present and future devices that become part of the IoT, especially those devices that will manage financial transactions.

Admittedly, while the wireless connection of electronic devices on the IoT will present additional problems in terms of possible jamming and interference, especially when devices are within range of each other and operating at similar frequencies and bandwidths, these security measures will help to minimize unwanted theft of identity and electronic financial information. mw

JEAN-JACQUES DELISLE | Technical Engineering Editor

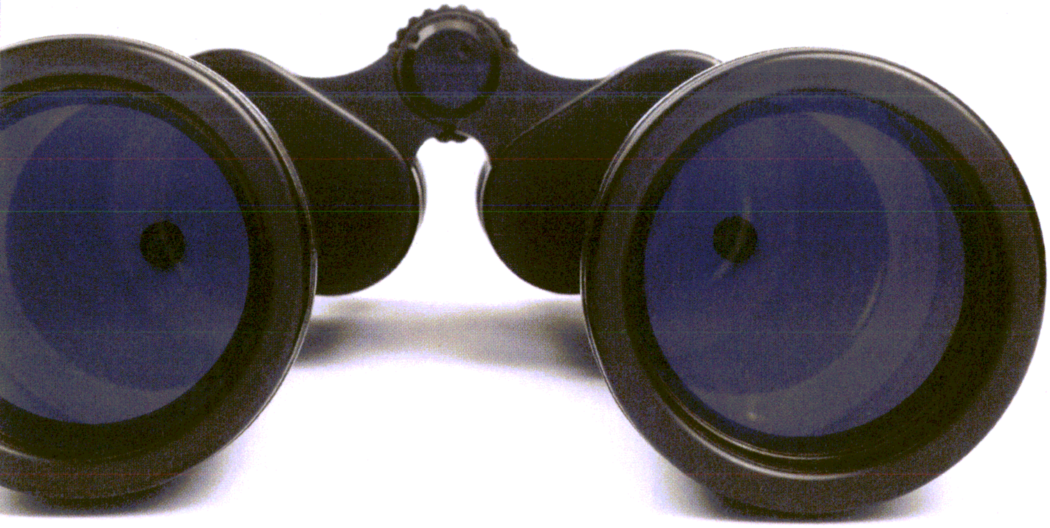

TECHNOLOGIES TO WATCH

Communications Inspires Technology Advances

FROM THE LATEST WIRELESS STANDARDS AND TEST EQUIPMENT TO CUTTING-EDGE PROCESS TECHNOLOGIES AND MODULATION APPROACHES, RF AND MICROWAVE FIRMS ARE LEADING AN EXCITING EVOLUTION WHILE PROVIDING SOME POSSIBLE GAME-CHANGING TECHNOLOGY APPROACHES.

In the microwave and RF arena, semiconductors, communications approaches, and the wireless standards they use are either the focus of research and development or the inspiration behind developments in other areas. Advances in RF semiconductors give designers access to higher frequencies, power, dynamic range, and lower noise parameters, enabling them to design the next generation of RF electronics.

Meanwhile, wireless standards provide a roadmap for companies and designers to coordinate their efforts and provide relevant technologies that are compatible with a changing and expanding infrastructure. Evolving communication techniques allow designers to cleverly use the present technology beyond previously thought boundaries, increasing range, throughput, and signal-to-noise ratio (SNR).

By focusing on new innovations and developments surrounding these pillars of the RF/microwave industry, it is

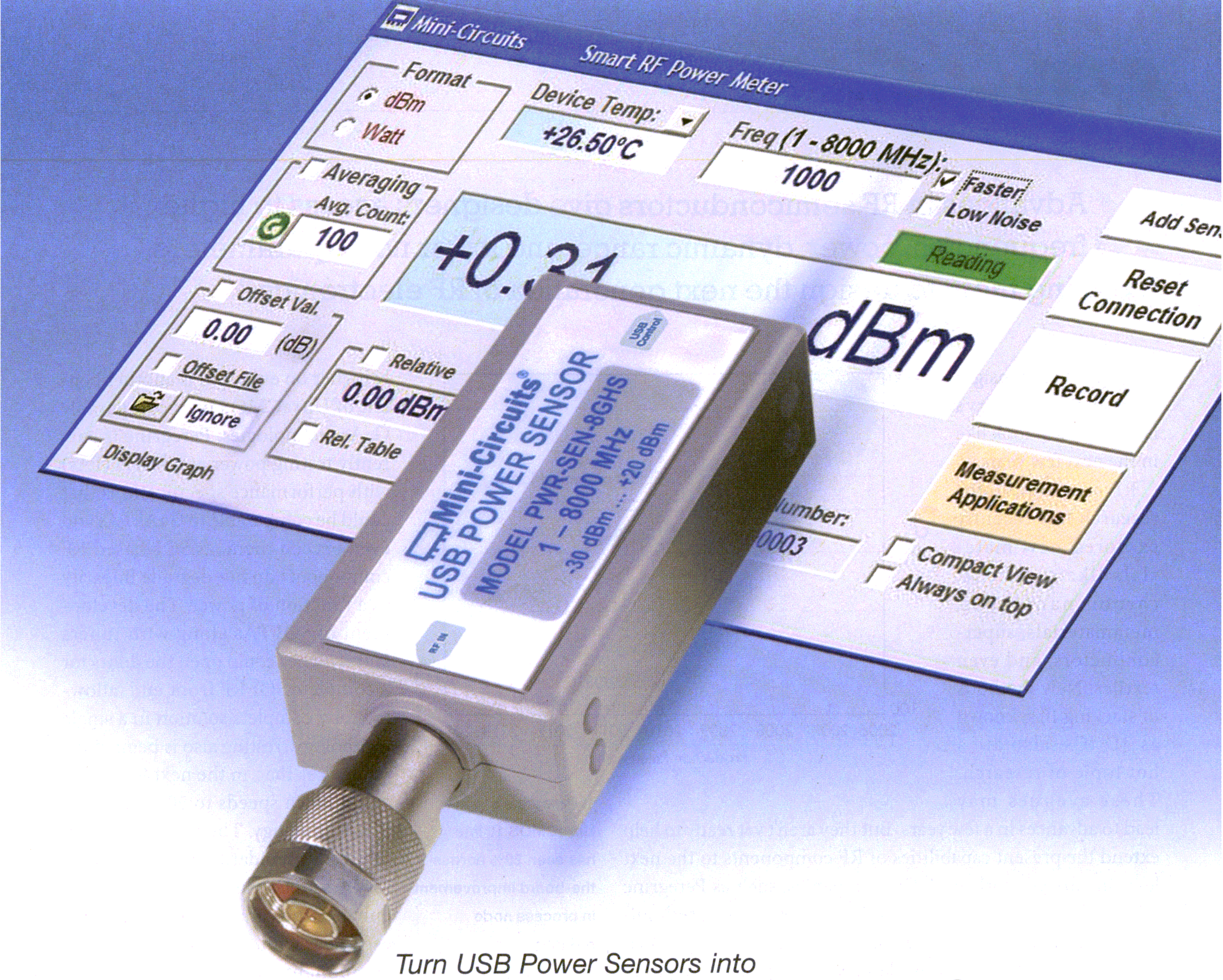

Turn USB Power Sensors into

Smart RF POWER METERS

from -35 up to +20 dBm 9 kHz to 8 GHz

• ***True RMS model now available!*** • *Lightning-fast measurement, as quick as 10 ms**
• *Compatible with most test software†* • *Up to 55 dB dynamic range* • *Measurement averaging*

Don't break your bank with expensive conventional power meters. Mini-Circuits USB Power Sensors turn almost any Linux® or Windows® based computer into a low-cost testing platform for all kinds of RF components. Reference calibration is built in, and your USB port supplies required power. Our GUI offers a full range of watt or dB measurements, including averaging, frequency sweeps, and multi-sensor support.

Our power sensors can be carried in your pocket, or mounted remotely for manual or automated system monitoring (internet connectivity required). Data can be viewed on-screen or exported to Excel® spreadsheets for reporting and analytic tools. Mini-Circuits Power Sensors cost half as much as you might expect, so why do without? Place an order today, and we can have it in your hands as early as tomorrow.

All Power Sensor models include:

- *Power Sensor Unit*
- *Power Data Analysis Software*
- *SMA Adaptor (50Ω only)*
- *USB Cable*

** Measurement speed as fast as 10 ms with PWR 8 FS. All other models as fast as 30 ms.*

† See datasheets for an extensive list of compatible software.

Windows and Excel are registered trademarks of Microsoft Corporation in the US and other countries. Linux is a registered trademark of Linus Torvalds. Neither Mini-Circuits nor Mini-Circuits Power Sensors are affiliated with or endorsed by the owners of the above-referenced trademarks.

Model	Frequency	Price $ ea. (Qty 1-4)
PWR-4GHS	9 kHz-4 GHz	795.00
PWR-2.5GHS-75	100 kHz-2.5 GHz	795.00
PWR-6GHS	1 MHz-6 GHz	695.00
PWR-8GHS	1 MHz-8 GHz	869.00
PWR-8FS	1 MHz-8 GHz	969.00
NEW! PWR-4RMS	50 MHz-4 GHz	1169.00

RoHS compliant

Mini-Circuits®

www.minicircuits.com P.O. Box 35166, Brooklyn, NY 11235-0003 (718) 934-4500 sales@minicircuits.com

"Advances in RF semiconductors give designers access to higher frequencies, power, dynamic range, and lower noise parameters, enabling them to design the next generation of RF electronics."

possible to gain insight into what the industry's landscape will look like in the next few years.

RF semiconductor research has recently explored new materials like graphene, carbon nanotubes, metamaterials, superconductors, and even textiles. New methods of stacking ICs, known as 3D ICs, also are a hot topic of research. These avenues may lead to advances in a few years. But they aren't yet ready to help extend the present capabilities of RF components to the next level in current markets. A few companies, such as Peregrine Semiconductor (www.psemi.com), are using proven technologies with small leaps in development to provide roadmapped improvements that will be available for next-generation parts.

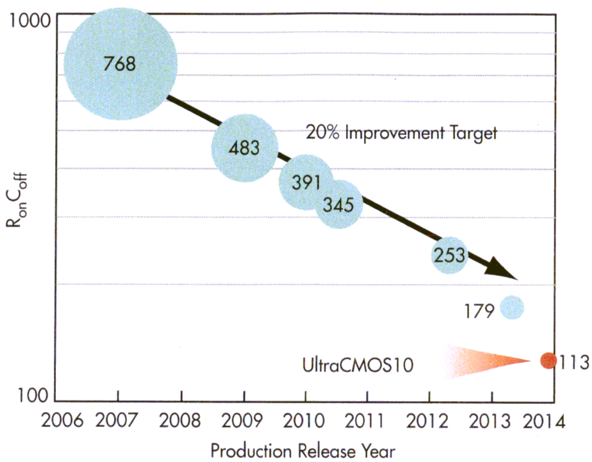

1. Peregrine's UltraCMOS 10 line has seen 20% across-the-board improvement in process node reduction.

Peregrine's silicon-on-insulator (SOI) UltraCMOS 10 is such a process. Peregrine claims it improves 20% consistently every year and is able to support LTE-Advanced (LTE-A) operational requirements *(Fig. 1)*. In many markets, it is thought to have the potential to outpace gallium arsenide (GaAs) as the semiconductor of choice. As noted by Duncan Pilgrim, director of strategic marketing, "When silicon matches GaAs in a market, it takes over."

The UltraCMOS 10 technology boasts a high-resistance substrate, which allows RF device speeds while incorporating analog and digital blocks on the same substrate. The ability to combine these three regimes lowers costs, increases speeds, and allows for higher yields with advanced integration. To implement the improvements to the UltraCMOS line of products, Peregrine partnered with Siotec and GlobalFoundries to create the 130-nm UltraCMOS 10 process and help accelerate process-node reduction.

Good electrostatic-discharge (ESD) performance of 2000 V and potentially higher on every pin is another benefit of UltraCMOS over comparable GaAs technologies. Peregrine is currently testing power amplifiers (PAs) with performance specifications that could be comparable to GaAs PAs and even exceed them, as SOI-based RF components do not degrade linearity as a function of power. The development of SOI PAs along with tuners and switches could open the doors for a complete SOI RF front end, allowing for a complete solution in a single technology. Testing also is being done on devices that, in the next few years, could reach speeds to 50 GHz using SOI technology. The next generation of wireless standards is a driving force for RF semiconductor technologies to enhance the capability of RF switches/tuners while lowering the cost of components. Long Term Evolution Advanced (LTE-A), for example, pushes the boundaries of RF semiconductors by allowing bandwidths to 100 MHz and multiple-input multiple-output (MIMO) operation.

Developed by the 3rd Generation Partnership Project (3GPP), LTE-A is designed to meet or exceed the requirements of the International Telecommunication Union (ITU) for the fourth generation (4G) of radio communication—a standard known as IMT-Advanced. Starting with Release 10

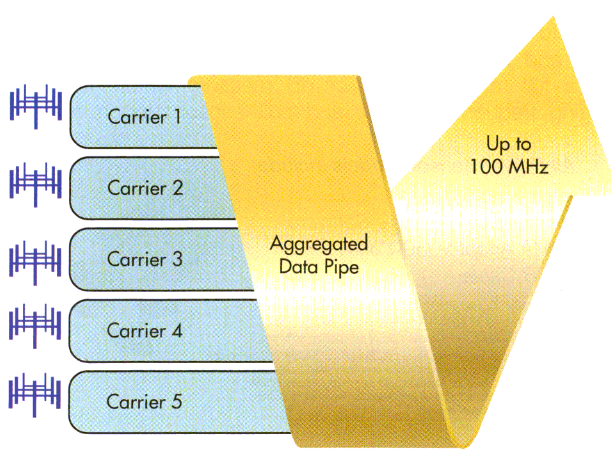

2. Carrier aggregation could lead to a combined LTE-A downlink data rate of up to 100 MHz to a device pairing with up to five carriers.

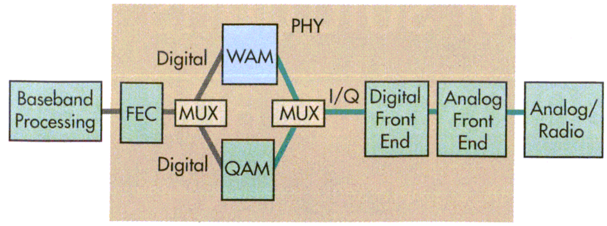

3. WAM added to a back-compatible QAM system could lead to significant modulation improvements for modern wireless and wired communication devices alike.

and including later releases, LTE-A is described with higher capacity and increased data rates up to 3 Gb/s for downlink (DL) and 1.5 Gb/s for uplink (UL). Improved performance for cell edges, higher spectral efficiency, and an increase in simultaneous active subscribers also are critical improvements in the Advanced standard over the previous LTE standard. The main new functional additions of the standard include MIMO antenna techniques to 8×8, enhanced uplink, support for relay nodes (RNs), and carrier-aggregation capabilities.

Carrier aggregation offers the ability to use the fragmented bandwidths of a variety of carriers and aggregate them to the 100-MHz maximum bandwidth *(Fig. 2)*. This helps in situations where certain carriers' bandwidth offerings don't meet necessary DL or UL requirements for a particular device, but multiple carriers combined could provide adequate data rates. By using an RN as a part of a telecommunications system, signals could be passed from a transmitter potentially much further away or with a much weaker signal to a device that otherwise wouldn't be able to communicate with adequate signal to noise for high data rates.

There are different types of relays. A Layer 1 relay is merely a repeater that amplifies the signals from transmitter to device while a Layer 2 relay demodulates the signal and modulates/transmits the signal with higher power for noise-reduction purposes. For its part, a Layer 3 relay completely deconstructs/reconstructs the communication signals in the link for higher noise reduction and standards specification benefits. A MIMO antenna system coordinates the frequency capabilities from multiple antennas to allow data rates far greater than a single antenna could accomplish. This multiple-bandwidth operation creates a variety of design difficulties stemming from working with such a large range of RF signals and having to switch and tune the variety of antennas simultaneously. The benefit is that the channels for communication are doubled with each additional antenna that is added to the matrix. As a result, data rates can hit the 3 Gb/s defined by the standard.

As these standards continue to advance in frequency, bandwidth, and complexity, new and more versatile test and measurement equipment is necessary to characterize and refine the designs of complex communication structures. National Instruments (www.ni.com) proposes a solution to the complex LTE-A test scenario with its new PXI Express-based vector signal transceiver (VST). This transceiver is a software-programmable combination of a signal analyzer and generator in a PXI package. Agilent Technologies (www.agilent.com) also offers a variety of LTE-A test and measurement solutions in a PXI Express platform.

The evolution toward enhanced standards and resulting increase of RF-component performance is one way to meet the demands of next-generation communications systems. Yet companies like MagnaCom (www.magna-com.com) are looking deeper into the root of communication methods to squeeze the most out of already congested communication systems. MagnaCom's technology, dubbed WAve Modulation (WAM), describes a method of digital modulation that takes a huge advance over the omnipresent quadrature amplitude modulation (QAM) with the same spectral mask. QAM is based on a system of two modulated signals that must operate within the linear region of the RF components with only a two-dimensional (2D) constellation of possible phases for the two signals.

In contrast, WAM is designed from the bottom up to assume nonlinearity and multidimensional signal constellations. Because this modulation is purely digital, it does not require any hardware adaptations, is not a compression algorithm, and is a purely backward-compatible replacement of QAM (*Fig. 3*).

Nonlinearities like white noise, phase intermodulation distortion (PIM), and the nonlinear region of amplifier operation are accounted for automatically with WAM and do not degrade performance, according to Yossi Cohen, CEO of MagnaCom. WAM could allow for PAs and other RF electronics to operate beyond their normal region of linearity, allowing for wider dynamic range from the same hardware. This leads to a proposed benefit of up to 10 dB for the same footprint as a similar QAM4096 system.

With higher spectral compression, a WAM system could offer increased signal rates over a QAM system at much lower-order constellation alphabets (64 with WAM compared to 4096 with QAM). WAM also benefits from the same scalability as QAM, increasing in operational performance as the order gets higher in the constellation alphabet.

According to the company, WAM could enable higher system gains, lower power, a boost in range, an increase in throughput, and lower-cost digital designs. The benefit for the designer is that he or she could choose per application. This technique also could provide a solution to the phase-noise issues present at much higher carrier frequencies. MagnaCom is currently looking to apply its technology in point-to-point systems like wireless backhaul, military, and satellite communications. mw

JEAN-JACQUES DELISLE | Technical Engineering Editor

The Future Of Connectivity: Mobile & Automobiles

With more applications becoming integrated with communication networks, the next natural frontier is car drivers' in-vehicle experience.

AS ESTABLISHED TECHNOLOGIES improve, clever designers and industry experts have a way of finding new applications and markets for growing technologies. This is very much the case with RF and microwave technologies, as the consumer demand for staying constantly connected spills over into other industries. This trend is now extending to automobiles *(Fig. 1)*. Wireless coverage has to catch up to the demand of its data-hungry users. To meet this demand, terrestrial-based wireless communications are being augmented by ever-more-capable communications satellites.

Most mobile RF applications would not be possible without the semiconductor-based solutions that transformed RF components from rack-mounted units to pocket-portable tools for everyday life. Insights on what to expect from the RF industry can be gleaned by taking a look into the production of RF integrated circuits (ICs) and the industries for which they are produced. An updated study by IC Insights, titled "IC Market Drivers 2013—A study of Emerging and Major End-Use Applications Fueling Demand for Integrated Circuits," notes that the communications-IC market grew with a compound annual growth rate (CAGR) of 16% from 2009 to 2013. It surpassed the computer-IC market by reaching as much as $100 billion dollars in 2013. This coincides with a report from IDC, which predicts that smartphones will overtake feature-phone sales by more than 10% in 2014. The need for smartphones to have additional antenna elements and radio streams increases the necessary RF components of the smartphone beyond feature-phone requirements.

While mobile-phone sales grow, mobile-communications standards are advancing to provide higher data rates while incorporating multiple antennas and advanced features. These advancements, which require more RF-semiconductor development, have demonstrated a rise in production of these components. At the RF MEMS Conference in 2013, a forecast report by Yole Development predicted that the RF microelectromechanical-systems (MEMS) switch and variable capacitor market will grow from more than 50+ million in 2013 to more than 450 million in 2018 *(Fig. 2)*. The forecast noted that the mobile-device market dominates this demand with over 50% of the market share.

Cisco shares many statistics and predictions on the mobile communications market in its report, "Visual Networking Index Forecast (VNI)." According to the forecast, there will be 841 million mobile-connected devices in 2017—an increase of almost 400 million compared to 2012. With an estimated increase from 1.26 mobile connections per capita in 2012 to 2.2 from the report, it would stand to reason that mobile data traffic would scale as well. The report predicts that mobile data traffic will hit over 1 exabytes per month, used by over 300 million people in 2017. It also indicates that 7% of the mobile data traffic in 2017 will be from machine-to-machine (M2M) connections with almost 350 million mobile-connected M2M modules. As more "smart" systems are incorporated into daily life every year, such reports show

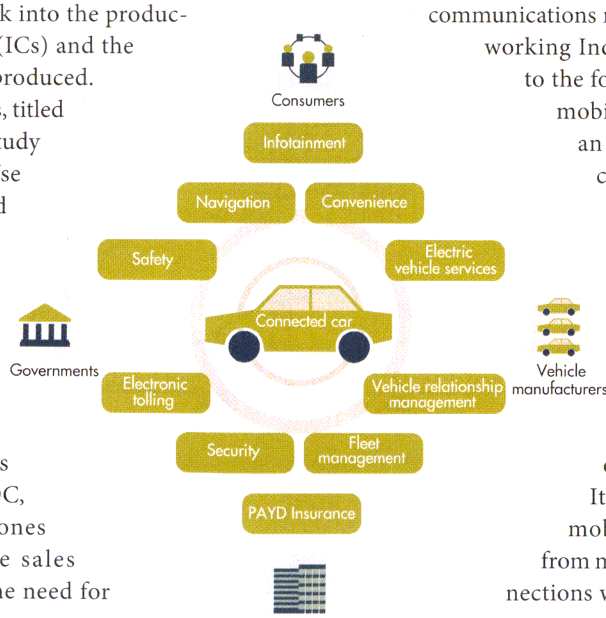

1. A connected car could eventually boast many applications, thanks to the advanced features of its telematics capability. (Image courtesy of "2025 Every Car Connected: Forecasting the Growth and Opportunity")

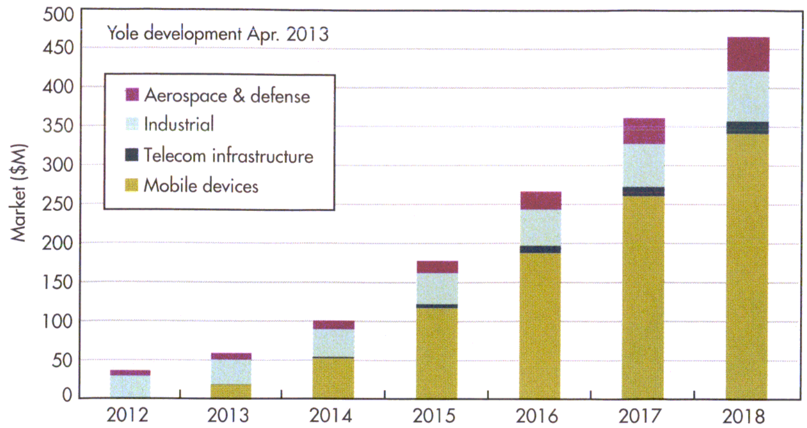

2. The RF MEMS switch and variable capacitor market will grow to more than 450 million in 2018. (Information courtesy of Machina Research)

that machine and human communications will spread to more diverse platforms. Automobile communication, or telematics, is an industry that is poised to take advantage of this boom.

With a 25.4-minute average commute (according to the U.S. Census Bureau), most Americans spend almost 1.5 hours a day traveling (according to the Bureau of Labor Statistics American Time Use Survey). This could attribute to the forecasting by Machina Research, which predicts that over 120 petabytes of information will be transmitted a year just for entertainment and Internet traffic in in-vehicle mobility systems by 2020 *(Fig. 3)*. Common telematics solutions include feature enhancements and added features to the automobile ecosystem, such as security/tracking, emergency/eCall, entertainment and Internet, navigation, insurance, and lease/rental/share car management. In a whitepaper written by SBD for GSMA, "2025 Every Car Connected: Forecasting the Growth and Opportunity," an estimation of the growth of embedded in-car telematics over the next 15 years is predicted to reach over 5% of all connected devices by 2025. In other words, roughly 0.1% of connected devices would be embedded in-car telematics solutions. Although there is a high demand from consumers to see telematics systems in everyday cars, there are reasons that the forecast for embedded telematics is predicted to only grow significantly in the late 2010s.

For instance, automobile design cycles operate on a 3-5 year basis, whereas mobile technologies update annually. The life spans of automobiles typically range from 7-10 years. This means that in-vehicle telematics solutions must be able to be updated remotely, require few hardware updates, and be highly resistant to the stresses of vehicular travel. Additionally, automakers want solutions that can be adjusted to changes in markets, business models, mobile operators, and vehicle ownership. This need could lead to embedded devices, tethered devices, or integrated devices with mobile handsets.

All of these telematics solutions require a reliable communications network in which automakers can assure users of 99.999% functionality, according to GSMA's white paper, "Connecting Cars: The Technology Roadmap." This requirement—along with historical cooperation difficulties between mobile network operators (MNOs) and automakers—has led to delays in telematics solutions. An additional complication stems from recent changes in the European Union (EU) wireless regulations. Automakers' telematics solutions may take some time to arrive to market, which means aftermarket telematics solutions might grow to fill consumer demand.

One such solution could be the new embedded subscriber identity module (SIM) technology, which enables operator swapping without the need to physically possess the device. In an excerpt from a white paper written by SBD for GSMA, "2015 Every Car Connected: Forecasting the Growth and Opportunity," the following hypothesis is provided:

"At some point in the future, every car will need to be connected to the outside world through a cellular network. The most user-friendly and secure way to enable this is by embedding a SIM card and a communication module inside the car. Therefore, the automotive market will naturally converge towards embedded telematics in the long term unless major barriers prevent this from occurring."

Connecting cars may add many opportunities and benefits. Yet such capability also invites the potential for technological assaults on the telematics solutions within the vehicle. Each connectivity option allows for another method of potential intrusion. As such, high-tech thefts are a key consideration for automakers. mw

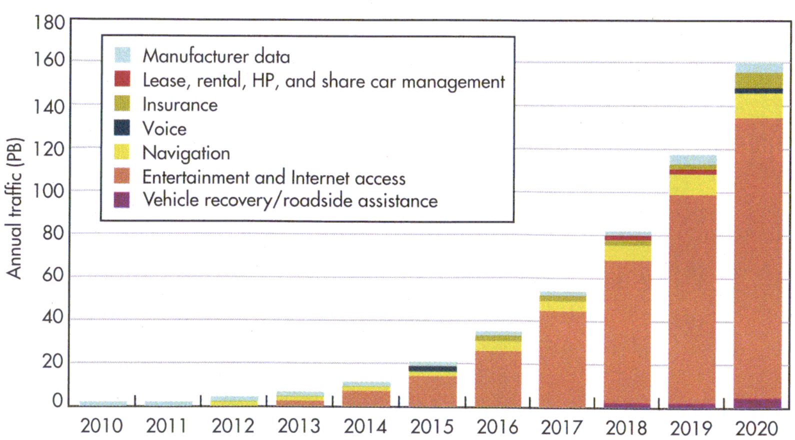

3. In-car telematics continues to be dominated by Internet/entertainment. (Courtesy of GSMA)

JEAN-JACQUES DELISLE | Technical Engineering Editor

Gazing At The Tiers of Wireless Power Solutions

Since the early 2000s, there has been a good deal of talk about losing the cord while charging our daily blend of portable devices. Are we finally on the verge of seeing real wireless power solutions?

IN LATE 2008, the Wireless Power Consortium (WPC) began supporting an inductive-coupling standard. Since that moment, large companies competing in the portable-electronic-device (PED) market have been struggling to define an effective and universal standard to deliver power wirelessly to their devices *(Fig. 1)*.

Other associations, such as the Power Matters Alliance (PMA; an inductive-coupling standard) and Alliance for Wireless Power (A4WP; a magnetic-resonant standard), also have considerably large companies backing their efforts. As recently as October of 2013, the IEEE Standards Association announced the IEEE Wireless Power and Charging Systems Working Group (WPCS-WG). Its goal is to control the standards for wireless power transfer (WPT) and help lead a unified front for developing WPT technologies starting with inductive coupling. With so much activity, many are trying to discern why there is such a struggle over WPT systems, the difference between all of the standards, and the impact of WPT on design engineers.

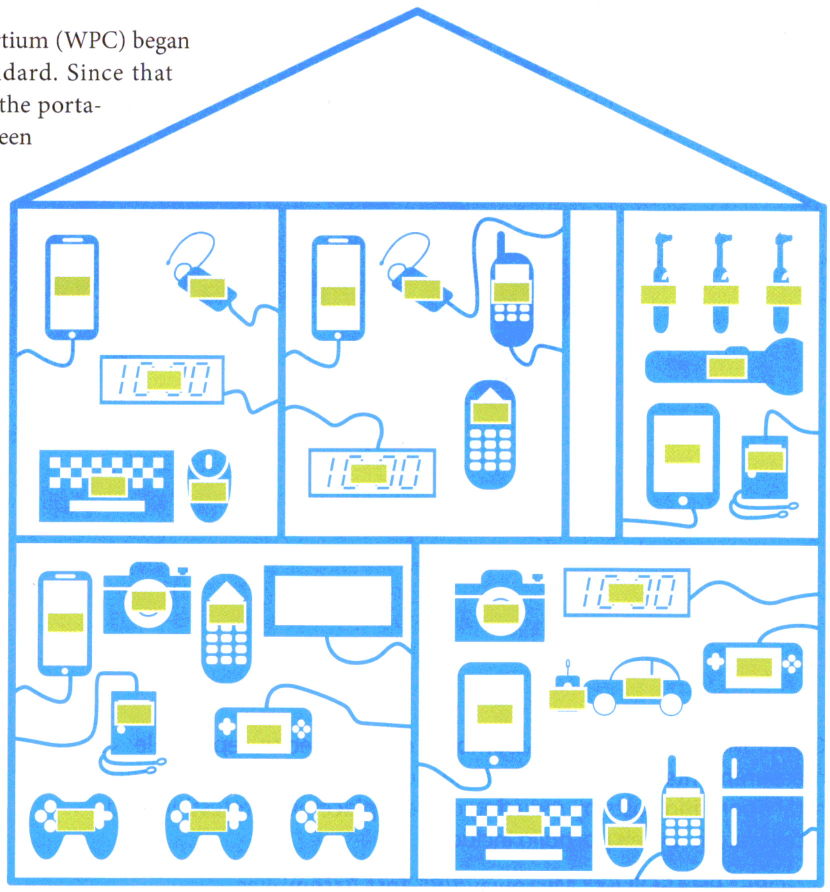

1. A standard household has tens to hundreds of low-power or battery-powered devices, many of which are portable electronic devices (PEDs). (Courtesy of www.osiainc.com)

WPT was the brainchild of the wily scientist and showman, Nikola Tesla. His grandiose vision led him to build a WPT tower system that was meant to transmit energy across the globe in 1901. (Wardenclyffe Tower, which was located in Long Island, N.Y., was demolished in 1917.) Much has changed in the WPT world since 1901. The goal is no longer to transfer huge amounts of energy over vast distances with massive towers, but to transfer just enough energy to useful devices over very short distances.

Building a smart and efficient WPT infrastructure for highly diverse and numerous devices wasn't economical until computers started fitting into pockets, as there was no demand or real use for such a system. With estimates of yearly PED sales at the hundreds of millions and growing, many companies with their fingers in the PED pie are trying to catch up with increasing accessibility for these devices. According to Mark Hunsicker, Senior Director of Wireless Power Solutions for Qualcomm, "From Qualcomm's perspective, smartphones were the catalyst."

As the computational capability of PEDs increases far beyond

battery technology's capacity to provide safe and adequate power with reasonable charging times, consumers and manufacturers of PEDs are looking for other ways to keep PEDs running. This conundrum has led to a scramble as top companies like Duracell, Procter & Gamble, Qualcomm, Samsung, LG, Energizer, Starbucks, Nokia, and hundreds of others either create their own standards or jump on board with other large companies' standards. Meanwhile, the standards organizations—WPC, A4WP, and PMA—are vying for technology presence within PEDs to decide what standard will dominate.

Both the PMA and WPC standards operate in the hundreds-of-kilohertz range using two inductively coupled coils. Although they exhibit highly efficient energy transfer, they require close physical proximity with exact placement. The A4WP standard, Rezence, operates at 6.78 MHz within the Industrial, Scientific, and Medical (ISM) band and uses magnetic-resonant technology *(Fig. 2)*. For a WPT system, magnetic resonance allows for efficient power transfer and position flexibility within several inches vertically/horizontally, through surface charging. These aspects permit incorporation into existing work surfaces.

Regardless of the electromagnetic (EM) method of energy transfer, the standards themselves include design guidelines for safety, interference, compliance, transmission, reception, antenna design, power, and telemetry. All of these technologies have functional examples and a few even have early product versions available. This year, all of them are looking to enlarge their presence in higher-volume arenas like smartphones, tablets, cars, and lounge/business areas like coffee shops.

Many companies that produce components for PEDs, such as Texas Instruments, are part of all of the WPT standards associations. They are betting on every standard so that they can capitalize on the market with whatever standard wins out. With the Chair of the WPCS-WG also being the Technical Director of the PMA, designers should expect a wide adoption of the PMA standards in large component manufacturers in the short term. The WPCS-WG also is allowing the next-generation implementation of WPT to embrace magnetic resonance as the technology matures. After all, magnetic resonance does possess many user-oriented benefits over inductive coupling. Right now, all of these standards focus on applications in which the device must physically be placed on or near a powering station and can only service a few devices simultaneously. Yet some companies are looking past current expectations into a more energy-accessible future, where PEDs are not the only devices looking to lose the cord.

For example, Hatem Zaine, CEO of Ossia, has spent 12 years developing COTA technology, which is geared toward putting "Star Trek" -level power availability in every home. The COTA system works on a different principle of phased-array-focused energy transfer along the path of optimal efficiency. It delivers at least 1 W of constant power up to 30 ft. within the radius of the transmitter, with less power being available beyond 30 ft.

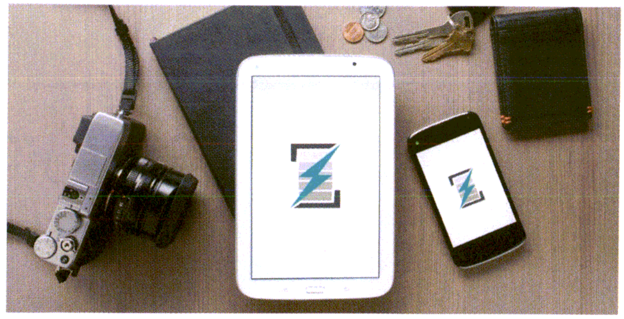

2. The Alliance For Wireless Power (AW4P) has recently established the brand name for its new wireless power transfer standard, Rezence. (Courtesy of www.rezence.com)

The transceiver/charger is roughly a subwoofer-sized mixture of a non-planar phased array with tens of thousands of elements and a computer dedicated to optimizing the long-distance energy transfer. A receiver is equipped with a 5-×-5-mm chip, which could easily be incorporated into phones, cases, batteries, smoke alarms, appliances, and more. That chip sends out a low-power omnidirectional signal, which the transceiver uses to take a 3D electromagnetic hologram of the room. It then decides upon the most efficient energy path to charge the receiver device.

The energy transmit path could include bouncing signals off walls, desks, tables or any other non-absorptive structure. This method intrinsically avoids sending RF power signals toward objects non-conducive to RF signal transfer, adding to the safety of the system. The RF hologram is generated at a rate of 100 times per second, which allows for easy avoidance of moving objects that would rather not absorb RF energy (like people).

The COTA system stands out because it is not just designed to kick the common smartphone cord. Rather, its goal is to replace cords and charging concerns in all battery/low-powered household/commercial devices. This all sounds extremely space age and theoretical, but Ossia is demonstrating the technology at this month's International CES in Las Vegas, Nev. (CES; www.cesweb.org). Following CES, the Ossia team is working on integrating the receiver technology so that it can be incorporated into AA and AAA batteries. According to Hatem, the market can expect COTA systems by 2015. Given the movement around the growing WPT industry, the product and solution landscape should already be quite diverse at that point. mw

ADDITIONAL RESOURCES:

www.powermatters.org

http://standards.ieee.org/develop/wg/WPCS-WG.html

www.rezence.com

www.wirelesspowerconsortium.com

www.ossiainc.com

CHIN-LEONG LIM | Engineer
*Avago Technologies, 11900 Bayan Lepas, Penang, Malaysia;
(604) 610-2525, e-mail: C.L.Lim@ieee.org, www.avagotech.com*

COMPACT LNA Drives 2.5-GHz Base Stations

This balanced-amplifier design combines small size with high performance and is a suitable candidate for reliable operation in TMA applications in cellular communications towers with limited space.

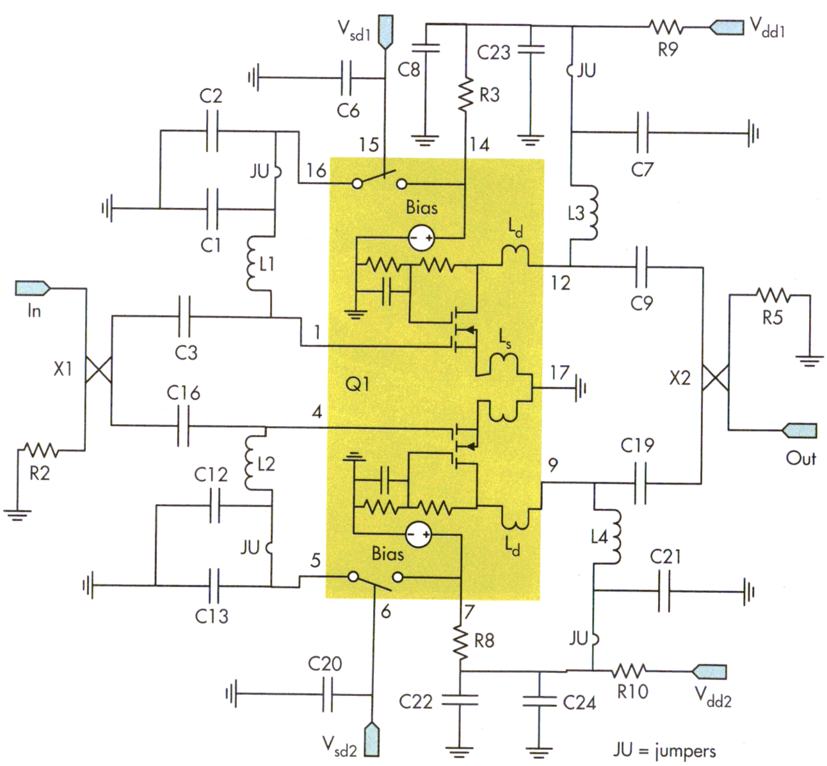

1. Integration of dual amplifiers, impedance matching, active bias, ESD protection, and shutdown functions can be achieved in a compact balanced amplifier design.

Low-noise amplifiers (LNAs) are essential to many communications systems, such as cellular communications networks. Achieving low noise figures requires determining such parameters as the optimum impedance matching points, such as for G_{opt} and conjugate S^*_{11} impedance matching points, for active devices. Balanced LNAs were developed in the 1960s by finding transistor amplifiers' noncoinciding noise G_{opt} and conjugate S^*_{11} matching points,[1,2] achieving low mismatches by self-cancellation of the reflected energies in quadrature 3-dB couplers (also known as the 90-deg. or hybrid couplers) employed in the LNA design. By ensuring good impedance match, an LNA's constituent amplifiers can then be tuned for minimum noise.

Although an isolator can perform the same function, the cost is comparatively higher. Additionally, a balanced LNA configuration improves upon the reliability, linearity, and bandwidth of its single-ended counterpart and is inherently self-stabilizing (i.e., high stability, both in-band and out of band, is possible even when it is constructed from two potentially unstable amplifiers).[3] However, a balanced LNA needs twice the current and components of its single-ended counterpart.

Furthermore, the quadrature couplers represent an additional cost and occupy substantial printed-circuit-board (PCB) space, especially for distributed implementations. Their insertion losses degrade amplifier noise figure (NF), gain, and output power. If commercial drop-in couplers are used, their RF performance levels are generally proportional to their cost and size. More critically, a balanced LNA's

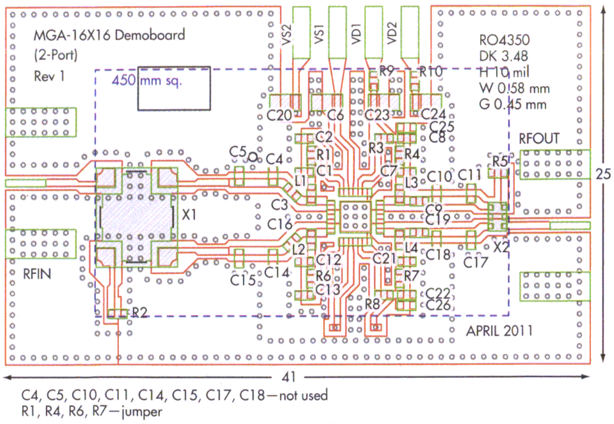

2. For this balanced design, a complete LNA fits inside an area of only 450 mm^2 (inside the dashed box) on the PCB.

doubled size and weight diminish its viability as a tower-mounted amplifier (TMA) in confined spaces atop cellular towers.

Three broad approaches to miniaturizing a balanced LNA are (a) shrinking the couplers,[4,5] (b) integrating the couplers into the amplifying device monolithically[6] or in hybrid form,[7] and (c) integrating dual amplifiers in either hybrid form[8,9] or monolithic form.[10,11] However, TMAs also require cutting-edge performance, and this is an obstacle to miniaturization.

Many TMA-centric balanced LNA designs of the past decade have been based on discrete devices,[4,5,12,13] but these require a large number of supporting components. To achieve significant reduction in size and component count, dual amplifiers, biasing, and shutdown functions have been integrated into a monolithic microwave integrated circuit (MMIC) and then combined with miniature couplers to create a high-performance, compact 2.5-GHz balanced LNA. The design's viability as a TMA is contingent upon meeting a number of critical specifications: a sub-1-dB noise figure, 17.6-dB gain in a single stage, better than 18-dB input match, +30-dBm output third-order intercept point (OIP3), and unconditional stability. This may also be the first dual-amplifier design with integrated shutdown function.

The compact GaAs MMIC comprises dual amplifiers, electrostatic-discharge (ESD) protection, adjustable active biasing, and shutdown functions (the yellow box in *Fig. 1*). The proximity of the bias function to the amplifier on the same chip also beneficially stabilizes the operating current against gate threshold voltage and temperature variations.

For chip fabrication, a proprietary 0.25-μm enhancement-mode pseudomorphic high-electron-mobility-transistor (ePHEMT) process technology on a 6-in. wafer was selected because it best matches the cost-versus-performance requirements. Because this process technology has previously enabled a single-ended LNA to achieve a 0.7-dB NF at 2.5 GHz,[14] a balanced design with sub-1-dB NF was anticipated after factoring in about 0.2-dB coupler loss.

The semiconductor process has relatively high transition frequency (f_T) and peak transconductance (greater than 30 GHz and about 615 mS/mm, respectively) which should provide the leverage to meet the target gain with a single amplifier stage. Additionally, this process technology's stable linearity down to 2-VDC drain-source voltage (V_{DS})[15] is beneficial for a cascode arrangement where each transistor only sees one-half the supply. The MMIC is assembled into a 16-pin, 4- × 4- × 0.85-mm quad-flat-no-lead (QFN) package using conventional lead-frame wire bonding technology.

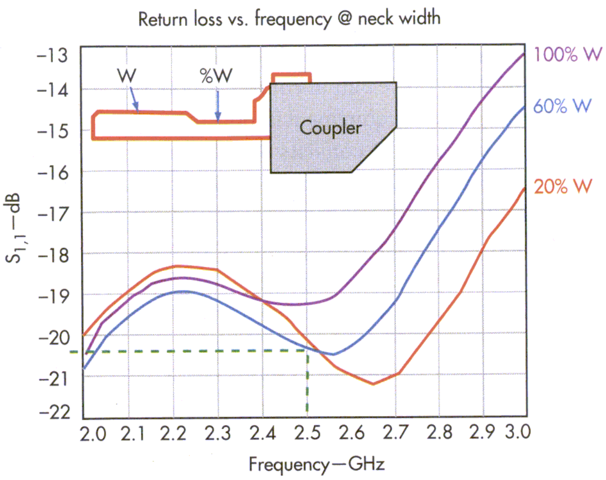

3. A short section (1.4 mm long) of microstrip trace next to the coupler was narrowed to achieve a 1-dB improvement in input impedance match.

The target 17-dB gain can be achieved with a cascade of two common source stages or one cascade stage. The latter was selected for its lower current—i.e., the cascade configuration's series-connected transistors consume one-half the current of a cascade configuration. The cascode configuration is biased by connecting the upper gate to a resistor divider, while the lower gate is connected to active bias via off-chip inductors L1 and L2. On-chip inductors were not used in these positions since they cannot meet the low RF loss characteristics of off-chip inductors as needed to meet the target NF performance.

In addition to supplying bias, these inductors form highpass networks (in conjunction with capacitors C3 and C16) to roll off excessive low-frequency gain. These input networks need not perform impedance transformation because the ePHEMT device periphery and source inductance L_s have been optimized for impedance matching and low noise in the 2-to-4-GHz band. Internal prematching by the drain inductance, L_d, simplifies the output networks, L3-C9 and L4-C19.

The on-chip shutdown circuit consists of a transistor switch in series with the active bias. Shutdown is initiated by applying high logic (≥2 V) at $V_{sd1/2}$ to open the switch. Conversely, a low logic signal—i.e., $V_{sd1/2}$ ≤ 500 mV—enables the amplifiers. The transition from normal operation to shutdown takes less than 32 ns if the large (≥0.1 μF) decoupling capacitors—C8, C22, C23, and C24—are omitted. However, these capacitors are generally recommended because they prevent low-frequency instability and dampen supply transients.

Although the monolithic integration of Lange couplers can achieve the smallest circuit dimensions, the resulting noise figure (e.g., about 7 dB[6]) is too high for TMA applications. For this reason, the signal splitting and combining functions in the current design were performed using commercially available surface-mount couplers, X1 and X2.

These backward-wave couplers are fabricated on high-dielectric-constant ceramic substrates to achieve compact dimensions: They are about halfway in size between Lange and branch-line couplers. The 2.6-GHz versions of these couplers have enough bandwidth to straddle Fourth-Generation (4G) WiMAX and cellular Long-Term-Evolution (LTE) bands.

To minimize input loss, a larger (6.4 × 5.1 mm) coupler is used at the input port, while a smaller (2.0 × 1.3 mm) coupler is used at the output port to save space and cost. To ensure that a better than 18-dB input match can be consistently met in volume production, controls were instituted on the two most critical param-

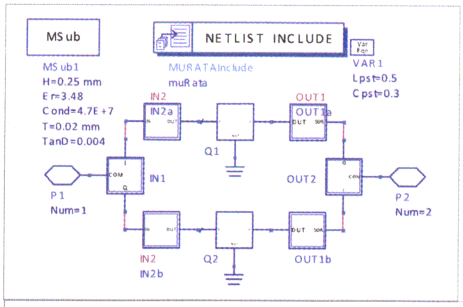

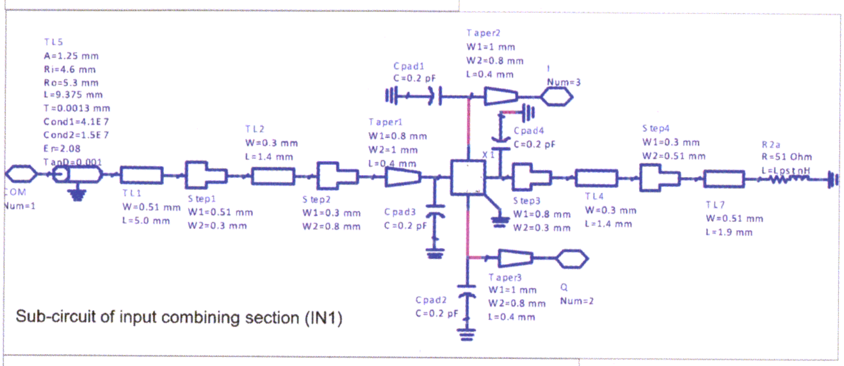

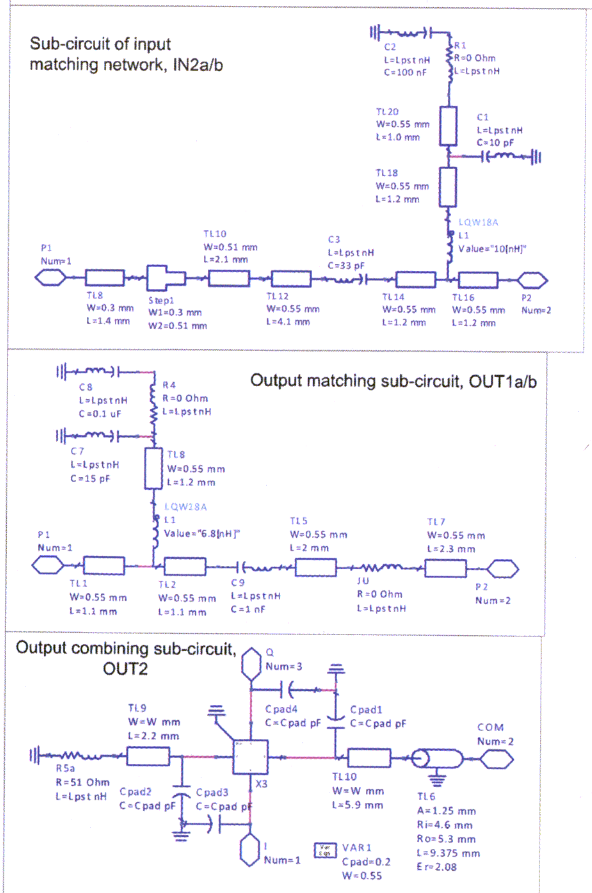

4. The balanced amplifiers'8 equivalent-circuit models include circuits for input impedance matching, output impedance matching, and input combining.

eters: (a) correlating the amplifiers' input match to $|S_{11a} - S_{11b}| < 0.025$ dB and (b) specifying an input coupler with better than 23-dB isolation.[16] The output coupler is noncritical since the TMA output match requirement is more relaxed.

The amplifier PCB consists of a 10-mil-thick layer of RO4350B printed-circuit-board (PCB) material from Rogers Corp. (www.rogerscorp.com) with an FR-4 layer added to increase the stack height to 1.6 mm (*Fig. 2*). RF test connections are made via edge-launched SMA receptacles. Measurements are referenced to these connectors. The occupied circuit area, populated mostly with 0402-sized passive components, is 450 × 450 mm. The occupied area can possibly be reduced by about 20% if the empty area between input coupler X1 and the input matching networks (L1 – C3) is removed.

The PCB's microstrip width (0.58 mm) is nominally dimensioned for an impedance of 50 Ω, but the traces next to the input coupler's mounting pads are necked down to compensate for the pads' parasitic capacitances (*Fig. 3*). Narrowing the trace width to 60% of its nominal value can improve the 2.5-GHz input match.

For circuit simulation, the design is modelled using a two-level nested hierarchy (*Fig. 4*). The upper level consists of blocks representing the MMIC, the signal dividing/combining, and the impedance-matching functions. Each of the dual amplifiers, Q1 and Q2, is represented by an identical set of scattering (S) parameters (.s2p). The device .s2p was previously extracted from an MMIC sample mounted on a test fixture of similar PCB material and thickness, using a thru-reflect-line (TRL) technique to compensate for the fixture.

The device's noise and linearity [third-order intercept point (IP3)] parameters were also extracted on the same test fixture using automated source and load-pull tuners. The minimum noise figure, NF_{MIN}, of about 0.4 dB is particularly challenging to extract because it is very close to the combined loss of the tuner, cables, and connector adapters. The inductors and couplers are modelled with their manufacturers' .s2p data. Other passive components are modelled using their equivalent-circuit values, including first-order parasitic values.

The prototype was evaluated with a +4.8-VDC supply voltage and 2.5-GHz nominal test frequency and found to meet the target sub-1-dB NF at the design frequency. The experimental NF was found to be 0.95 dB at midband, with negligible variability in NF (<0.05 dB) for five samples over a 1-GHz span. The predicted NF follows the same trend as the measured NF, but with value that is lower by about 0.3 dB. This discrepancy is probably due to a modelling error, since the device's NF_{min} is close to the measurement limit of the noise characterization equipment.

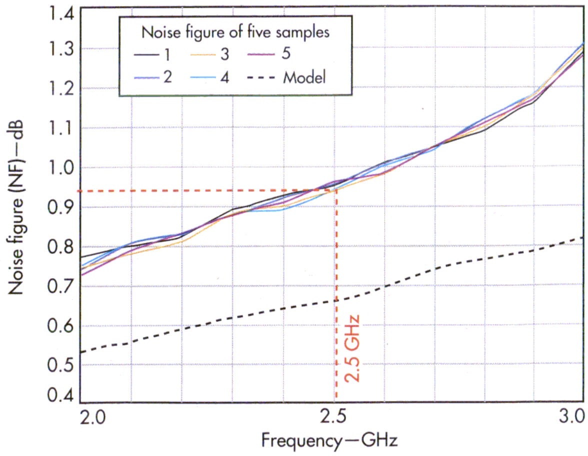

5. The experimental noise figure (NF) is consistently around 0.95 dB at 2.5 GHz.

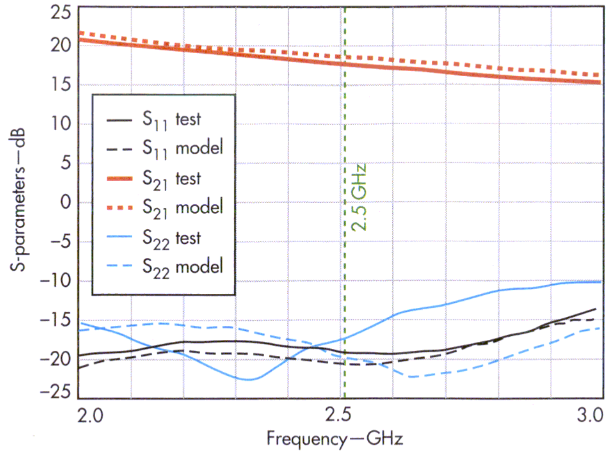

6. The single-stage balanced LNA achieves 18-dB midband gain.

The design capably meets the TMA's gain and input match requirements. The experimental gain is 18 dB at midband (*Fig. 6*). The predicted gain is in good agreement with the measured over a 1-GHz span. The experimental input and output return losses are 19 and 17 dB, respectively. In theory, optimum matching should occur at the center frequency of the couplers. The experimental input match for the couplers is optimum at 2.6 GHz, which coincides with the input coupler's center frequency. The best output match is at 2.3 GHz, however, which does not coincide with prediction (probably due to coupler tolerance). The return-loss amplitude is primarily a function of the coupler's isolation, although how identical the amplifiers are—as well as discontinuities in the microstrip transmission lines—can contribute to variations in return-loss amplitude.

Because the amplifier behaves like a nonreflective attenuator during shutdown, an LNA bypass switch can be potentially eliminated. When the MMIC shutdown is activated, the circuit exhibits 26-dB attenuation, 26-dB input return loss, and 10.5-dB output return loss at 2.5 GHz (*Fig. 7*). Matching remains good in shutdown mode because reflections from the unpowered amplifiers are self-cancelled in the couplers. The 2.5-GHz output match is worse than expected because the minimum output return loss shifts to 2.15 GHz, possibly because of coupler tolerance. Because of the good match during shutdown, an LNA bypass switch is not required to prevent aerial or filter detuning.

The fabricated balanced LNA is unconditionally stable. Both modelled and measured stability factors, μ, exceed unity from 50 MHz to 20 GHz (*Fig. 8*). The accuracy of the simulated μ is poor above 3 GHz since the simple equivalent circuits used to model the amplifier's passive components do not account for the higher resonances above about 3 GHz. What is remarkable is the potential instability of the constituent amplifiers, as indicated by less than unity μ from 7 to 18 GHz, although the balanced topology's self-stabilizing promise is validated in this design. It is also remarkable that the frequency range where stability is improved, from 7 to 18 GHz, is well above the couplers' passbands.

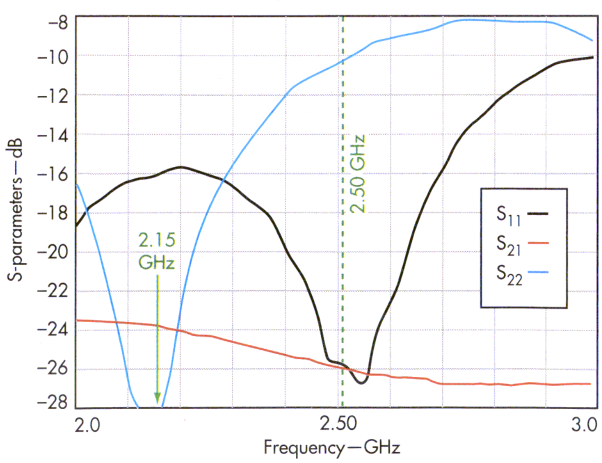

7. The amplifier achieves better than 10-dB return loss in shutdown mode to minimize the need for a bypass switch.

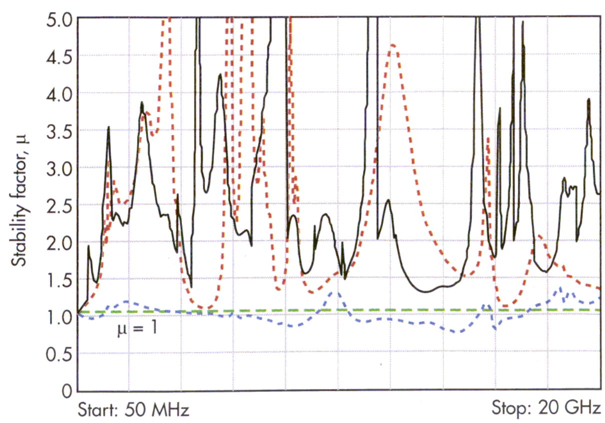

8. This plot of stability, μ, versus frequency shows unconditional stability for the balanced amplifier, even though its constituent parts are relatively unstable.

This amplifier design has sufficient linearity to operate reliably in a cellular tower's noisy RF environment. The 2.5-GHz experimental OIP3 is +38 dBm, about 1-dB lower than the 2.0-GHz peak (*Fig. 9*). The OIP3 peaks away from 2.5 GHz because the amplifiers' output networks are tuned for maximum gain. At the expense of reduced gain, it should be possible to improve the 2.5-GHz OIP3 to about +39 dBm by matching for linearity. The OIP3 simulated with load-pull data agrees well with the experimental results, with less than 0.2-dB error at 2.6 GHz. The linearity figure of merit calculated from the ratio of OIP3 to DC power is about 12.4. The midband gain compression point, P1dB, is +21.1 dBm. A high P1dB implies immunity to strong blockers.

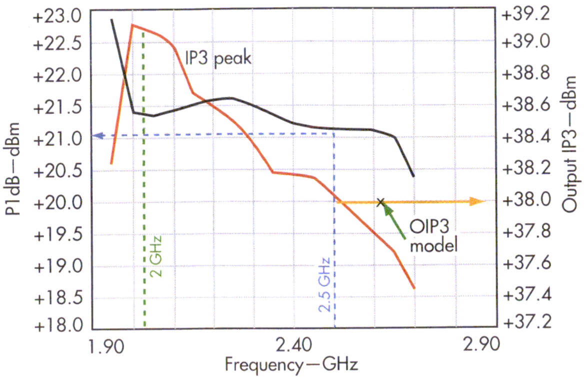

9. The amplifier achieves experimental OIP3 of +38 dBm and output power at 1-dB compression of +21.1 dBm.

Among GaAs MMICs intended for balanced cellular LNA applications, this design has one of the smallest footprints, at 16 mm^2. With three functions on the device, the area per function is only 5.3 mm^2 compared to previous work[7-10] with footprints ranging from 16 to 419 mm^2, and even an MMIC footprint of only 16 mm^2 at Avago for a single-function device.[11] The current design is also the only MMIC cellular LNA with an integral shutdown function.

This design has demonstrated the best performance-to-size ratio among TMA-capable balanced LNAs in the 2-to-3-GHz range. Comparison of different designs can be facilitated by a figure of merit (FOM), such as LNAFOM = (OIP3 9 mW)/ P_{DC} (mW) × NF (dB).[17] The current design has an LNAFOM of 13.2. In comparison, designs with large couplers[8,9,12] have the highest LNAFOMs but also occupy large PCB areas. The current design combines high performance and compactness.

The proposed balanced LNA design successfully marries high performance and small size, usually conflicting TMA requirements. It substantially reduces component count by integrating dual amplifiers, bias regulators, and shutdown circuits in an MMIC. (A table showing a bill of materials for the LNA is available on the online version of this article, at www.mwrf.com.) When the MMIC is coupled with miniature hybrid couplers, the balanced LNA's PCB size can be reduced further. This MMIC's low-noise performance allows input coupler loss to be traded off for size reduction. A bonus is good impedance match during shutdown, which may eliminate the need for bypass switches. This new design may overcome traditional barriers to the use of balanced amplifier topologies in TMAs. mw

ACKNOWLEDGMENTS
The author wishes to thank H.A. Zulfa, W.H. Chiok, and R. Chuah for the MMIC design and characterization, M.D. Suhaiza and S. Punithevati for assembling the prototypes, and S.A. Asrul and the management of Avago Technologies for approving the publication of this work. Anaren Communications (Suzhou) provided the couplers at no charge.

REFERENCES

1. M. Eisele, R.S. Engelbrecht, and K. Kurokawa, "Balanced Transistor Amplifiers for Precise Wideband Microwave Applications," IEEE International Solid-State Circuits Conference, February 1965.
2. R.S. Engelbrecht and K. Kurokawa, "A Wideband Low Noise L-Band Balanced Transistor Amplifier," Proceedings of the IEEE, Vol. 53, No. 3, March 1965, pp. 237-247.
3. Steve C. Cripps, RF power amplifiers for wireless communications, Artech House, Norwood, MA, 1999, Section 10.2 "Balanced amplifiers."
4. J.S. Mandeep and H. Abdullah, "A compact, balanced low noise amplifier for WIMAX base station applications," Microwave Journal, November 2010.
5. A.F. Osman and N. Mohd. Noh, "A design for SDR radio using balanced amplifier topology," 4th Asia Symposium on Quality Electronic Design, 2012.
6. S. Seo, D. Pavlidis, and J.S. Moon, "Wideband balanced AlGaN/GaN HEMT MMIC low noise amplifier," Electronics Letters, Vol. 41, No. 16, August 2005.
7. B. Jensen, "Build LNAs with an integrated approach," Microwaves & RF, December 2002.
8. T. Chong, "A Low-Noise, High-Linearity Balanced Amplifier in Enhancement-mode GaAs pHEMT Technology for Wireless Base-Stations," Proceedings of the European Microwave Conference, Paris, France, October 2005.
9. T. Chong and S. Rendava, "Design and Performance of a 1.6-2.2-GHz Low-Noise, High Gain Dual Amplifier in GaAs E-pHEMT," Asia-Pacific Microwave Conference, Suzhou, China, December 2005.
10. Ommic application note, "CGY2105XHV/AB2500 2.5-2.7 GHz balanced low noise amplifier application board," www.ommic.com.
11. Avago Technologies, Application Note 5442, "LNA Design with the MGA-17516 Matched Pair, Low Noise Amplifier," www.avagotech.com.
12. I. Piper, S. Seward, A. Ward, H.P. Hostergaard, and S. Tozin, "Balanced LNA suits cellular base stations," Microwaves & RF, April 2002, pp. 70-80.
13. J.-L. Olvera-Cervantes, A. Corona-Chavez, R. Chavez-Perez, H. Lobato-Morales, J.-R. Ortega-Solis, and J.-L. Medina-Monroy, "A wideband quadrature power divider/combiner and its application to an improved balanced amplifier," Progress In Electromagnetics Research C, Vol. 34, 2013, pp. 29-39.
14. Avago Technologies, Application Note 5479, "MGA-635P8 GaAs epHEMT MMIC 2.5-GHz low-noise amplifier with superior noise and linearity performance," www.avagotech.com.
15. J. Madden, "Low voltage operation of GaAs power amplifier," Microwave Journal, September 2006, pp. 130-134
16. Anaren Co., Product specification, "X3C26P1-035 hybrid coupler," Rev. C, www.anaren.com.
17. "IMS 2011 student design competitions," IEEE Microwave Magazine, February 2011, pp. 98-99.

RAYMOND A. BAKER
Field Applications Engineer

WALTER H. NAGY
Principal Engineer

DAVID W. RUNTON
Vice President, Engineering

ROBERT A. SADLER
Principal RF Applications Engineer

Nitronex Corp., 523 Davis Dr., Ste. 500, Morrisville, NC 27560; (919) 807-9100, FAX: (919) 472-0692, e-mail: info@nitronex.com, www.nitronex.com

High-Voltage GaN-Deliver High Power

These high-voltage GaN-on-Si devices are capable of providing broadband frequency coverage with high gain and generous output-power levels while operating at +48 VDC.

Gallium-nitride (GaN) semiconductor devices offer great promise for designers of high-frequency active circuits, especially when high output-power levels are needed at higher frequencies. GaN devices offer the mobility and transconductance of gallium-arsenide (GaAs) active devices, with the added capability of operating at high voltage levels to achieve high output-power levels. As with silicon laterally diffused metal-oxide-semiconductor (LDMOS) devices, GaN active devices are capable of output-power levels of tens to hundreds of watts, but with a fraction of the input and output capacitances of those Si LDMOS devices, for high output power over broad bandwidths and with high efficiency.

With +48-VDC GaN devices now available, design engineers have further options using GaN devices in commercial and military applications. Understanding the differences between these emerging +48-VDC GaN devices compared to existing +28-VDC GaN devices can help in matching these higher-voltage devices to suitable applications.

These higher +48-VDC drain supply voltages offer both obvious and subtle benefits. Because device channel size is largely set by peak current requirements, a higher supply voltage reduces the transistor size required for a given RF power rating. *Table 1* shows how power density, as measured by gate periphery for typical GaN-on-Si devices, approximately scales by the voltage ratio.

Migrating existing +28-VDC processes to allow for +48-VDC operation requires redesigning the device structure to improve reliability due to the increased electric field. In the X-Y direction, the underlying substrate, epitaxial structure, and channel characteristics remain largely the same for higher-voltage operation, with increased gate-to-drain spacing needed to raise the breakdown voltage. In the Z-direction (vertically), the gate oxide is thickened and changes to the gate metal allow for both higher reliability and increased standoff voltages.

Of greater importance to RF/microwave amplifier designers, *Table 1* shows that device output capacitance (C_{OUT}) scales by device size. Because of the increased power density, the resulting C_{OUT} for a given power level is reduced. This reduction in output capacitance is the largest differentiator for higher-voltage operation since the resulting change in load impedance offers a major advantage in device operation.

Perhaps the biggest challenge that designers face at higher power levels and frequencies is matching the low output

TABLE 1: ASSESSING VOLTAGE-RELATED PARAMETERS FOR +28- AND +48-VDC GaN-ON-Si DEVICES

	28 V	48 V	Units of measure
Power density	3	4.5	W/mm
I_{DQ} (typical)	20-25	20-25	mA/mm
C_{OUT}	0.6	0.5	pF/mm
Gate-drain spacing	1	1.55	(relative)

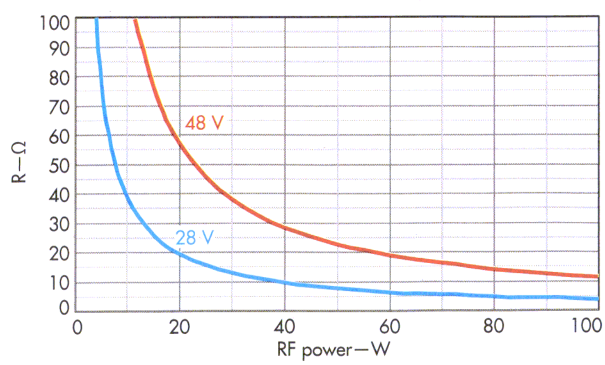

1. These curves compare load resistance versus output power for active devices operating with +28- and +48-VDC supplies.

on-Si Devices

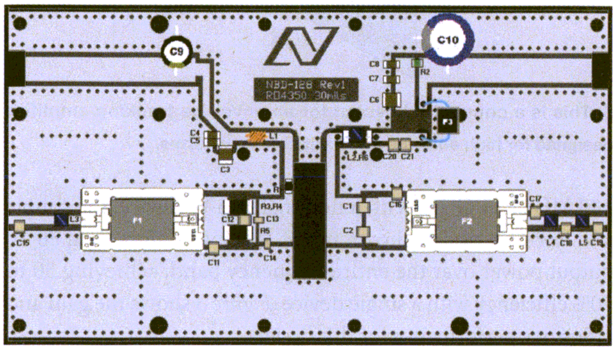

2. This reference design provides 80 W broadband output power at +48 VDC with high efficiency.

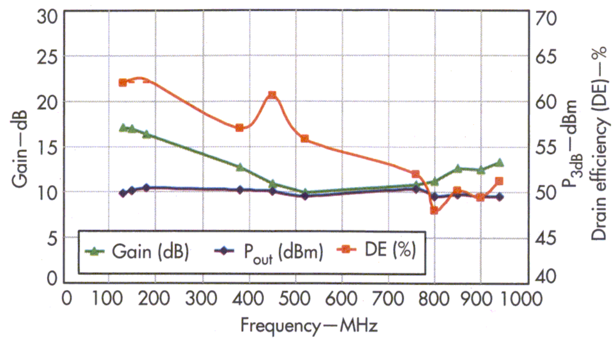

3. These curves show the gain, output power, and efficiency for the reference design from 100 MHz to 1 GHz.

impedances of larger devices. A parallel resistor-capacitor (R-C) circuit is a good model for the transistor output, corresponding to the equivalent R with C_{OUT} *(Table 1)*. Given the supply voltage (V) and desired power (P) of an ideal amplifier, a simple equation estimates the output resistance (R_{OUT}):

$P \approx V^2/2R_{OUT}$ (1)

Figure 1 plots R_{OUT} for both +28- and +48-VDC device operation across a typical output-power range. It shows how an amplifier designed for +28-VDC operation is well optimized for output-power levels of 8 to 10 W, requiring minimal impedance transformation for 50-Ω systems. It becomes obvious from *Fig. 1* how +48-VDC operation is capable of nearly 25-W output power with minimal impedance matching needed for the same 50-Ω system compared to +28-VDC operation.

In addition to increased R_{OUT}, +48-VDC operation also provides further benefits that can ease matching complexity. All things being equal, the usable bandwidth for an amplifier is fundamentally limited by the metrics of impedance transformation ratio and device quality factor (Q):

Impedance transformation ratio = $Re(Z_{DEVICE})/50\ \Omega$ Device Q, where $Q \approx Im(Z_{DEVICE})/Re(Z_{DEVICE})$ and $Z_{DEVICE} \approx R_{OUT} + 1/j\omega C_{OUT}$ (2)

The impact of these limitations varies with frequency, but there are general trends. With +28-VDC devices, the transformation ratio becomes the limiting factor—i.e., low R_{OUT} tends to limit the available bandwidth. With +48-VDC devices, smaller C_{OUT} and larger R_{OUT} mitigate both factors, and device Q tends to set the limit. Parameter C_{OUT} limits the usable maximum frequency in all cases.

A further complication arises at higher power levels—typically around 100-W device output power. At this level, R_{OUT} and C_{OUT} for +28-VDC devices result in low output impedances that approach 2 Ω or less, making it difficult to achieve impedance matching for 50-Ω systems. A typical +28-VDC LDMOS device at 100 W adds an output impedance prematch to provide an amplifier designer more reasonable terminal impedances. The added complexity increases the package size, however, nearly doubling the printed-circuit-board (PCB) area needed for a +28-VDC device for the same power level.

Comparing +28- and +48-VDC devices—looking only at the resistance and capacitance characteristics of the amplifying die—it is possible to show that the available bandwidth for a given mismatch also follows the voltage ratio. A +48-VDC device will provide about 70% increased bandwidth potential compared to an equivalent powered +28-VDC device.

If the system requires only moderate bandwidth, there are still good reasons for using a +48-VDC solution. The lower Q or transformation ratio allows for more simplistic matching topologies since the load impedances require less transformation. These simplistic topologies also tend to be more resistant to manufacturing tolerances (i.e., PCB and matching component variations due to assembly).

For a realistic comparison, *Table 2* shows fundamental properties for two similar 100-W GaN-on-Si devices, the +28-VDC model NPT1010 and +48-VDC model NPT2010 devices. Both devices use a 100-W die with no output impedance prematching and the same substrate thickness, die attach tech-

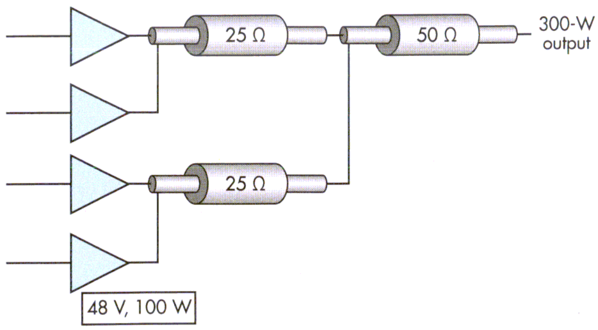

4. This is a wideband quad combining configuration for four +48-VDC, 100-W power devices.

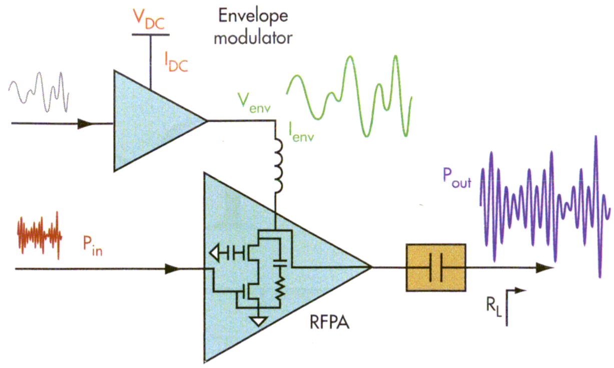

5. This is a conceptual design for an envelope tracking amplifier designed for high efficiency with variable waveforms.

nique, and metal air cavity package. Among these measures, two differences stand out. The optimum load impedance of the +48-VDC device is significantly higher with the ratio of the real part at 3:1, consistent with theory.

The second obvious difference is thermal resistance ($R_{\theta JC}$). This is the exception in the comparison of devices, whereby the smaller +48-VDC die can push performance in the wrong direction on account of more power being produced in a smaller area. Both devices are designed to operate with adequate margin to achieve rated output power levels below maximum rated junction temperatures for a given ambient condition.

A significant thermal limitation for these high-power devices is the AC360 air-cavity flange package. The limitations of the package serve as a reminder of the need for more enhanced thermal packaging techniques to further enhance +48-VDC device operation.

In addition to enabling broader bandwidths, higher output impedances also enable alternative matching topologies, some of which were previously impractical. One of these, for example, is a broadband amplifier targeting 90-W output power from 100 MHz to 1 GHz. A ferrite-based impedance transformer is the best choice for a decade-plus bandwidth in the VHF/UHF bands. These topologies are ideally suited for N^2:1 impedance ratios such as 1:1, 4:1, and 9:1.

From Eq. 1, an amplifier based on +28-VDC devices would require a load resistance of about 4.5 Ω, and 9:1 would be the ideal ratio for a transformation to 50 Ω. But a 9:1 impedance transformer is difficult to realize. The higher permeability materials needed to enable the low-frequency transformation become lossy at high frequencies, preventing full band coverage.[1] Realistically, a high-power ferrite transformer with 9:1 transformation ratio will suffer from high loss and struggle to work above a few hundred MHz.

With a +48-VDC drain supply, the load resistance is much higher, nearly 12.5 Ω, and a lower-ratio 4:1 transformer is better suited to make the impedance transformation to 50 Ω. This lower transformer ratio is ideal for frequency coverage from 100 MHz to 1 GHz. With a nominal 100-W device, the simple and low-cost design shown in *Fig. 2* delivers more than 80 W output power over the entire frequency band, achieving 50 to 70% efficiency with a single device. *Figure 3* shows the gain and efficiency performance for this design.

A balanced design (push-pull) amplifier configuration also benefits from higher output impedances. Two +48-VDC devices, each with 12.5-Ω load resistance at 90-W output power, present an impedance of 25 Ω to the primary in a push-pull configuration. *Figure 4* shows how four devices can be set in a balanced push-pull configuration combined using coaxial sleeve baluns, allowing operation over a wide bandwidth.[2] Higher output impedances enable other transmission-line transformer and combinational networks. Depending on the frequency band and required bandwidth, many tailored topologies are available for consideration.[3]

Power amplifiers (PAs) for wireless infrastructure applications with wideband-code-division-multiple-access (WCDMA), Long Term Evolution (LTE), orthogonal-frequency-division-multiplex (OFDM), and other high-peak-to-average (PAR) waveforms face a real challenge. Achieving even modest

TABLE 2: COMPARING +28- AND +48-VDC GaN-ON-Si DEVICES

	NPT1010	NPT2010	Units of measure
V_{DD}	28	48	V
P_{SAT} at 900 MHz	100	125	W
Efficiency at P_{SAT}	70	71	%
Typical quiescent bias	700	600	mA
Small-signal gain	21	22	dB
Z_L	1.9 + j0.6	5.7 + j3.2	Ω
$R_{\theta JC}$	1.4	1.75	°C/W

amplifier efficiency is difficult when the RF amplifier is appropriately sized for peak power levels that are 8 to 10 dB higher than the average power level.

Envelope tracking (ET) is one of several effective techniques to address this issue. ET raises and lowers the drain voltage to follow the instantaneous peak amplitude of the device, effectively adjusting the compression point of the amplifier in real time to increase amplifier efficiency *(Fig. 5)*. A peak-to-average ratio (PAR) of 10 dB, or 10×, implies a voltage ratio of approximately 3:1. This is a typical ratio seen in commercial systems.

For ET with +28-VDC devices, the drain supply typically varies between +10 and +30 VDC. This presents a problem for both GaN and LDMOS devices at the low end of this range because small-signal gain becomes nonlinear as a function of supply voltage. Above about +12 VDC, the gain increases linearly with voltage, but below +10 to +12 VDC, the gain enters a nonlinear region and can drop several dB below its nominal level at higher voltages. The statistical nature of a high-PAR signal implies an ET PA operates in this low-voltage region most of its time, thus encountering this unwelcome nonlinear gain condition. With a +48-VDC device, a typical ET system varies the drain between +20 and +60 VDC and the minimum voltage remains well above the onset of the nonlinear gain condition.

A +48-VDC GaN device provides an additional benefit over an LDMOS device because of the reduced C_{OUT} of the device. As mentioned previously, the higher C_{OUT} of LDMOS devices mandates internal pre-matching on the output to provide more friendly terminal impedances. The chosen topology for this output pre-match is usually a shunt-L match in the RF path. The shunt-L is designed to resonate with C_{OUT} to improve the terminal impedance.

All active transistor devices have terminal capacitances that vary versus applied voltage. When the drain supply voltage is modulated to follow the signal envelope, the drain-to-source capacitance (C_{DS}) also varies and the shunt inductance (L) resonance is impacted, changing the terminal impedance of the device in real-time with the drain voltage. This leads to a nonoptimal impedance match for ET applications.[5]

In addition, because the shunt-L match requires a large shunt DC-blocking capacitor, there is additional strain on the envelope modulator design *(Fig. 5)*, which is already challenged to swing large voltages with high current capability at high data bandwidths. The large blocking capacitor prevents the envelope modulator from being able to raise and lower the supply voltage in time with the modulation bandwidth. The low C_{OUT} of GaN devices means this matching topology is not needed, making +48-VDC GaN devices inherently optimized for ET applications.

A transition to a +48-VDC drain supply may raise concerns given the higher voltage. Although there may be thoughts that a higher voltage causes additional stress and lower reliability, this has not been found to be the case. Between +28 and +48 VDC, no difference has been found in DC reliability studies, with both voltage optimized technologies achieving 1×10^6 hours mean time before failure (MTBF) at a junction temperature of +200°C.

It is important for RF system design engineers to realize the connection between junction temperature and device reliability. The key to reliable design is maintaining device junction temperature below specified limits. Designers need to monitor ambient temperature and operating conditions (power dissipation) to guarantee reliable operation.[6]

Compared to +28-VDC devices, +48-VDC devices are physically smaller for a given RF power rating and the advantages of performance come primarily from this difference. This flows down into every aspect of the device, from the difficulty and performance of the impedance match to the usable bandwidth and relative achievable performance.

Legacy commercial and military RF systems are well rooted in the use of +28-VDC power-amplifying devices. While LDMOS and GaN device suppliers will continue to support and increase +28-VDC offerings, new systems with the flexibility to do so should consider higher-voltage devices like the +48-VDC GaN-on-Si offerings. mw

REFERENCES

1. Jerry Sevick, Transmission Line Transformers, 4th ed., Scitech Publishing, Raleigh, NC, 2001.
2. Amin K. Ezzeddine and Ho C. Huang, "10-W Ultra-Broadband Power Amplifier," IEEE MTT-S International Microwave Symposium Digest, 2008, pp. 643-646.
3. Chris Trask, "Designing Wide-band Transformers for HF and VHF Power Amplifiers," QEX March/April 2005, pp. 3-15.
4. Jonmei J. Yan, Chin Hsia, Donald F. Kimball, and Peter M. Asbeck, "Design of a 4-W Envelope Tracking Power Amplifier With More Than One Octave Carrier Bandwidth," IEEE Journal of Solid-State Circuits, Vol 47, No. 10, October 2012, pp. 2298-2308.
5. Jeffrey B. Shealy, Michael Lefevre, Bobby Anderson, David W. Runton, Matthew J. Poulton, and James Martin, "Optimization of gallium nitride high power technology for commercial and military applications," Proceeding of Bipolar/BiCMOS Circuits and Technology Meeting, 2009. IEEE BCTM 2009.
6. "GaN Essentials, AN-012: Thermal Considerations for GaN Technology," www.nitronex.com.

FANGFANG FAN | Doctor WEI WANG | Master ZEHONG YAN | Professor
Science and Technology on Antennas and Microwave Laboratory, Xidian University, Xi'an, Shaanxi, 710071, People's Republic of China; e-mail: fffan@mail.xidian.edu.cn, www.xidian.edu.cn

SIW Fashions CP X-Band Antenna

This antenna, which is relatively simple to fabricate with standard circuit materials, is a high-gain candidate for use in satellite-communications applications.

Novel transmission-line structures, such as those employing substrate-integrated-waveguide (SIW) technology, can equip antennas with high gain at high frequencies for a variety of communications applications. To demonstrate, a square ring-slot, single-layer, circularly polarized SIW antenna was designed and developed for X-band applications. Through the use of two shorted square ring-slots in the top wall of the SIW substrate, along with shorting via holes, a circularly polarized (CP) antenna design was achieved. The antenna features a good radiation pattern with high gain, with measured impedance bandwidth of 6.5% and axial ratio (AR) bandwidth of 1.5%. This high-gain antenna is suitable for satellite-communications (satcom) applications at X-band frequencies.

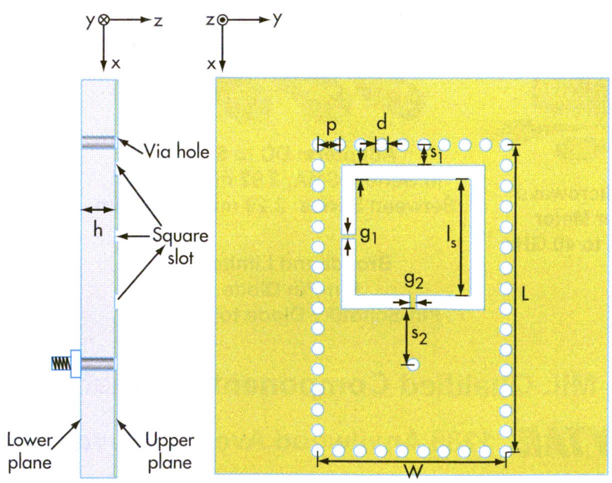

1. The key parameters of the SIW CP antenna are detailed in these side (left) and top (right) views.

Additionally, CP antennas are used in radar and other communications applications. They are useful since they can resolve problems in wireless channels such as polarization mismatch generated by Faraday effects and interference generated by multipath effects. SIW technology, as first proposed by Wu,[1] enables easy integration with planar circuits by replacing conventional microstrip and stripline transmission-line designs.

SIW technology features lower cost than conventional waveguide, with low loss, high-power capacity, and high quality factor (Q). In fact, SIW-based CP antennas have been reported by various researchers.[2-7]

These designs employed different approaches for CP performance. In ref. 2, for example, a 16-element top-wall SIW slot antenna used two compounded slot pairs to obtain CP performance centered at 16 GHz, albeit with a usable impedance bandwidth of just 2.3%. In ref. 3, a single grounded coplanar waveguide (CPW) structure was used to feed an X-band cavity-backed crossed-slot antenna, although this structure also suffered from a narrow impedance bandwidth of less than 3%, along with a narrow axial ratio (AR) bandwidth of about 1% for an AR of less than 3 dB.

NOW **USB & ETHERNET**

RF SWITCH MATRIX

Efficiency for your test setup. Economy for your budget.

DC to 18 GHz from $385 ea.

We're adding more models and more functionality to our line of RF switch matrices. All models now feature switch cycle counting with automatic calibration interval alerts based on actual usage, an industry first! This function improves test reliability and saves you money. Our new RC-series models feature both USB and Ethernet control, so you can run your test setup from anywhere in the world! Rugged aluminum cases on all models house our patented mechanical switches with extra-long life of 10 years/100 million cycles of guaranteed performance!*

Our easy-to-install, easy-to-use GUI will have you up and running in minutes for step-by-step control, full automation, or remote operation. They're fully compatible with most third-party lab software,† adding capabilities and efficiency to existing setups with ease! Visit minicircuits.com today for technical specifications, performance data, quantity pricing, and real time availability – or call us to discuss your custom programming needs – and think how much time and money you can save!

USB Control Switch Matrices

Model	# Switches (SPDT)	IL (dB)	VSWR (:1)	Isolation (dB)	RF P_{MAX} (W)	Price $ (Qty. 1-9)
USB-1SPDT-A18	1	0.25	1.2	85	10	385.00
USB-2SPDT-A18	2	0.25	1.2	85	10	685.00
USB-3SPDT-A18	3	0.25	1.2	85	10	980.00
USB-4SPDT-A18	4	0.25	1.2	85	10	1180.00
USB-8SPDT-A18	8	0.25	1.2	85	10	2495.00
NEW USB-1SP4T-A18	1 (SP4T)	0.25	1.2	85	2	795.00

NEW USB and Ethernet Control Switch Matrices

Model	# Switches (SPDT)	IL (dB)	VSWR (:1)	Isolation (dB)	RF P_{MAX} (W)	Price $ (Qty. 1-9)
RC-1SPDT-A18	1	0.25	1.2	85	10	485.00
RC-2SPDT-A18	2	0.25	1.2	85	10	785.00
RC-3SPDT-A18	3	0.25	1.2	85	10	1080.00
RC-4SPDT-A18	4	0.25	1.2	85	10	1280.00
RC-8SPDT-A18	8	0.25	1.2	85	10	2595.00
RC-1SP4T-A18	1 (SP4T)	0.25	1.2	85	2	895.00

*The mechanical switches within each model are offered with an optional 10 year extended warranty. Agreement required. See data sheets on our website for terms and conditions. Switches protected by US patents 5,272,458; 6,650,210; 6,414,577; 7,633,361; 7,843,289; and additional patents pending.

†See data sheet for a full list of compatible software

Mini-Circuits®

www.minicircuits.com P.O. Box 35166, Brooklyn, NY 11235-0003 (718) 934-4500 sales@minicircuits.com

521 rev A

"CP antennas are used in radar and other communications applications. They are useful since they can resolve problems in wireless channels, such as polarization mismatch generated by Faraday effects and interference generated by multipath effects."

In refs. 4-6, shorting via holes were used to connect the metal area bounded by the ring-slot at the top wall and the bottom wall of SIW to obtain a CP wave, so the locations of the shorting via holes and fabrication errors associated with them greatly affected the CP characteristics.

In ref. 5, the authors studied SIW cavity-backed antennas using microstrip-to-SIW and coaxial-to-SIW transitions. A good level of cross-polarization was obtained with the coaxial-to-SIW transition, with antenna gain of about 7 dBi. The AR bandwidth and the impedance bandwidth were almost the same as for a circular ring-slot antenna.[4] However, the antenna occupies a relatively large area, and its design is complex.

In the present report, a square ring-slot SIW CP antenna was developed for X-band applications. Two shorted strips are etched into the slot to obtain the CP wave. The design is simple, and fabrication for the shorted strip is easier than for the antenna with the shorting via hole.

Figure 1 shows the antenna's geometrical configuration (side view on left and top view on right). The overall size of the SIW antenna is 34 × 34 mm^2. It consists of three parts: the SIW structure, the square ring-slot with two shorted strips, and a coaxial feeding probe. The SIW is created by two rows of via holes, with its one end shorted.

Parameter P is the distance between two via holes and d is the diameter of the via holes, while parameters W and L represent the width and length of the SIW structure, respectively. These SIW values should imply that it operates in fundamental mode, TE_{10}. Parameters g_1 and g_2 are the length of the shorted strips, and their width is as long as the width of the ring-slot denoted as w_s.

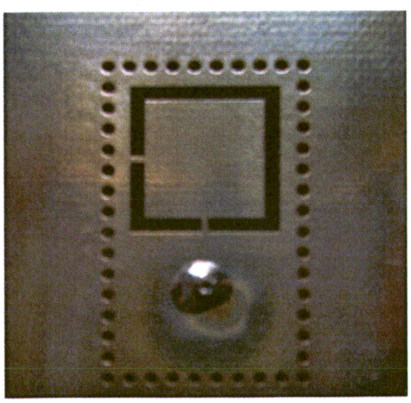

2. The SIW antenna was fabricated on TLX-8 PCB material from Taconic Advanced Dielectric Division (www.taconic-add.com).

Next, the distance that's between the feeding probe and the bottom of the square ring-slot is denoted as s_2, and it is located in the center of the SIW in the y-direction. Parameter s_1 is the distance between the top of the square ring-slot and the shorted end, with the inner dimension of the square ring-slot denoted as l_s.

The antenna was designed with the help of Version 10.0 of the High-Frequency Structure Simulator (HFSS) finite-element-method (FEM) simulation software from ANSYS (www.ansys.com). It is based on TLX-8 printed-circuit-board (PCB) material from Taconic Advanced Dielectric Division (www.taconic-add.com) with a relative permittivity of 2.55. A height of 1.52 mm was used for the antenna.

During computer simulation and optimization, it was concluded that parameter l_s affects the operating frequency of the antenna, while parameters g_1 and g_2 determine the quality of the CP wave. The final parameter values for the antenna are shown in the *table*.

Figure 2 shows the fabricated SIW antenna, with an SMA connector soldered to the feed port. The voltage standing wave ratio (VSWR) was measured with the assistance of a model E8363B vector network analyzer (VNA) from Agilent Technologies (www.agilent.com).

Figure 3 shows the simulated and measured VSWR results, where it can be seen that the measured impedance bandwidth with VSWR less than 2.0:1 is 6.5% (from 9.04 to 9.64 GHz). A measured frequency that is higher than the simulated fre-

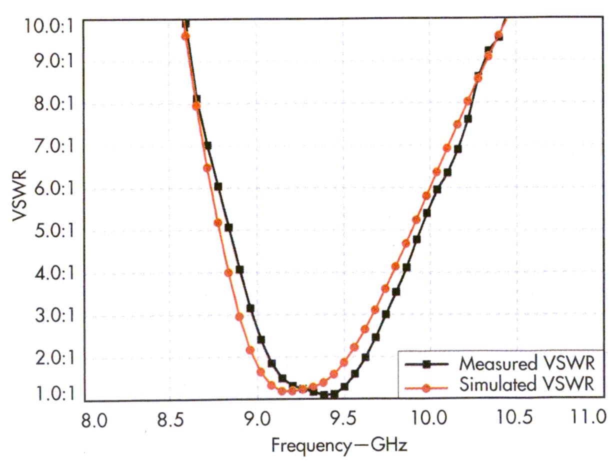

3. The antenna's measured VSWR is compared with its computer simulated performance.

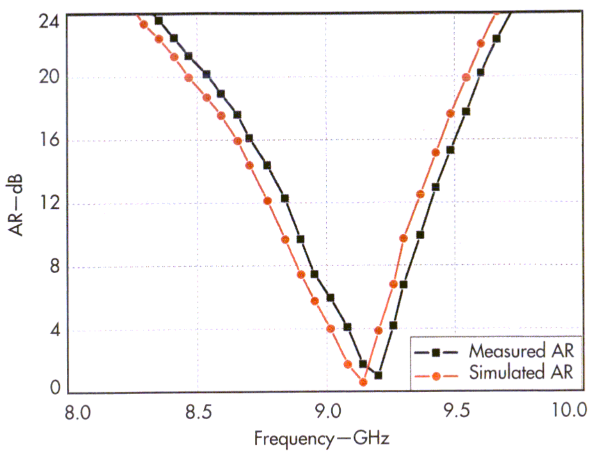

4. These plots show the simulated and measured AR versus frequency for the SIW antenna.

quency range may be due to the tolerance error in the manufacturing process of the SIW structure.

Figure 4 shows that the measured AR also appears as a frequency shift from the simulated AR, and the AR bandwidth is 1.5%. *Figure 5* delineates simultaneously right-handed-circular-polarization (RHCP) and left-handed-circular-polarization (LHCP) gains for the SIW antenna in the xz- and yz-planes at 9.2 GHz. It indicates that the SIW antenna radiates an RHCP wave with cross polarization in the boresight direction. The measured gain is 8.05 dBi in the boresight direction at 9.2 GHz.

In summary, the SIW antenna is relatively simple and easy to fabricate and provides performance suitable for satcom applications at X-band frequencies. It achieves high gain at 9.2 GHz with a 6.5% impedance bandwidth and 1.5% AR bandwidth, with gain of 8.05 dBi at boresight with low cross-polarization. Through its use of a novel shorting configuration and SIW substrate technology to achieve the CP wave, the CP antenna can be fabricated with a relatively low profile and compact structure on standard PCB material. mw

ACKNOWLEDGMENTS

This work was supported by the National Natural Science Foundation of China Project (Grant No. 61301068) and the Fundamental Research Funds for the Central Universities (Grant Nos. K50511020018 and K5051302075).

REFERENCES

1. F. Xu and K. Wu, "Guided-wave and leakage characteristic of substrate integrated waveguide," IEEE Transactions on Microwave Theory and Techniques, Vol. 53, No. 1, January 2005, pp. 66-73.
2. Chen Peng, Hong Wei, Kuai Zhenqi, et al., "A substrate integrated waveguide circular polarized slot radiator and its linear array," IEEE Antennas and Wireless Propagation Letters, Vol. 8, 2009, pp. 120-123.
3. G.Q. Luo, Z.F. Hu, Y. Liang, L.Y. Yu, and L.L. Sun, "Development of low profile cavity backed crossed slot antennas for planar integration," IEEE Transactions on Antennas and Propagation, Vol. 57, No. 10, October 2009, pp. 2972-2979.
4. D. Kim, J. W. Lee, C.S. Cho, et al., "X-band circular ring-slot antenna embedded in single-layered SIW for circular polarization," Electronics Letters, Vol. 45, No. 13, June 2009, pp. 668-669.
5. D. Kim, J. W. Lee, T.K. Lee, et al., "Design of SIW cavity-backed circular-polarized antennas using two different feeding transitions," IEEE Transactions on Antennas and Propagation, Vol. 59, No. 4, April 2011, pp. 1398-1403.
6. Jaroslav Lacik, "Circularly polarized SIW square ring-slot antenna for X-band applications," Microwave and Optical Technology Letters, Vol. 54, No. 11, November 2012, pp. 2590-2593.
7. Yue Li, Zhi Ning Chen, Xianming Qing, et al., "Axial ratio bandwidth enhancement of 60-GHz substrate integrated waveguide-fed circularly polarized LTCC antenna array," IEEE Transactions on Antennas and Propagation, Vol. 60, No. 10, October 2012, pp. 4619-4626.

SUMMARIZING THE SIW ANTENNA'S PARAMETERS

Parameter	W	L	L_s	W_s	p	d	G_1	G_2	S_1	S_2
Value (mm)	16.2	26.4	10	1.2	1.8	1	0.5	0.5	1.7	4.8

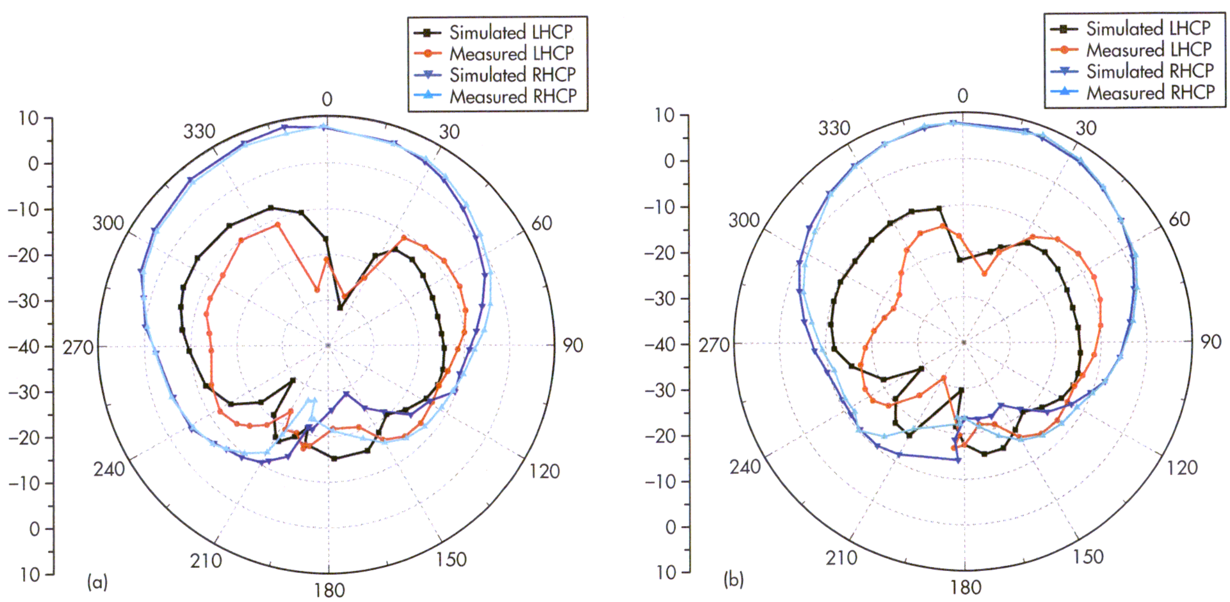

5. These plots show the SIW antenna's simulated and measured radiation patterns at 9.2 GHz (in the xz and yz planes).

ULTRA WIDE BANDWIDTH VCO

Model	Frequency Range (MHz)	Tuning Voltage (VDC)	DC Bias (VDC)	Typical Phase Noise @10kHz (dBc/Hz)
DCMO25-5	20 -50	0.5 - 24	+5 @ 40 mA	-114
DCMO514-5	50 -140	0.5 - 24	+5 @ 35 mA	-110
DCMO616-5	65 -160	0.5 - 24	+5 @ 35 mA	-108
DCMO1027	100 -270	0.5 - 24	+5 - 12 @ 25 mA	-112
DCMO1129	110 -330	0.5 - 24	+5 - 12 @ 27 mA	-112
DCMO1545	150 -450	0.5 - 24	+5 - 12 @ 35 mA	-108
DCMO1857	180 -560	0.5 - 24	+5 - 12 @ 32 mA	-108
DCYR2060-5	200 -600	0.5 - 28	+5 @ 65 mA	-119
DCMO2260-5	220 -600	0.5 - 24	+5 @ 35 mA	-108
DCMO2476	240 -760	0.5 - 24	+5 - 12 @ 27 mA	-108
DCMO2550-12	250 -500	0.5 - 20	+12 @ 37 mA	-112
DCMO3288-5	320 -880	0.5 - 24	+5 @ 28 mA	-109
DCMO3288-12	320 -880	0.5 - 24	+12 @ 39 mA	-105
DCFO35105-5	350 -1050	0.5 - 25	+5 @ 60 mA	-110
DCMO40110-5	400 -1100	0.5 - 24	+5 @ 45 mA	-103
DCMO40110-8	400 -1100	0.5 - 24	+8 @ 45 mA	-104
DCMO40110-12	400 -1100	0.5 - 24	+12 @ 45 mA	-105
DCMO50120-5	500 -1200	0.5 - 24	+5 @ 40 mA	-102
DCMO50120-12	500 -1200	0.5 - 24	+12 @ 35 mA	-103
DCYR50125-10	500 -1250	0.5 - 24	+10 @ 45 mA	-110
DCMO60170-5	600 -1700	0.5 - 25	+5 @ 40 mA	-100
DCMO60170-12	600 -1700	0.5 - 24	+12 @ 35 mA	-102
DCMO80210-5	800 -2100	0.5 - 24	+5 @ 35 mA	-96
DCMO80210-10	800 -2100	0.5 - 24	+10 @ 35 mA	-100
DCMO90220-5	900 -2200	0.5 - 24	+5 @ 35 mA	-98
DCMO90220-12	900 -2200	0.5 - 24	+12 @ 35 mA	-99
DCMO92200-12	925 -2000	0.5 - 18	+12 @ 35 mA	-101
DCMO100230-5	1000 -2300	0.5 - 24	+5 @ 35 mA	-98
DCMO100230-12	1000 -2300	0.5 - 24	+12 @ 35 mA	-101
DCYS100200-12	1000 -2000	0.5 - 28	+12 @ 40 mA	-105
DCMO110250-5	1100 -2500	0.5 - 28	+5 @ 35 mA	-100
DCMO110250-8	1100 -2500	0.5 - 28	+8 @ 35 mA	-102
DCMO130275-5	1300 -2750	0.5 - 24	+5 @ 30 mA	-93
DCMO135270-8	1350 -2700	0.5 - 20	+8 @ 40 mA	-93
DCMO150318-10	1500 -3100	0.5 - 22	+10 @ 35 mA	-96
DCMO150318-5	1500 -3200	0.5 - 20	+5 @ 30 mA	-93
DCMO150320-5	1500 -3200	0.5 - 18	+5 @ 60 mA	-92
DCYS160360-5	1600 -3600	0.5 - 20	+5 @ 60 mA	-94
DCMO170340-3	1700 -3400	0.5 - 20	+3.5 @ 20 mA	-85
DCMO170345-5	1700 -3450	0.5 - 16	+5 @ 50 mA	-88
DCMO172332-5	1720 -3320	0.5 - 24	+5 @ 30 mA	-94
DCMO190410-5	1900 -4100	0.5 - 18	+5 @ 50 mA	-90
DCYS200400-5	2000 -4000	0.5 - 16	+5 @ 50 mA	-90
DCYS200400P-5	2000 -3900	0.5 - 22	+5 @ 60 mA	-93
DCMO250512-5	2500 -5125	0.5 - 14	+5 @ 55 mA	-76
DCYS250500-5	2500 -5000	0.5 - 14	+5 @ 55 mA	-76
DCYS250510-5	2500 -5100	0.5 - 16	+5 @ 55 mA	-78
DCYS300600-5	3000 -6000	0.3 - 17	+5 @ 50 mA	-75

Patented Technology

SYNERGY®
MICROWAVE CORPORATION

Phone: (973) 881-8800 | Fax: (973) 881-8361
E-mail: sales@synergymwave.com
Web: WWW.SYNERGYMWAVE.COM
Mail: 201 McLean Boulevard, Paterson, NJ 07504

PCBs AT MICROWAVE FREQUENCIES: DESIGN GUIDELINES

LAMINATE PRINTED-CIRCUIT BOARDS (PCBs) are a commonly used substrate for designing low-cost subsystems that can operate to 40 GHz. With their ability to support high-performance surface-mount technology packages (SMTs) containing RF integrated circuits (ICs) while supporting a wide range of interface connections, PCBs are ideal for many RF/microwave applications. However, significant considerations must be applied to every step of the design to ensure proper operation. Such considerations have grown due to the reduction in size of RF ICs, which has led to a reduction in parasitic capacitance and a subsequent increase in attainable frequencies of operation. In a seven-page application note titled "Technology Overview Designing Laminate PCBs at Microwave Frequencies," Plextek details some of these critical design considerations.

If appropriate measures are not taken, for example, grounding inductances can induce a series inductive feedback around an RF SMT IC. Two possible approaches to help reduce grounding inductances are the use of an array of tightly spaced vias within the groundplane of the SMT IC and selecting a suitably thin substrate height to reduce the individual via inductances. Knowing the level of tolerable grounding inductance and how to estimate the grounding inductance are necessary metrics to design with cost efficiency and timeliness.

Plextek Consulting
London Road,
Great Chesterford,
Essex CB10 1NY, UK
+44 1799 533200
www.plextek.com

The exact material and sizes of the PCB substrate also are critical for effective RF PCB design. Modern RF PCB substrates are well suited to mass manufacture and generally have dielectric constants around 3.5. To ensure appropriate operation of on-PCB transmission lines or microstrip waveguides, the maximum substrate thickness should be less than one-tenth of the highest wavelength of operation.

The thickness of the copper metallization, known as weights of copper cladding, must be known to design according to the required direct-current carrying capability as well as the maximum skin depth. The exact dimensions of the pads and metallization of attached discrete components and printed components correlate directly to the parasitic elements within the circuitry. They must therefore be accounted for accordingly. Based on the frequencies of operation, connections made with external devices (which usually incorporate on-board coaxial connections) and adequate grounding and mechanic attachment strength also should be taken into consideration.

SURVEY PROVIDES IN-DEPTH OVERVIEW OF SPECTRUM ANALYZERS

MODERN SPECTRUM ANALYZERS have capabilities far beyond the frequency-selective and peak-responding voltmeters that are calibrated to display RMS values of their sine waves of origin. A swept-tuned spectrum analyzer uses a superheterodyne receiver to down-convert the spectrum of the input signal to the center frequency of a band-pass filter using a mixer and voltage-controlled oscillator. The 120-page application note by Agilent, "Application Note 150: Spectrum Analysis Basics," offers a rigorous walk-through of the capabilities and understanding behind the operation of swept-tuned superheterodyne spectrum analyzers. Analyzing electrical signal spectra can give the designer valuable information on the spectral components of a signal not easily detectable in time-domain waveforms.

Agilent Technologies
5301 Stevens Creek Blvd.
Santa Clara, CA 95051
(408) 345-8886
www.agilent.com

A spectrum is a properly combined collection of sine waves that produce a desired time-domain signal. The value of monitoring a spectrum lies in the ability to measure the energy throughout a frequency domain. For example, this knowledge is necessary in determining if signal energy is spilling into other frequency bands for cellular communications and to determine what interference with other electronics can be expected during device operation.

Spectrum analyzers are made from hundreds of high-precision and high-performing parts, which are carefully matched and tuned to maintain optimum performance. These complex parts all play a role in measuring the various aspects of the signal response of a device under test. To meet modern demands, spectrum analyzers have included many of the capabilities traditionally held by vector signal analysis and Fourier signal analyzers—for example, the all-digital intermediate-frequency operation, which Agilent claims to have implemented with many operational benefits. Some of these benefits include a combination of Fast Fourier Transform analysis for narrow spans and swept analysis for wide spans for a more optimal approach. Other modern spectrum analyzers also sport application-specific measurement functions such as vector signal analysis and adjacent channel power.

Overall, the note strives to provide an in-depth summary of the building blocks of spectrum-analyzer operation, covering amplitude/frequency accuracy, sensitivity/noise, dynamic range, and frequency range. Included is a special dedication to the note's original author Blake Peterson, who received the *Microwaves & RF* "Living Legend" award in June 2013.

Cover Story

ULRICH ROHDE
Chairman

AJAY PODDAR
Chief Scientist

DORIN CALBAZA
Senior Design Engineer

Synergy Microwave Corp., 201 McLean Blvd., Paterson, NY 07504; (973) 881-8800, FAX: (973) 881-8361, E-mail: sales@synergymwave.com, www.synergymwave.com

Searching For Low-Phase

A hybrid approach shows great promise in achieving frequency synthesized microwave signals with low phase both close to and far from the carrier.

Clean, quiet frequency synthesizers are essential for modern communications systems. But the performance of RF/microwave frequency synthesizers is often tied to a lower-frequency reference oscillator, such as an oven-controlled crystal oscillator (OCXO), and great effort is often required to produce a microwave frequency synthesizer with low phase noise. To demonstrate, a 10.24-GHz frequency synthesizer with OCXO reference source was developed, and the design path to that synthesizer will be traced.

Phase noise is a vital parameter for oscillators and synthesizers in communications and other systems. It is measured as the ratio between the power density in one phase noise modulation sideband, per hertz, and total signal power.[1] Typically, a wideband synthesizer will exhibit more noise than a single-frequency synthesizer. When low noise is required, a single-frequency synthesizer can be combined with frequency mixers to build a wideband synthesizer with low noise.

The phase noise of the signal produced by the synthesizer is determined by the performance of the oscillator used to build the synthesizer, the performance of the reference, and the transfer characteristic and intrinsic noise of the synchronization method. Major contributors to phase noise are the internal oscillator and the reference source (for noise offset far from and close to the carrier, respectively). An OCXO may be used as the reference for low-noise applications, possibly locked to a rubidium clock or a 1-pulse-per-second GPS source.

The phase noise performance of the oscillators has a fundamental limit imposed by the Johnson-Nyquist theory. A resistor at room temperature (300 K) produces about −173.82-dBm/Hz noise, with this power level equally split in two sidebands. A signal with 0-dBm power will have a lower phase-noise limit of −177 dBc/Hz, improving upon −177 dBc/Hz only if the signal carries more than 0-dBm power, as with some low-noise OXCOs.[2,3] The best low-noise oscillators are capable of approaching this limit at far offset frequencies. For close-in frequency offsets the phase noise will be determined by the quality factor (Q) of the resonator.

The frequency offset at which the phase noise approaches the theoretical limit is roughly proportional to the frequency of the oscillator, increasing as the frequency increases. *Figure 1* shows typical performance levels for different low-noise oscillators, including a 100-MHz OCXO, a 1-GHz surface-acoustic-wave (SAW) oscillator, a 10-GHz dielectric-resonator oscillator (DRO), a 10.24-GHz sapphire oscillator (SO), and a 10-GHz opto-electronic oscillator (OEO).[4-10]

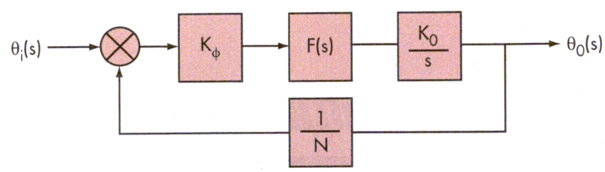

3. This block diagram represents a second-order phase-locked loop (PLL) for low-noise frequency synthesis.

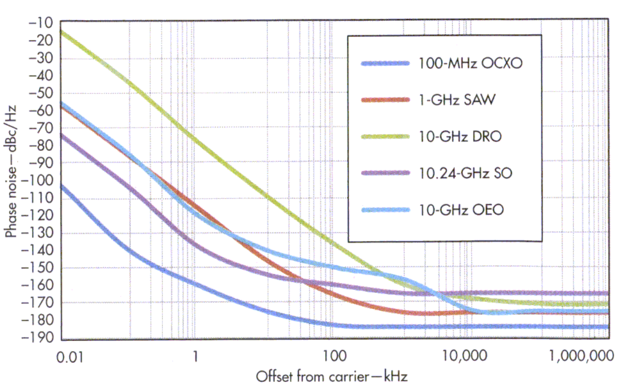

1. These curves plot typical phase-noise performance levels for various low-noise oscillators.

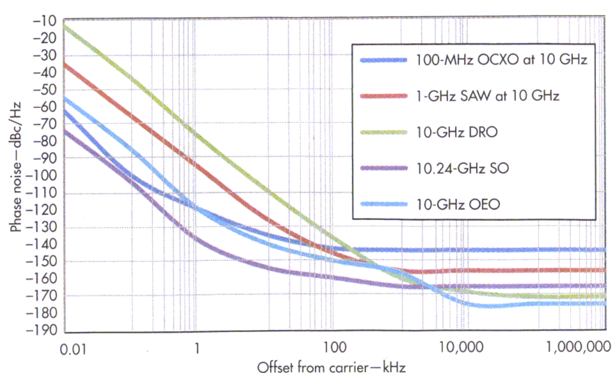

2. This plot shows the phase noise of a low-noise oscillator scaled to a 10-GHz output frequency.

-Noise SYNTHESIZERS

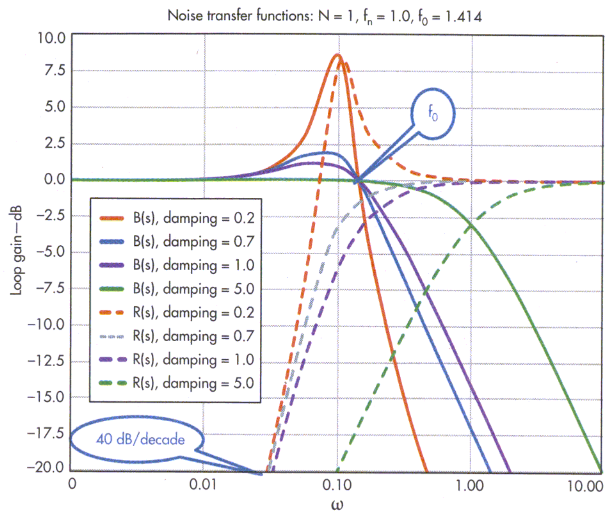

4. Noise transfer functions: Input to Output (solid lines), VCO to Output (dashed lines).

In *Fig. 1*, the OCXO phase noise exceeds the –177-dBc limit, because its power is 13 dB higher than the 0-dBm limit. The lowest-frequency oscillators typically exhibit the lowest noise floors. They also show lower close-in phase noise, since the quality factor (Q) of lower-frequency resonators is higher, and because the flicker characteristics associated with these resonators is better. When using these oscillators as the reference of a synthesizer, their noise contribution is scaled by $20\log(F_{out}/F_{ref})$. Thus, the noise contribution of a 100-MHz OCXO will be increased by 40 dB when producing a 10-GHz signal. *Figure 2* shows the expected noise from these oscillators when used to generate a 10-GHz signal.

The lowest close-in phase noise is from the sapphire oscillator (SO), followed closely by the OCXO. The lowest phase noise far from the carrier is for the optoelectronic oscillator (OEO) and the dielectric-resonator oscillator (DRO). Combining the SO or OCXO with the OEO or DRO could achieve lower noise levels. (Additional specifications are available in *Table 1* at www.mwrf.com/active-components/searching-low-phase-noise-synthesizers.)

TABLE 1: TYPICAL PERFORMANCE SPECIFICATIONS FOR DIFFERENT OSCILLATORS

Parameter	OCXO	SAW	DRO	Sapphire	OEO
Size (in.)^3	1.5 × 1.1 × 0.7	0.5 × 0.5 × 0.2	1.3 × 3.1 × 0.8	8.5 × 8.5 × 2.5	4.5 × 5.9 × 0.94
Weight	0.9 oz.	0.1 oz.	0.2 lb.	15.5 lb.	--
Power consumption (W)	1.5	0.175	5	34.5	28
Cost	Moderate	Low	Moderate	Very high	--
Operating temperature range (°C)	–20 to +60	–20 to +70	–15 to +75	0 to +50	+15 to +45
Output power (dBm)	+15	+2	8dBm	>10dBm	>10dBm
Harmonics (dBc)	-40	-25	-40	--	-40
Spurious (dBc)	--	--	--	-130	-95

Figure 3 shows a typical second-order PLL circuit that can be used as the starting point for building a frequency synthesizer. It uses a phase detector, loop filter, oscillator, and feedback divider.[10-12] Parameter K_φ is the gain of the phase detector, F(s) is the transfer characteristic of the loop filter, K_0 is the VCO sensitivity, and N is the feedback divider ratio. Considering the PLL a control system, the closed-loop transfer function (transfer function of the input phase noise to the output signal) can be described by Eq. 1:

$B(s) = \varphi_0(s)/\varphi_i(s) = N[(2\xi\omega_n s + \omega^2{}_n/(s^2 + 2\xi\omega_n s + \omega^2{}_n]$ (1)

with F(s), the natural pulsation (ω_n), and the damping factor of the control system (ξ) described by Eqs. 2, 3, and 4, respectively:

$F(s) = (1 + \tau_2 s)/(\tau_1 s)$ (2)

$\omega_n = [K_\varphi K_0/(N\tau_2)]^{0.5}$ (3)

$\xi = \omega_n\tau_2/2$ (4)

By analyzing Eq. 1, as the input phase-noise frequency offset decreases towards zero, the transfer function approaches N. The feedback divider ratio amplifies the input phase noise, increasing by a factor of 20logN (in dBc). The unity gain frequency (f_0) is independent on the damping factor and is given by Eq. 5[13]:

$f_0 = [(2)^{0.5}/2\pi]\rho_n$ (5)

The VCO noise transfers to the output of the PLL by a second-order highpass relationship given by Eq. 6:

$R(s) = s^2/(s^2 + 2\xi\omega_n s + \omega^2_n$ (6)

For low offset frequencies, the VCO noise is attenuated with a 40-dB/decade slope, while for far offset frequencies, the VCO noise passing to the output is unaffected by the loop.

The magnitudes of the B(s) and K(s) noise transfer functions are plotted in *Fig. 4*. For a damping factor of 0.707, shown by the blue trace on *Fig. 4*, the peaking has a value of 2.09 dB. If the PLL is underdamped ($\xi < 0.707$), peaking can be large, making the system unstable. Peaking can be reduced by increasing the damping factor, but this takes the B(s) and R(s) trace decrease less sharply beyond the natural frequency.

Noise models can be categorized as linear time invariant (LTIV), linear time variant (LTV), and nonlinear time variant (NLTV) models, in order of increasing complexity. Leeson's model[15] is based on LTIV oscillator properties, such as resonator Q, feedback gain, and noise figure. Additional models include an LTV model[16] and an NLTV configuration using a perturbation model based on numerical techniques.[17-20]

Phase noise has been analyzed by means of a number of different models, with both time- and frequency-domain techniques applied.[21-26] (The relative strengths and weaknesses of the three phase-noise models are compared in *Table 2*, included in the online version of this article). When comparing noise models for harmonic (LC-resonator-type) and nonharmonic oscillator circuits (RC-oscillator-type) oscillator circuits, a designer must choose the noise model, since none of the models provide closed-form solutions for phase noise.

In typical implementations, a synthesizer would use a feedback divider to control the frequency produced by the oscillator. The feedback divider's output noise exhibits the same lowpass transfer characteristics [B(s)] as the input noise, with the divider's close-in noise of greater importance than its noise level. Such a divider is built with logic gates, using typical technologies as TTL, CMOS/BiCMOS, and ECL, but rarely as a regenerative divider based on frequency mixers. TTL dividers can achieve low noise levels[28], to −170 dBc/Hz, with good close-in noise, but their maximum clock frequency rarely exceeds 150 MHz.

Reducing the reference frequency from 100 MHz to 10 MHz would result in degradation of output phase noise of 20 dB, making the TTL divider unsuitable for locking with 100-MHz signals. CMOS/BiCMOS dividers can achieve similar noise levels at offsets greater than 10 MHz, but with more flicker in higher close-in noise levels that makes them poor choices for low-noise synthesizers. A better choice would be using ECL dividers, which typically exhibit noise levels of −155 dBc/Hz.

TABLE 2: COMPARING THE THREE PHASE-NOISE MODELS

Model	Leeson	Lee and Hajimiri	Kaertner and Demir
Assumptions	LTIV	LTV	NLTV
Perturbing noise source	Constant white noise (kTB)	Cyclostationary 1/fk for any k that is an element of N	Modulated 1/fk for any k that is an element of N
Accuracy	Reasonable	Good	Exact
Simplicity	Simple	Moderate	Involved
Computer dependence	Independent (Calculation by hand)	Computer to evaluate ISF	Computer dependent (no closed form solutions)
Predicts close-in phase noise	No	Yes	Yes
Retained circuit parameters	Loaded Q-factor (QL), output power (Ps)	Q_{max}	None

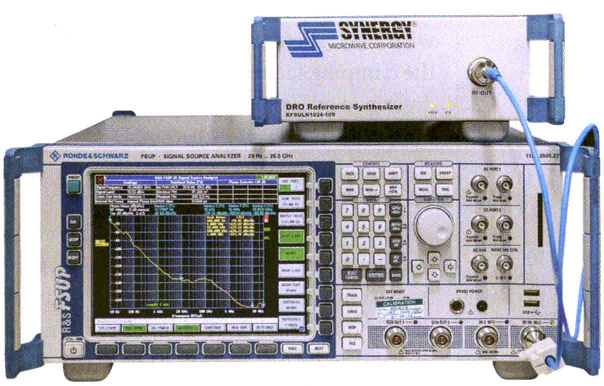

5 This measurement setup was used to test the DRO reference synthesizer.

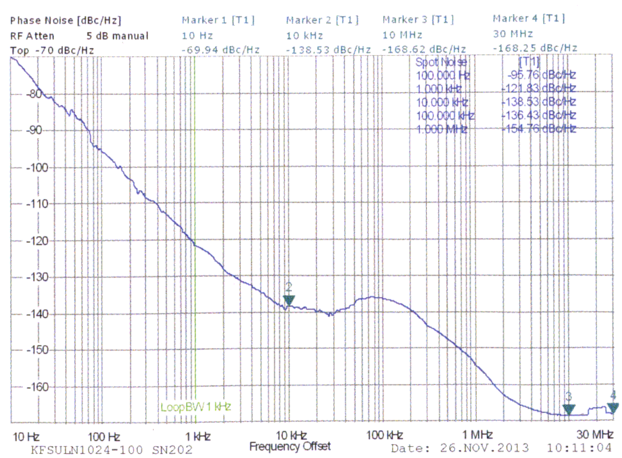

6. This is a plot of the phase-noise performance of the 10.24-GHz signal produced by the KFSULN1024-100 source.

WORLD'S WIDEST SELECTION

VCOs

12 to 6840 MHz from 11^{95} ea. (qty. 5)

Want a miniature surface mount, shielded plug-in, or rugged coaxial voltage controlled oscillator with the right stuff for your project? Go to minicircuits.com! You'll find over 800 standard catalog models, ***always in stock***. They're optimized to meet specific requirements, from narrow, broad, or octave bandwidths to linear tuning, low phase noise, dual output, 5V PLL/synthesizer implementation, or size, as small as 0.25 x 0.25 x 0.1". Selection is a snap, even with so many models to choose from! Just enter your requirements, and our patented search engine, Yoni2, searches *actual test data* to find the models that meet your needs. And if you need a custom design, challenge us with a phone call or email! We constantly design new models to meet new needs—so you'll get a quick response, fast turnaround times, and all at a surprisingly low price. Give your competition *real competition*...specify a Mini-Circuits VCO!

All SMT components are glued, as well as soldered, in place for long-term, reliable performance even after multiple reflow operations.

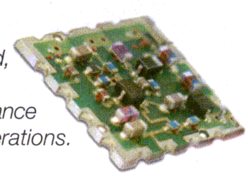

RoHS compliant

Mini-Circuits®

www.minicircuits.com P.O. Box 35166, Brooklyn, NY 11235-0003 (718) 934-4500 sales@minicircuits.com

359 rev V

Direct frequency synthesis can achieve lower noise than when using feedback dividers and phase-detector combinations. Direct synthesis employs harmonic multipliers, based on step-recovery, PIN, or Schottky diodes, to generate higher-frequency signals. Such diodes allow multiplication of the 100-MHz signal from an OCXO with minimal degradation in noise, with an equivalent noise floor of about −174 dBc/Hz. The synthesis approach can achieve a slightly better noise performance when using references having power levels considerably higher than 0 dBm. The drawback of this method is the high far-offset output noise, with 20logN degradation.

LOWERING NOISE

Improved noise performance can be achieved by combining the direct frequency synthesis approach with a PLL method. A high-frequency phase detector is used to lock the oscillator to the harmonic of the reference clock produced by diode harmonic multipliers. By using a low-noise OCXO with a low-noise high-frequency oscillator, such as a DRO or SAW oscillator, this hybrid method is capable of achieving excellent noise levels. Close-in performance is determined by the OCXO and harmonic multiplier, while far-offset performance is determined by the high-frequency oscillator.

The KFSULN1024-100 DRO reference synthesizer is an implementation of such an approach, providing a 10.24-GHz output signal with low noise. The design locks a 10.24-GHz DRO from Synergy Microwave Corp. (www.synergymwave.com) to the harmonics of an internal OCXO reference, using a low-noise PLL with double-balanced mixer serving as phase detector. By using frequency multiplication from the reference, the noise performance required from the mixer and loop filter is relaxed by about 40 dB. The design employs low-noise operational amplifiers to achieve low noise levels.

The synthesizer was characterized with a model FSUP signal source analyzer from Rohde & Schwarz (www.rohde-schwarz.com). The synthesizer and test system were both placed inside a Faraday cage to minimize the effects of outside noise sources. *Figure 5* shows the test system, while *Fig. 6* shows the test results. The synthesizer produces a +10-dBm signal at 10.24 GHz. The low-noise internal OCXO determines the synthesizer's performance for offset frequencies between 10 Hz and 1 kHz, with −70-dBc/Hz phase noise at 10-Hz offset and −121 dBc/Hz at 1-kHz offset. Low-noise

synthesis techniques produce a low noise floor of −138 dBc at 10-kHz offset. Above 1 MHz, the noise floor is determined by the DRO and reaches −168 dBc/Hz. mw

REFERENCES

1. IEEE STD 1139-2008, IEEE Standard Definitions of Physical Quantities for Fundamental Frequency and Time Metrology-Random Instabilities," February 2008, Digital Object Identifier: 10.1109/IEEESTD.2008.4797525, pp. c1-35.
2. U.L. Rohde and A.K. Poddar, "Technique to Minimize Phase noise of Crystal Oscillators," Microwave Journal, May 2013, pp. 132-150.
3. Synergy Microwave Corp., www.synergymwave.com/products/?n=99&p=&pId=22.
4. U.L. Rohde and A.K. Poddar, " Latest Technology, Technological Challenges, and Market Trends for Frequency Generating and Timing Devices," IEEE Microwave Magazine, October 2012, pp.120-134.
5. U.L. Rohde and A.K. Poddar, "DRO Drops phase-noise levels," Microwaves & RF, February 2013, pp. 80-84.
6. U.L. Rohde, A.K. Poddar, and A. Apte, "Getting Its Measure," IEEE Microwave Magazine, Vol. 14, No. 6, pp. 73-86.
7. U.L. Rohde, A.K. Poddar, and A. Apte, "How Low Can They Go, Oscillator Phase Noise Model, Theoretical, Experimental Validation, and Phase Noise Measurements," IEEE Microwave Magazine, Vol. 14, No. 6, pp. 50-72.
8. Li Zhang, A.K. Poddar, U.L. Rohde, and A.S. Daryoush, "Analytical and Experimental Evaluation of SSB Phase Noise Reduction in Self-Injection Locked Oscillators Using Optical Delay Loops," IEEE Photonics Journal, Vol. 5, No. 6, pp. 1-18.
9. A.K. Poddar, "Slow Wave Resonator Based Tunable Multi-Band Multi-Mode Injection-Locked Oscillators" Dr.-Inh.-habil Thesis, BTU Cottbus, Germany (draft thesis submitted for defense on March 2013).
10. U.L. Rohde, Microwave Wireless Synthesizers: Theory and Design, Wiley, New York, 1997, p. 25.
11. U.L. Rohde and A.K. Poddar, "A Digital Frequency Synthesizer Using Adaptive Mode-Coupled Resonator Mechanism for Low Noise and Low Jitter Applications," IEEE International Symposium on Circuits and Systems (ISCAS), 2011.
12. U.L. Rohde and A.K. Poddar, "VCSO Technology Silences Synthesizers," Microwaves & RF, February 2011.
13. J.A. Crawford, "Advanced Phase-Locked Techniques," Artech, Norwood, MA, p. 28.
14. Behzad Razavi, RF Microelectronics, Prentice-Hall, Englewood Cliffs, NJ, 2011, p. 613.
15. D.B. Leeson, "A Simple Model of Feedback Oscillator Noise Spectrum," IEEE Proceedings, 1966, pp. 329-332.
16. T.H. Lee and A. Hajimiri, "Oscillator Phase Noise: A Tutorial," IEEE Journal of Solid-State Circuits, Vol. 35, No. 3, March 2000, pp. 326-336.
17. A. Demir, A. Mehrotra, and J. Roychowdhury, "Phase noise in oscillators: a unifying theory and numerical methods for characterization," IEEE Transactions on Circuits & Systems I, Vol. 47, No. 5, May 2000, pp. 655-674.
18. M. Nick, "New Q-Enhanced Planar Resonators for Low Phase-Noise Radio Frequency Oscillators," Ph.D. Dissertation, Electrical Engineering, University of Michigan, 2011.
19. F.X. Kaertner, "Analysis of White and üb Noise in Oscillators," International Journal of Circuit Theory and Application, Vol. 18, 1990, pp. 485-519.
20. A. Demir, "Phase Noise and Timing Jitter in Oscillators with Colored-Noise Sources," IEEE Transactions on Circuits and Systems 1, Vol. 49, No. 12, December 2002, pp. 1782-1791.
21. J.C. Nallatamby, M. Prigent, M. Camiade, and J. Obregon, "Phase noise in oscillators – Leeson formula revisited," IEEE Transactions on Microwave Theory and Techniques, Vol. 51, No. 4, April 2003, pp. 1386-1394.
22. A. Suárez, S. Sancho, S. Ver Hoeye, and J. Portilla, "Analytical comparison between time- and frequency-domain techniques for phase-noise analysis," IEEE Transactions on Microwave Theory and Techniques, Vol. 50, No. 10, October 2002, pp. 2353-2361.
23. S. Ver Hoeye, A. Suárez, and J. Portilla, "Techniques for oscillator nonlinear optimization and phase-noise analysis using commercial Harmonic-Balance software," 2000 IEEE MTT-S Digest, pp. 95-98.
24. V. Rizzoli, F. Mastri, and D. Masotti, "General noise analysis of nonlinear microwave circuits by the piecewise Harmonic Balance technique," IEEE Transactions on Microwave Theory and Techniques, Vol. 42, No. 5, May 1994, pp. 807-819.
25. A. Abidi, "How phase noise appears in oscillators," www.rfdh.com/ez/system/db/pds_tn/upload/271/phase_noise.pdf.
26. U.L. Rohde and D.P. Newkirk, "RF/Microwave Circuit Design for Wireless Applications," Wiley-Interscience, New York, 2000, p. 644.
27. U.L. Rohde, Digital PLL Frequency Synthesizers - Theory and Design, Prentice-Hall, Englewood Cliffs, NJ, 1983.
28. U.L. Rohde, "A New and Efficient Method of Designing Low Noise Microwave Oscillators," Dr.-Ing. Thesis, BTU Cottbus, Germany, 2004.


AEROFLEX
INMET
Models 6FH & 18FH
6 and 18 GHz Full Hex
2-Watt Attenuators
Model AHC/RP
6 GHz Reverse-Polarity
2-Watt Attenuator

JEAN-JACQUES DELISLE | Technical Engineering Editor

Adapters And Couplers Ride The Millimeter Wave

As wireless communications and electronic warfare push the frequency performance of test and operating systems ever higher, adapters and couplers are responding by carrying wider-band signals at higher frequencies.

COUPLERS AND ADAPTERS are necessary links between components in the test and operation of RF systems. As these components are add-ins to the RF signal stream, they produce distortion, attenuation, and delay. Minimizing these performance degraders is a high priority for designers of adapters and couplers, who are preparing their product lines to meet future demands for higher-frequency and wider-band operation. The materials used, quality of construction, finishing, size, and connector type all have significant impact on the performance of adapters and couplers (*Fig. 1*). For adapters in particular, they impact frequency range, voltage-standing-wave ratio (VSWR), maximum power, and passive intermodulation distortion (PIM). Couplers are affected in terms of frequency range, VSWR, PIM, coupling, accuracy, insertion loss, directivity, and maximum power.

Adapters are used in almost every RF system to bridge the gap between RF components. The most common off-the-shelf RF adapters are coaxial connector adapters, which are either between-series (i.e., between two different standard types of coaxial connector) or in-series (joining two coaxial cable connectors with the same standard type). The goal of between-series adapters is to provide a convenient transition between common coaxial connector types, minimizing length while providing good electrical performance, small size, low VSWR, and broadband coverage. Other RF adapters, such as waveguide-to-coaxial adapters, are offered by Anritsu Co. (www.anritsu.com), Ducommun Technologies (www.ducommun.com), and Sage Millimeter (www.sagemillimeter.com; *Fig. 2*).

Most between-series adapters are made of machined stainless steel with a passivated finish, nickel-plated brass, and gold-plated brass. The insulators are commonly tetrafluoroethylene (TFE), teflon, polytetra-

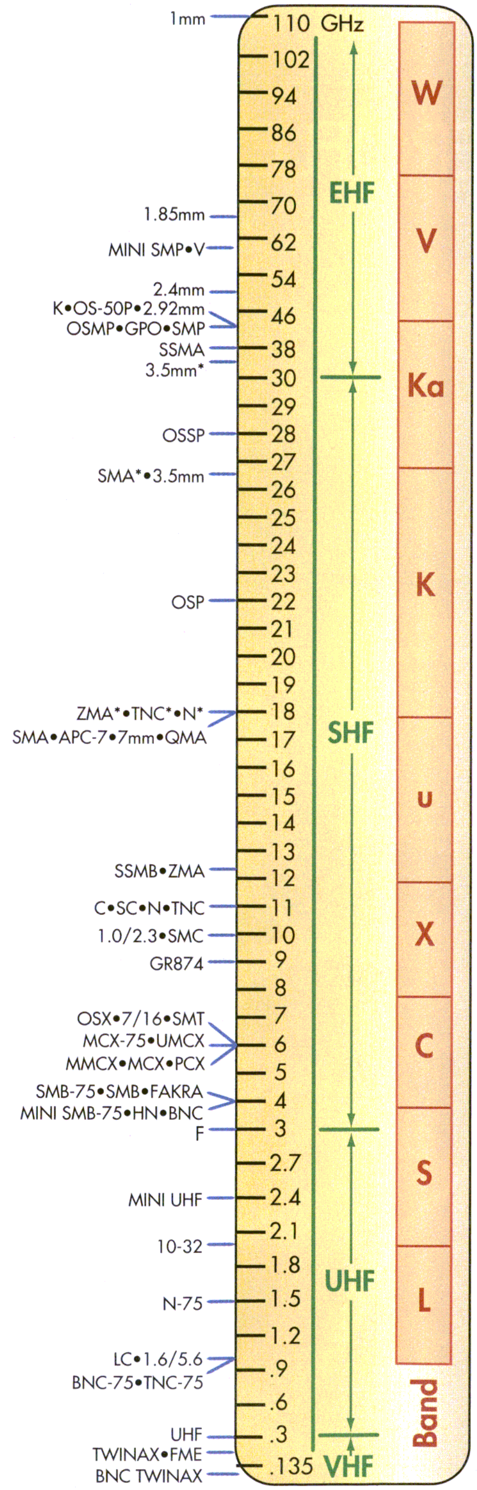

1. This frequency chart displays the VHF, UHF, SHF, and EHF ranges with commonly available coaxial connector sand their maximum operating frequency.

fluoroethylene (PTFE), polyethylene solid/foam, and even air. They are all commonly used as dielectrics for different frequency range and environmental applications. The contact pins are made of copper, gold, or—for high-frequency applications—beryllium copper with gold plating. An adapter's connector type is the major limiting factor in frequency performance, as larger types of connectors cannot support transverse-electromagnetic (TEM) modes for higher frequencies. Modern adapter types are constructed with sufficient precision, refined materials, and small dimensions to allow for VSWR as low as 1.2:1 to 110 GHz. Pasternack (www.pasternack.com) and Agilent (www.agilent.com; *Fig. 3*), for example, has a range of adapter offerings into the 1.0-mm and 1.85-mm adapter range with operation to millimeter-wave frequencies. To avoid being the limiting factor in a design, adapters are being forced to outpace the coupler market in maximum frequency and performance.

> "Minimizing performance degraders is crucial for designers of adapters and couplers, who are preparing their products to meet future demands for higher-frequency and wider-band operation."

Couplers, for their part, are used in a variety of military, space, telecommunications, and test/measurement systems to extract a portion of the transmission (Tx) or reception (Rx) signal, the coupling factor. Specifically, directional couplers are designed with the ability to extract a significant portion of only the Tx or Rx, depending upon how it is configured (known as directivity and isolation). Directional couplers are created by placing a conducting (often metal) coupling structure in proximity to the main transmission line of operation. The coupling structure's dimensions and the materials used are designed specifically to achieve the frequency response for the desired application.

Traditionally, directional couplers only came in coaxial connectorized models. But modern directional couplers are offered with through-hole, plug-in, and surface-mount connectivity. The transmission lines and coupling structures are often made using printed-circuit-board (PCB) technology to ensure tight tolerances for fabrication, thanks to the availability of laminates with high dielectrics for RF applications. For instance, Mini-Circuits (www.minicircuits.com) offers surface-mount directional couplers as small as 0.12 × 0.06 in.

Modern directional couplers operate from 0.5 to 60.0 GHz with common coupling factors (assumed negative) of 6, 10, 20, and 30 dB. Some companies, such as Connecticut Microwave (www.connecticut.microwave.com), make specialized directional couplers for PIM operation as low as −140 dB with coupling factors from 40 to 65 dB. Like adapters, the maximum frequency is dictated by the quality of materials, machining, and connectivity type. Maximum insertion loss ranges from 2.5 to 0.05 dB with broadband directional couplers sacrificing insertion loss for wider frequency response. Narrowband directional couplers lead with higher directivity ranging from 25 to 10 dB.

Maximum VSWR ranges from 1.1:1 to 1.8:1 with broadband directional couplers, which generally suffer higher maximum VSWR ratings. In general, the lower-coupling-strength and narrower-bandwidth directional couplers offer better electrical response. Companies like Krytar (www.krytar.com) and AtlanTecRF (www.atlantecrf.com; *Fig. 4*) offer directional couplers to 40 GHz, while companies like Narda Microwave (www.nardamicrowave.com) have offerings to 60 GHz. mw

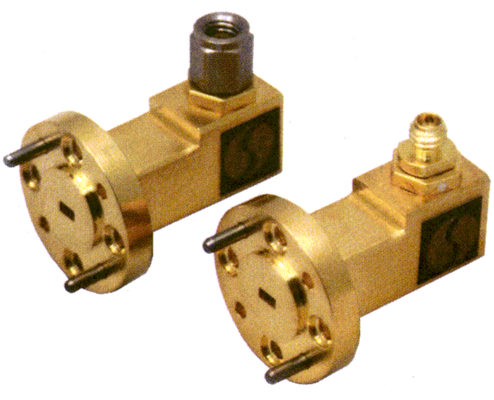

2. Sage Millimeter's waveguide-to-coaxial directional couplers.

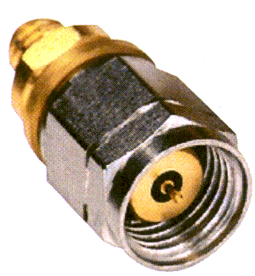

3. Agilent's 1-mm female to 1.85-mm male coaxial adapter.

4. AtlanTecRF's broadband directional coupler.

Senior Design Engineer: Required by RF Micro Devices for a position in San Jose, CA. Collaborate with customers/marketing engineers to architect/define/specify highly integrated solutions to wireless transceiver products for battery powered applications. Will develop low cost solutions to high volume, commercial RFIC's using GaAs and Silicon IC Technologies. Perform conceptual and detailed IC design of critical RF elements associated RF ASIC's. Critical RF elements include power amplifiers, switches, couplers, filters, power detectors, etc. Company Proprietary IC design information, confidential market information. Interacts with all areas of the company. Public interaction at conferences and in written articles/papers. PC and Workstation CAD/CAE tools used in the IC design process, RFIC design knowledge. These include Agilent ADS and 2.5/3D EM tools such as Momentum, Sonnet, and HFSS. Knowledge of GaAs HBT, GaAs pHEMT, InGaP HBT, SiGe HBT, and CMOS. Requires BSEE (or foreign equivalent) and two years experience. Full time position. Qualified candidates should send resumes to **employment@rfmd.com** and refer to Job Code: **JLWAN**.

This index is provided as an additional service by the publisher, who assumes no responsibility for errors or omissions.

Subscription Assistance and Information:
(ISSN 0745-2993)
Microwaves & RF is published monthly, except semi-monthly in December. Microwaves & RF is sent free to individuals actively engaged in high-frequency electronics engineering. In addition, paid subscriptions are available. Subscription rates for U.S. are $95 for 1 year ($120 in Canada, $150 for International). Published by Penton Media, Inc., 9800 Metcalfe Ave., Overland Park, KS 66212-2216. Periodicals Postage Paid at Shawnee Mission, KS and at additional mailing offices.
POSTMASTER: Send change of address to Microwaves & RF, Penton Media Inc., P.O. Box 2095, Skokie, IL 60076-7995. For paid subscription requests, please contact: Penton Media Inc., P.O. Box 2100, Skokie, IL 60076-7800. Canadian Post Publications Mail agreement No. 40612608. Canadian GST# R126431964. Canada return address: IMEX Global Solutions, P.O Box 25542,London, ON N6C6B2.

Back issues of MicroWaves and Microwaves & RF are available on microfilm and can be purchased from National Archive Publishing Company (NAPC). For more information, call NAPC at 734-302-6500 or 800-420-NAPC (6272) x 6578.

Ceramic Packages Extend To 40 GHz

A LINE of hermetically sealable, high-temperature-cofired-ceramic packages incorporates air cavity designs for low loss at high frequencies. These quad-flat-pack-no-lead packages are available in six sizes from 3 to 8 mm with standard JEDEC MO-220 footprints. The maximum insertion loss is 0.5 dB from DC to 18 GHz, 1.5 dB from 18 to 35 GHz, and

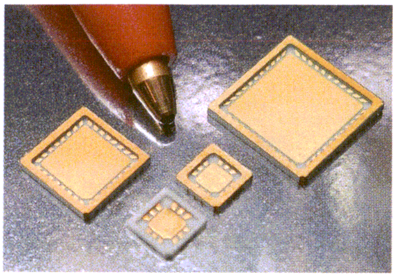

4 dB from 35 to 40 GHz. The packages—which exhibit higher thermal conductivity than low-temperature-cofired-ceramic (LTCC) packages, making them well suited for high-power applications—are available with either a plain seal for epoxy or metallized grounded seal ring for solder lid attachment. Lids are also available.

BARRY INDUSTRIES INC., 60 Walton St., Attleboro, MA 02703; (508) 226-3350, FAX: (508) 226-3317, e-mail: sales@barryind.com, *www.barryind.com*

USB Controls Phase Shifters

MODELS LPS-402 and LPS-123 have been added to the Lab Brick family of phase shifters. The former operates from 2 to 4 GHz while the latter runs from 8 to 12 GHz. These Universal Serial Bus (USB) controllable phase shifters can be set from an easy-to-install and easy-to-use software graphical user interface (GUI). The GUI can handle several phase shifters for use in multiple-device test setups. Over their frequency ranges, the phase shifters provide full 360-deg. phase control in 1-deg. increments. They achieve 5-dB typical insertion loss, 15-dB typical input/output return loss, 10-μs typical response time, and ±2.5-deg. phase adjustment accuracy. The phase shifters maintain linear operation for power levels to +10 dBm.

VAUNIX TECHNOLOGY CORP., 242 Neck Rd., Haverhill, MA 01835; (978) 662-7839, FAX: (978) 662-7842, e-mail: vaunixsales@vaunix.com, *www.vaunix.com*

Materials Absorb Microwave Energy

A FAMILY of tuned microwave absorbers can be used to attenuate unwanted signals at microwave frequencies. Different types of absorbers are available for both narrowband and broadband applications. By targeting discrete frequencies between 1 GHz and 18 GHz (such as 10.9 GHz), for example, these absorber materials deliver an average attenuation between 20 and 30 dB. They convert the unwanted electromagnetic energy into heat by means of high insertion loss or high reflection. The magnetically and dielectrically loaded absorbers are easy to install, economical, and

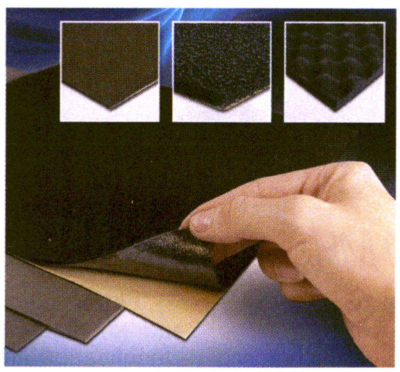

highly effective. They can be customized for a target frequency at no additional charge.

LEADER TECH, 12420 Race Track Rd., Tampa, FL 33626; (866) TECH-EMI, (813) 855-6921, FAX: (813) 855-3291, *www.leadertechinc.com*

GaN MMIC Amps Power 6 To 18 GHz

A HIGH-POWER monolithic-microwave-integrated-circuit (MMIC) amplifier based on gallium-nitride semiconductor technology has been developed for communications, test, and military applications from 6 to 18 GHz. Model HMC7149 provides 10-W output power from 6 to 18 GHz and typical small-signal gain of 20 dB. It provides +40-dBm saturated output power and draws 680 mA quiescent current from a +28-VDC supply. Model HMC7149,

supplied as a die measuring just 3.4 x 4.5 x 0.1 mm, achieves 10-dB gain at saturated output power with ±0.5-dB gain flatness. Input/output return loss is typically 17 dB while power-added efficiency (PAE) is typically 22%.

HITTITE MICROWAVE CORP., 2 Elizabeth Dr., Chelmsford, MA 01824; (978) 250-3343, FAX: (978) 250-3373, *www.hittite.com*

We've kept these ARRA Attenuators under our hat long enough...

Low Freq. Variable Attenuators

Phaseless Variable Attenuators

The "no-nonsense" attenuator...

For Audio, IF, and VHF.
Simple, straight forward, no frills. Not bad when this economy model performs in the same classy manner as other ARRA high precision units.

- SMA connectors, others available
- Off-the-shelf delivery
- 50 ohm impedance, 75 ohms available
- Specs that beat the competition's

Directly calibrated models

Freq Range (MHz)	Atten Range (dB)	Atten vs Freq (dB)	Model No.
DC-60	40	±1.0	0682-40F
DC-100	15	±0.3	0682-15F
DC-100	30	±0.5	0682-30F
DC-250	10	±0.5	0682-10F

Uncalibrated models

Freq Range (MHz)	Atten Range (dB)	Atten vs Freq (dB)	Model No.
DC-60	40	±1.0	0682-40
DC-100	20	±0.6	0682-20
DC-100	30	±0.5	0682-30
DC-200	30	±2.0	0682-30A
DC-250	15	±1.2	0682-15
DC-500	10	±0.25	0682-10

Visit our website at www.arra.com

The "incredible" attenuator...

Elegant, classic, exceptional. With all the extras you'd expect at the top of the ARRA line. So uniquely new in its approach, it's one of a kind. Nothing else like it on the market. It's got everything...

- Low phase
- High RF Power
- Low VSWR & Insertion loss
- Extremely flat frequency response
- 0-3 dB & high attenuation models
- Bands from 350-5000 MHz

...the last word in variable attenuators

ARRA INC.

15 Harold Court • Bay Shore NY 11706-2296

Tel 631-231-8400 Fax 631-434-1116

E-Mail: sales@arra.com